

***In silico* docking and ADMET studies on clinical targets for
type 2 diabetes correlated to *in vitro* inhibition of α -
glucosidase and pancreatic α -amylase by curcumin, 18 α -
glycyrrhetic acid, rosmarinic acid, and quercetin**

By

Kadima Samuel Tshiyoyo

Submitted in partial fulfilment of the requirement for the degree

Master of Science

In

Biochemistry

In the

Faculty of Natural and Agricultural Sciences

University of Pretoria

Pretoria

January 2022

Prof. Z. Apostolides

Prof. M. J. Bester



UNIVERSITEIT VAN PRETORIA
UNIVERSITY OF PRETORIA
YUNIBESITHI YA PRETORIA

DECLARATION OF ORIGINALITY

University of Pretoria

Faculty of Natural and Agricultural Sciences

Department of Biochemistry, Genetics and Microbiology

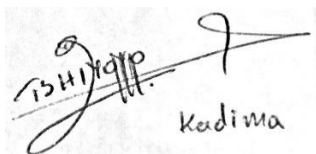
Subject of the work: *In silico* docking and ADMET studies on clinical targets for type 2 diabetes correlated to *in vitro* inhibition of α -glucosidase and pancreatic α -amylase by curcumin, 18 α -glycyrrhetic acid, rosmarinic acid, and quercetin

I, **Kadima Samuel Tshiyoyo**

Student number: 15308830

Declare that the dissertation, which I hereby submit for the degree Master of Science in Biochemistry at the University of Pretoria, is my own work and has not previously been submitted by me for a degree at this or any other tertiary institution.

SIGNATURE:



The image shows a handwritten signature in black ink on a light-colored background. The signature is written in a cursive style and includes the name 'Tshiyoyo' and 'Kadima' written below it.

DATE: 05 January 2022

ACKNOWLEDGEMENTS

First of all, I would like to thank the almighty God for the breath of life, for every blessing, and for giving me all the opportunities that I have in my life.

I would like to thank my supervisors Professors Apostolides and Bester to whom I owe an intellectual debt, thank you for your contribution, guidance, assistance and advise. Thank you for the opportunity to complete my master's degree under your supervision.

I would like to appreciate the assistance of the University of Pretoria and the Department of Biochemistry, Genetics and Microbiology for allowing me to undertake my studies at their facilities, and their staff for their support during this study. I would also like to thank Dr Serem and Ms. Nell from the Departments of Anatomy and Pharmacology respectively. Last but not least my gratitude goes to the members of CAM research group particularly Morné and Jamie, thank you for your support.

I would like to express my love and gratitude to my family, my beloved mother Monique, to my brothers and sisters Sylvie, Costa, Astrid, Fabrice, Trésor, Belinda and Emmanuel, to my other parents Constantin, Frederic, Dieudonné, Michel and Nadine. Thank you for your love, support, and constant prayers, all of you were my greatest fans and have always believed in me.

I would like to acknowledge all my friends for their encouragement and support. Particularly Grace, Joelle, Kevin, Martha, Phumi and TK to name a few, all of you were amazing.

I would like to acknowledge the National Research Foundation of South Africa for their financial support with a postgraduate scholarship. For young scientists and student helper grants and academic funding.

PUBLICATIONS AND CONFERENCES

To be submitted

- K.S Tshiyoyo, M. J Bester, J.C Serem & Z. Apostolides. *In silico* reverse docking and *in vitro* studies identified curcumin, 18 α -glycyrrhetic acid, rosmarinic acid, and quercetin as inhibitors of α -glucosidase and pancreatic α -amylase and lipid accumulation in HepG2 cells – important type 2 diabetes targets.

Congress

- Abstract accepted: K.S Tshiyoyo, M. J Bester & Z. Apostolides. *In silico* reverse docking and *in vitro* studies identified curcumin, 18 α -glycyrrhetic acid, rosmarinic acid, and quercetin as inhibitors of α -glucosidase and pancreatic α -amylase and lipid accumulation in HepG2 cells – important type 2 diabetes targets. *26th Congress of South African Society of Biochemistry and Molecular Biology (SASBMB)*, virtual congress, January 2022.
- K.S Tshiyoyo, M. J Bester & Z. Apostolides. *In silico* reverse docking and *in vitro* studies identified curcumin, 18 α -glycyrrhetic acid, rosmarinic acid, and quercetin as inhibitors of α -glucosidase and pancreatic α -amylase and lipid accumulation in HepG2 cells – important type 2 diabetes targets. *26th Annual Congress of South African Society of Biochemistry and Molecular Biology (SASBMB)*, virtual congress, January 2022 (Oral).

TABLE OF CONTENTS

DECLARATION OF ORIGINALITY	i
ACKNOWLEDGEMENTS	iii
PUBLICATIONS AND CONFERENCES	iv
Abbreviations	viii
List of Tables	ix
List of Figures	x
Abstract	xii
Introduction	1
1.1. Diabetes mellitus (DM)	1
1.2. Epidemiology of diabetes mellitus	1
1.3. Classification of diabetes mellitus	2
1.3.1. Type 1 diabetes	3
1.3.2. Type 2 diabetes	3
1.3.3. Gestational diabetes	3
1.3.4. Other types of diabetes	4
1.4. Complications associated with diabetes mellitus	4
1.4.1. Diabetes and non-alcoholic fatty liver disease	5
1.5. Carbohydrate digestion	6
1.5.1. Insulin mediated glucose uptake in tissue	9
1.6. Treatment of diabetes mellitus	10
1.7. Nutritional and medicinal values of plants	12
1.8. Strategies for identifying new antidiabetic plant derived molecules.	15
1.9. Virtual screening	16
1.9.1. Chemical structure	16
1.9.2. Ligand docking - scoring function	17
1.9.3. ADMET properties	18
1.10. Kinetic studies	19
1.11. In vitro and in vivo models	21
1.12. Aims	23
1.13. Null hypothesis	23
1.14. Objectives	23
Materials and methods	25
1.15. Materials	25
1.16. Methods	26

1.16.1.	Selection of compounds _____	26
1.16.2.	Computer simulation _____	26
1.16.3.	Preparation of reagents _____	27
1.16.4.	α -Glucosidase inhibition assay _____	29
1.16.5.	α -Amylase inhibition assay _____	30
1.16.6.	Cytotoxicity _____	32
1.16.7.	Glucose uptake assay _____	33
1.16.8.	Hepatic lipid accumulation _____	34
1.16.9.	Herbs/spices dose-related to acarbose dose _____	34
1.16.10.	Identification, profiling, and metabolomics of compounds in green tea _____	34
1.17.	Statistical analysis _____	36
Results	_____	37
1.18.	In silico studies _____	37
1.18.1.	Chemical structures of selected compounds _____	37
1.18.2.	Molecular docking _____	39
1.18.3.	ADMET proprieties _____	43
1.19.	In vitro enzyme inhibition _____	43
1.20.	Relationship between Docking scores and K_i _____	45
1.21.	In vitro cytotoxicity _____	47
1.22.	In vitro glucose uptake _____	49
1.23.	Hepatic lipid accumulation _____	50
1.24.	Herbs/spices dose-related to acarbose dose _____	53
1.25.	LC/MS and metabolomic analysis on green tea _____	54
1.25.1.	Identification of the peaks in the teas _____	54
1.25.2.	Quantification of metabolites in green tea _____	60
1.25.3.	Inhibition of α -amylase and α -glucosidase by green tea _____	60
1.25.4.	Correlation between peak areas in green tea brands and enzyme inhibition by green tea brands _____	61
1.25.5.	Multivariate data analysis _____	66
Discussion	_____	69
1.26.	In silico studies _____	69
1.27.	In vitro enzyme inhibition _____	71
1.28.	In vitro cytotoxicity _____	73
1.29.	In vitro glucose uptake _____	74
1.30.	Hepatic lipid accumulation _____	75
1.31.	Qualitative and quantitative analysis of green tea _____	76

Conclusion	78
References	80
Annexures	93
1.32. Annexure A: Binding interactions	93
1.33. Annexure B: Lineweaver burk plots	97
1.34. Annexure C: Cell viability graphs	99
1.35. Annexure D: Metabolites detected	101
1.36. Annexure E: Tentative identification of peaks	102
1.37. Annexure F: Ethical approval	103

Abbreviations

ADMET	Absorption, Distribution, Metabolism, Excretion/Elimination and Toxicity
CVD	Cardiovascular diseases
DIP	Diabetes in pregnancy
DM	Diabetes mellitus
DMEM	Dulbecco's Modified Eagle Medium
DMSO	Dimethylsulfoxide
DNSA	3,5-Dinitrosalicylic acid
ECG	Epicatechin gallate
EGCG	Epigallocatechin gallate
FBS	Fetal bovine serum
FCS	Fetal calf serum
GA	Glycyrrhetic acid
Glc	Glucose
GLUT-4	Glucose transporter type 4
HCC	Hepatocellular carcinoma
HDP	Hyperglycaemia during pregnancy
HIV	Human immunodeficiency virus
HOA	Human oral absorption
HTVS	High throughput virtual screening
IC ₅₀	Half inhibitory concentration
IDF	International diabetes federation
IRS	Insulin receptor substrate
K _i	Inhibitor constant
K _m	Michaelis constant
MODY	Maturity onset diabetes of young
NAFLD	Non-alcoholic fatty liver disease
NASH	Non-alcoholic steatohepatitis
NBDG	2-[N-(7-nitrobenz-2oxa-1,3-diazol-4-yl)amino]-2-deoxy-D-glucose
OA	Oleic acid
ORO	Oil Red Oil

PDB	Protein data bank
pNP	Para-nitrophenol
pNPG	Para-nitrophenyl α -D-glucopyranoside
QA	Quinic acid
SMILES	Simplified Molecular Input Line Entry System
SRB	Sulforhodamine B
TB	Tuberculosis
T1DM	Type 1 diabetes mellitus
T2DM	Type 2 diabetes mellitus
UP	Unidentified peak
V_{max}	Maximum Velocity
WHO	World Health Organisation

List of Tables

Table 1. Global diabetes estimates and projection	2
Table 2. Examples of herbs and spices and their origin in plants.	13
Table 3. Common compounds and antidiabetic effects thereof in some herbs and spices	13
Table 4. Strategies to identify new antidiabetic compounds	15
Table 5. Examples of ADMET properties predicted by different tools	18
Table 6. The structures of the compounds used in this study	38
Table 7. Docking scores of compounds docked to α -glucosidase	41
Table 8. Docking scores of compounds docked to α -amylase	41
Table 9. Spearman's and Pearson's correlation coefficients between Glide and AutoDock vina	42
Table 10. Predicted toxicity properties of selected compounds	43
Table 11. K_i values and types of inhibition of α -glucosidase by the selected compounds.....	45
Table 12. K_i values and types of inhibition of α -amylase by the selected compounds.	45
Table 13. Spearman's and Pearson's correlation coefficients between in vitro and silico studies for α -glucosidase.....	46
Table 14. Spearman's and Pearson's correlation coefficients between in vitro and silico studies for α -amylase	47
Table 15. IC_{50} of selected compounds on C2C12 cells	47
Table 16. IC_{50} of selected compounds on HepG2 cells	48
Table 17. IC_{50} of selected compounds on Caco2 cells.....	49
Table 18. Herb/spice dosage required relative to acarbose.....	53
Table 19. Peaks of standards according to the mass spectra from the negative ion mode.	54
Table 20. Average peak areas of the identified standards in the tea chromatograms	59
Table 21. Retention times and m/z ratios of the unidentified peaks (UP)	59
Table 22. Average peak areas of the unidentified peaks (UP) in the tea chromatograms.....	59
Table 23. Quantification of quinic acid, epicatechin gallate and epigallocatechin gallate in the 5 tea brands.	60

Table 24. IC ₅₀ of the green tea brands for the inhibition of α -amylase and α -glucosidase	60
Table 25. Spearman's and Pearson's correlation coefficients between peak areas of the identified standards and α -amylase inhibition by the green tea brands	61
Table 26. Spearman's and Pearson's correlation coefficients between peak areas of the identified standards and α -glucosidase inhibition by the green tea brands.....	62
Table 27. Spearman's and Pearson's correlation coefficients between the peak areas of the unidentified peaks (UP) and α -amylase inhibition by the green tea brands	62
Table 28. Spearman's and Pearson's correlation coefficients between the peak areas of the unidentified peaks (UP) and α -glucosidase inhibition by the green tea brands.....	63
Table 29. Details on UP3 and UP5 according to the obtained mass spectra	63

List of Figures

Figure 1. Estimated the comparative prevalence of diabetes in adults	2
Figure 2. Factors and agents that are either associated with or affects beta-cells function.....	5
Figure 3. Relationship between type 2 diabetes and non-alcoholic fatty liver disease.	6
Figure 4. Three dimensional structures of α -amylase (A) and α -glucosidase (B).....	8
Figure 5. Mechanism of α -amylase and α -glucosidase on carbohydrates	8
Figure 6. Insulin signalling pathway	9
Figure 7. Mechanism of actions of glucose lowering drugs in human.....	11
Figure 8. The structure of the catechins found in green tea.	15
Figure 9. Michaelis-Menten plot of velocity against substrate concentrations	20
Figure 10. Lineweaver-Burk plot of different types of inhibition.	21
Figure 11. The reaction of the substrate pNPG with α -glucosidase	29
Figure 12. The reaction of the colour reagent DNSA with the reducing sugar maltose.....	31
Figure 13. Chemical reaction of SRB with the cell protein content.	32
Figure 14. Representation of the compounds in the active side of α -amylase.	39
Figure 15. Representation of the compounds in the active side of α -glucosidase.....	40
Figure 16. The relationship between the Glide and AutoDock docking scores against alpha-glucosidase (Left) and alpha-amylase (Right).	42
Figure 17. Graphs showing the relationship between the docking scores Glide (Left) and AutoDock (Right) against the Ki of each compound for α -glucosidase.	46
Figure 18. Graphs showing the relationship between the docking scores Glide (Left) and AutoDock (Right) against the Ki of each compound for α -amylase.....	46
Figure 19. Glucose uptake by C2C12 cells.....	49
Figure 20. Glucose uptake by HepG2 cells.....	50
Figure 21. Lipid accumulation in HepG2 cells.	51
Figure 22. Light microscopy images showing the accumulation of lipid in HepG2 cells	52
Figure 23. Chromatogram of the standards cocktail in ESI negative.....	55
Figure 24. Chromatogram of the green tea in ESI negative.....	56
Figure 25. UV/Vis spectrum of the standards.....	57
Figure 26. UV/Vis spectra of the green tea.....	58
Figure 27. Molecular structures and ms/ms fragment ions of the proposed compounds UP3.	64
Figure 28. Molecular structures and ms/ms fragment ions of the proposed compounds UP5	65
Figure 30. PCA (A) and OPLS-DA (B) score plots of the metabolite content of the five green tea brands.	67

Figure 31. OPLS-DA (A) and volcano plot diagram(B) of α -amylase and α -glucosidase inhibition by the five green tea brands. 68

Abstract

Type 2 diabetes mellitus (T2DM) is a chronic disease characterised by prolonged hyperglycaemia due to the inability of the liver, muscle, and fat cells to absorb glucose following insulin stimulation. Several therapeutic targets have been identified and this includes the inhibition of α -amylase and α -glucosidase in the small intestine, promotion of glucose uptake by responsive tissue and the inhibition of hepatic lipid accumulation.

The *in silico* enzyme inhibitory abilities of 1070 compounds found in 30 commercially available herbs, spices, and medicinal plants were assessed using docking analysis with Maestro from Schrodinger and AutoDock vina from DIA-DB; four compounds (18 α -glycyrrhetic acid (18 α -GA), curcumin, quercetin and rosmarinic acid) with docking scores more negative or similar to acarbose were selected for further analysis. *In silico* ADMET properties were obtained using canvas QikProp, pkCSM online tool, and the results were compared with acarbose. *In vitro* biochemical assays were used to confirm docking studies; these were the dinitrosalicylic acid (DNSA) and para-nitrophenyl-D-glucopyranoside (pNPG) assays for α -amylase and α -glucosidase inhibition, respectively. The IC₅₀ of each compound was determined after 48 hrs exposure with the Sulforhodamine B (SRB) assay in the C2C12, HepG2 and Caco-2 cell lines, representing the muscle, liver, and intestinal tissue respectively. Using the 2-[N-(7-nitrobenz-2oxa-1,3-diazol-4-yl)amino]-2-deoxy-D-glucose (2-NBDG) assay, the ability of the compounds to promote glucose uptake was determined in the C2C12 and HepG2 cell lines. The reduction of lipid accumulation associated with non-alcoholic liver disease (NAFLD), a feature of T2DM was evaluated in the HepG2 cells exposed to oleic acid (OA). Effects were compared with known drugs, acarbose for α -amylase and α -glucosidase inhibition and metformin for glucose uptake and lipid accumulation studies.

Herbs and spices with high levels of these compounds were then identified. As green tea was also a rich source of compounds with antidiabetic effects, using UPLC-MS the levels of quinic acid, epicatechin gallate (ECG) and epigallocatechin gallate (EGCG) in five green tea *Camellia sinensis*, tea brands were determined. The aim was to identify, related to anti-diabetic effects the best tea that inhibits α -amylase and α -glucosidase.

The relationships between *in silico* and *in vitro* inhibition results correlated well; a more negative docking score *in silico* correlated with a lower inhibition constant (K_i) *in vitro*. For α -

glucosidase, the K_i values of curcumin, 18 α -GA, and quercetin were significantly lower ($p < 0.05$) than that of acarbose, while there was no significant difference ($p > 0.05$) between acarbose and rosmarinic acid. These compounds were then identified as potential inhibitors of α -glucosidase. For α -amylase, the K_i values of curcumin, 18 α -GA, quercetin, and rosmarinic acid were significantly higher ($p < 0.05$) than acarbose. An IC_{50} could be determined for 18 α -GA, quercetin and rosmarinic acid in the C2C12, 18 α -GA and rosmarinic acid in the HepG2 and curcumin and rosmarinic acid in the Caco-2 cell lines. All other compounds showed no cytotoxicity. Generally, at the concentrations used to evaluate glucose uptake and lipid accumulation the compounds were not cytotoxic. The compounds and metformin did not promote glucose uptake under the experimental conditions used but did significantly reduce ($p < 0.05$) the accumulation of OA induced lipid droplets in HepG2 cells.

Herbs and spices including green tea were identified as rich of these compounds and contained EGCG and ECG, known antidiabetic compounds. Further evaluation of five green tea brands confirmed α -amylase and α -glucosidase inhibition with Dilmah tea having the best inhibition. Other unidentified compounds in green tea may also contribute to activity.

Key findings were that these compounds are present in herbs, spices, and teas, which are cost-effective, easily cultivated, and readily available plant products that can contribute to the alleviation of T2DM symptoms. Curcumin, 18 α -GA, quercetin, and rosmarinic acid inhibited α -glucosidase, and reduced the accumulation of OA induced lipid droplets in HepG2 cells with the potential to alleviate the consequence of prolonged hyperglycemia such as the development of NAFLD. Curcumin is found abundantly in turmeric and EGCG in green tea; a dose of 1.3 g of turmeric or 1.2 g of green tea is equivalent to a 50 mg acarbose dosage per meal. One teabag contains 2.5 g of green tea; therefore, one cup of green tea per meal may be helpful in preventing prolonged hyperglycemia.

Introduction

1.1. *Diabetes mellitus (DM)*

Ancient Egyptians first discovered diabetes around 1500 B.C, and it is mainly known as diabetes mellitus (DM). The word diabetes is from Greek, and it means “pass-through,” Mellitus is from Latin, and it means “sweet” because of the sugar taste in the urine of patients (Polonsky, 2012).

Diabetes is a series of metabolic diseases associated with a high level of glucose in the blood, known as hyperglycaemia (Egan and Dinneen, 2019) and develops as a consequence of deficient secretion and/or action of insulin due to partial or complete malfunction of the pancreatic beta cells and the reduced response of tissue to insulin (Association, 2014). This can lead to macro and microvascular diseases such as kidney failure, blindness, renal dysfunction, and neuropathy (Nathan and Group, 2014). Some of these diseases are present at the early stages of diabetes (Egan and Dinneen, 2019), while others only develop later.

1.2. *Epidemiology of diabetes mellitus*

In developing countries the prevalence of DM has increased significantly (IDF, 2019). In contrast 40 to 50 years ago when it was less prevalent, today it is one of the leading causes of mortality and morbidity worldwide (Mohan *et al.*, 2007).

A recent report from the International Diabetes Federation (IDF) estimated that in 2019 approximately 9.3% of adults worldwide were living with diabetes, and if no interventions were implemented, it might increase to 10.2% and 10.9% in 2030 and 2045, respectively (IDF, 2019), as shown in Table 1.

According to a report from World Diabetes Day held in November 2019, DM caused more deaths than tuberculosis (TB), human immunodeficiency virus (HIV), and malaria combined (Rheeder, 2019). In 2016 in South Africa, DM after TB was the second disease with the highest mortality rate (Rheeder, 2019). As shown in Figure 1, South Africa is among the countries in Africa with the highest prevalence of DM in adults.

Table 1. Global diabetes estimates and projection (IDF, 2019)

	2019	2030	2045
World population	7.7 billion	8.6 billion	9.5 billion
Adults' population	5.0 billion	5.7 billion	6.4 billion
Diabetes mellitus (DM)			
Global prevalence	9.3%	10.2%	10.9%
Adults with DM	463.0 million	578.4 million	700.2 million
Death due to DM	4.2 million	-	-
Children with DM	1.1 million	-	-

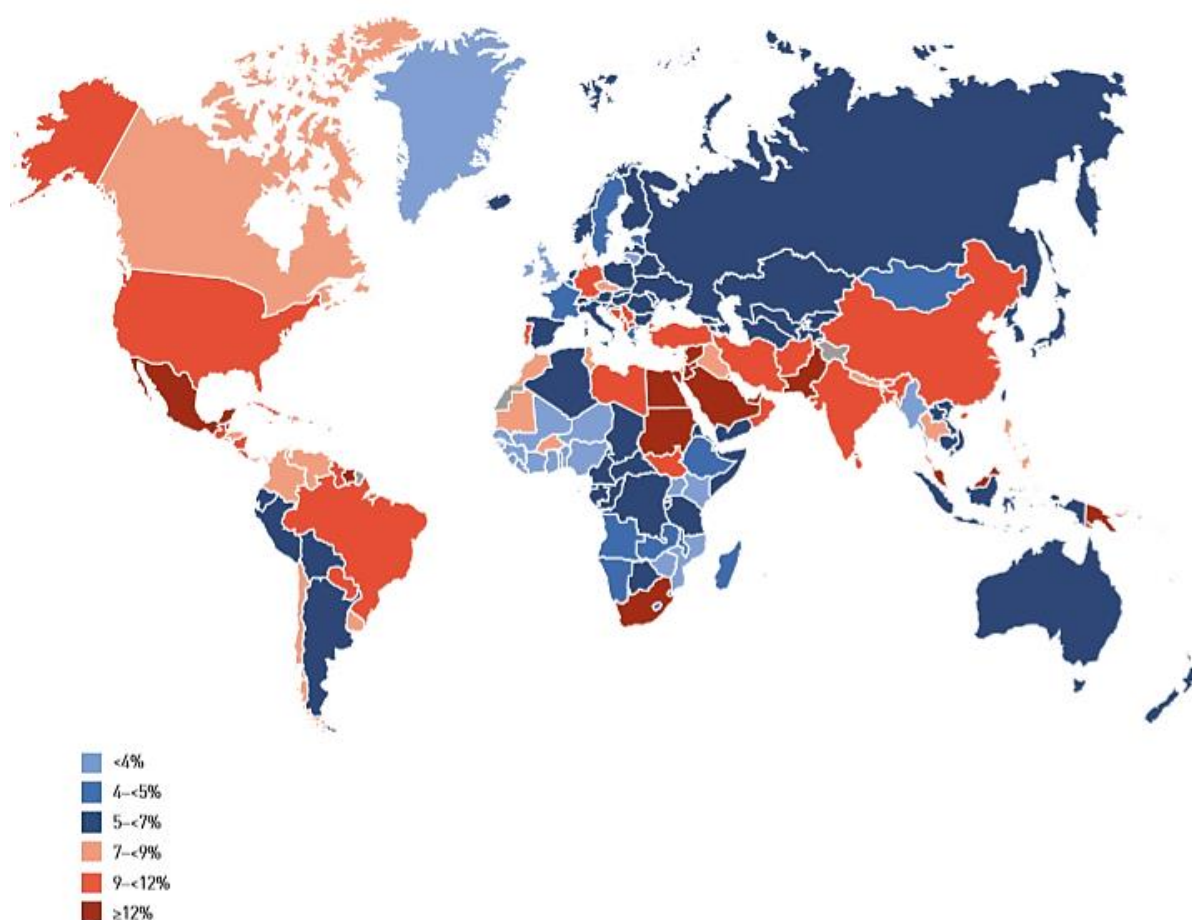


Figure 1 Estimated the comparative prevalence of diabetes in adults (20–79 years) in 2019 (IDF, 2019)

1.3. Classification of diabetes mellitus

The different types of diabetes mellitus include type 1 (T1DM), type 2 (T2DM) and gestational diabetes (GD) although other rarer forms do occur.

1.3.1. Type 1 diabetes

Type 1 diabetes mellitus is an autoimmune disease resulting in the destruction of pancreatic beta cells (Atkinson *et al.*, 2014), responsible for the production of insulin. The cause of T1DM is not fully understood, but a likely explanation is that cellular destruction is initiated by a combination of many genes and environmental factors (IDF, 2019). A consequence is a total deficiency of insulin (Egan and Dinneen, 2019) or very little insulin being secreted. Patients with T1DM require insulin injections to compensate for the shortage or absence of insulin and to minimize the increase in blood glucose levels.

This type of diabetes is mainly diagnosed in children or young adults and is more common in boys and young men than in women (Atkinson *et al.*, 2014). It is still one of the most chronic diseases of childhood, according to the IDF (IDF, 2019).

It is also known as “insulin-dependent” and “juvenile-onset” diabetes (Association, 2014) because of insulin deficiency and its occurrence in children, respectively.

1.3.2. Type 2 diabetes

Type 2 diabetes mellitus is the most common type of diabetes and approximately 90-95% of all diabetes patients are diagnosed with this disease. It occurs mainly in adults (Association, 2014) and is linked to genetic and adverse environmental factors with the contribution of the latter being greater (Kota *et al.*, 2012) and these include obesity, hypertension, and impaired fasting glucose.

In contrast to T1DM, T2DM is associated with a relative insulin deficiency and tissue insulin resistance (Chatterjee *et al.*, 2017) and is referred to as non-insulin-dependent diabetes because the insulin deficiency is not absolute, or as adult-onset diabetes (Association, 2014). However, T2DM is increasingly being diagnosed in children and young adults.

1.3.3. Gestational diabetes

Gestational diabetes (GD) is less common and is associated with any degree of glucose intolerance with onset or first recognition during pregnancy (Association, 2004). This type of diabetes is known as GD even if the condition continues after delivery, including the possibility that tolerance starts together with pregnancy (Association, 2014).

The World Health Organisation (WHO) classifies this type of diabetes as “hyperglycaemia during pregnancy” (HDP), and is present in women who had diabetes before pregnancy but were first diagnosed during pregnancy (IDF, 2019). However, most cases of hyperglycaemia during pregnancy are GD associated with approximately 75 – 90% of cases (IDF, 2019).

1.3.4. Other types of diabetes

There is an intermediate phase in which an individual has raised blood glucose levels higher than average but is not diagnosed with diabetes. That state is classified as prediabetes, and it is associated with impaired fasting glucose and glucose tolerance (Association, 2014). Blood glucose levels are higher than average but do not meet the criteria to be classified as diabetes according to the recommended diabetes diagnostic threshold (IDF, 2019). These individuals have a relatively high risk of being diagnosed with diabetes in the future.

Other types of diabetes are linked to genetic factors associated with impaired insulin production with reduced or no deficiency in the action of insulin (Association, 2014). The most common is maturity-onset diabetes of the young, known as MODY, which is associated with a mutation in beta-cell and some genes (Egan and Dinneen, 2019).

Another less common type is pancreatic diabetes, which is linked with exocrine pancreas dysfunction, which can later lead to T1DM or T2DM (Hardt *et al.*, 2008), also known as type 3c diabetes. Secondary diabetes is associated with pancreatic diseases such as hemochromatosis–related diabetes or corticosteroid hormone excess (Egan and Dinneen, 2019).

1.4. *Complications associated with diabetes mellitus*

Most tissue in the body requires glucose for energy, and insulin produced by pancreatic beta mediates this process. However, if the tissue becomes resistant to the effects of elevated blood glucose levels, it leads to hyperglycemia which is associated with certain complications, such as chronic damage and failure of different organs (Deshpande *et al.*, 2008). Symptoms accompanying hyperglycemia include polyuria, polydipsia, and blurred vision (Association, 2014). The primary affected organ is the pancreas, hence insulin deficiency, but hyperglycemia also affects other organs, such as the heart, kidney, eyes, blood vessels, and nerves (Association, 2014).

Diabetes is linked to insulin resistance or decreased insulin sensitivity because of pancreatic beta cell dysfunction (see Figure 2). Factors that contribute to the deterioration of beta cell function are glucotoxicity, lipotoxicity, autoimmunity, inflammation, leptin, islet amyloid, insulin resistance, and incretins (Cernea and Dobreanu, 2013). The pharmacological agents that reduce these effects are also shown in Figure 2.

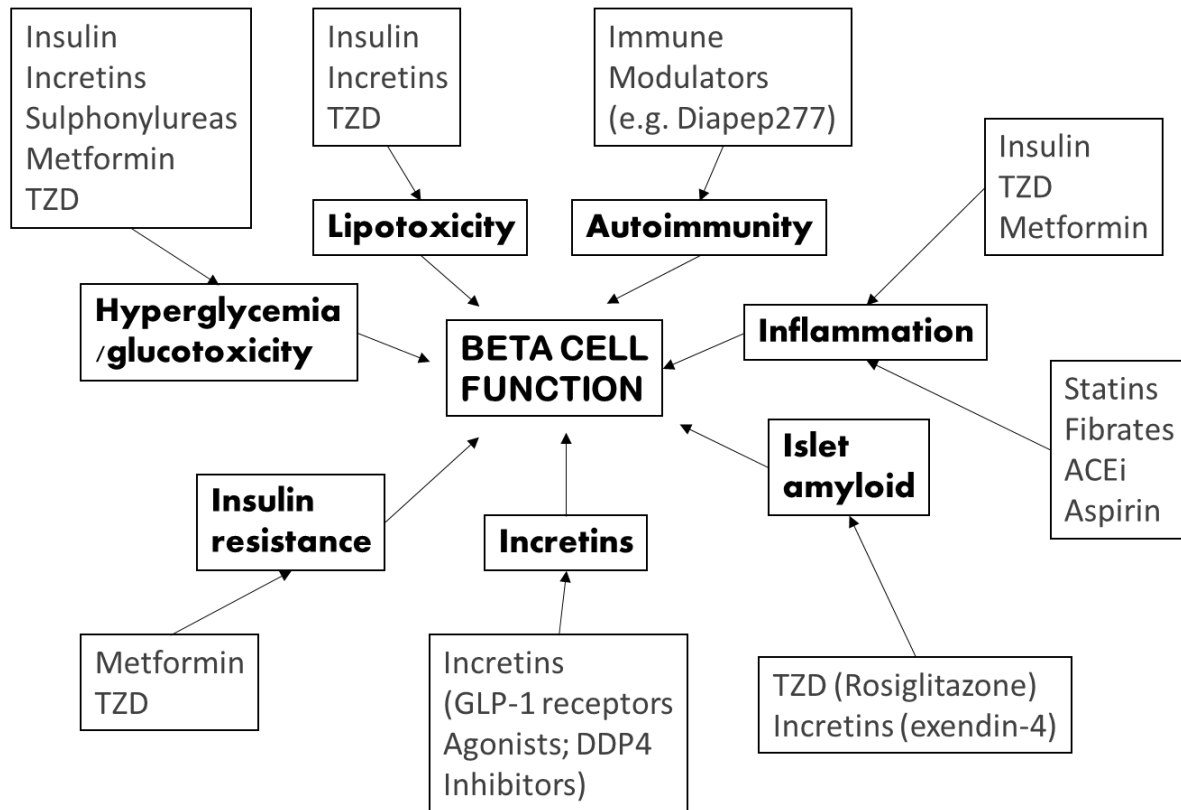


Figure 2. Factors and agents that are either associated with or affect pancreatic beta cells function. TZD - thiazolidinedione; GLP-1 - glucagon-like peptide-1; DPP4 - dipeptidyl peptidase-4; ACEi - angiotensin-converting enzyme inhibitors; ARB - angiotensin receptor blocker. (Cernea and Dobreanu, 2013).

1.4.1. Diabetes and non-alcoholic fatty liver disease

Factors that contribute to the development of T2DM are genetic, environmental, and physical factors. Obesity, age, and lack of physical activity are associated primarily with T2DM (Association, 2014) and often can lead to other complications, such as non-alcoholic fatty liver disease (NAFLD) (Pei *et al.*, 2020).

Non-alcoholic fatty liver disease is considered to be a major leading cause of liver disease globally and is linked with different factors such as fatty acid accumulation, ceramide

overload, and arachidonic acid metabolic disturbance. Lipotoxicity, insulin resistance, and disruption of insulin sensitivity all contribute to NAFLD (Pei *et al.*, 2020) and are associated with T2DM and cardiovascular disease (CVD). The presence of T2DM leads to a more severe form of NAFLD such as non-alcoholic steatohepatitis (NASH), cirrhosis, and hepatocellular carcinoma. Additionally, NAFLD contributes to the increased incidence of T2DM (Xia *et al.*, 2019) through increased glucose production and hepatic insulin resistance. The relationship between the development of T2DM and the progression of NAFLD increases hepatic and diabetic mortality worldwide. Figure 3 clearly shows the link between T2DM, oxidative stress and the development of NASH, cirrhosis, and hepatocellular carcinoma.

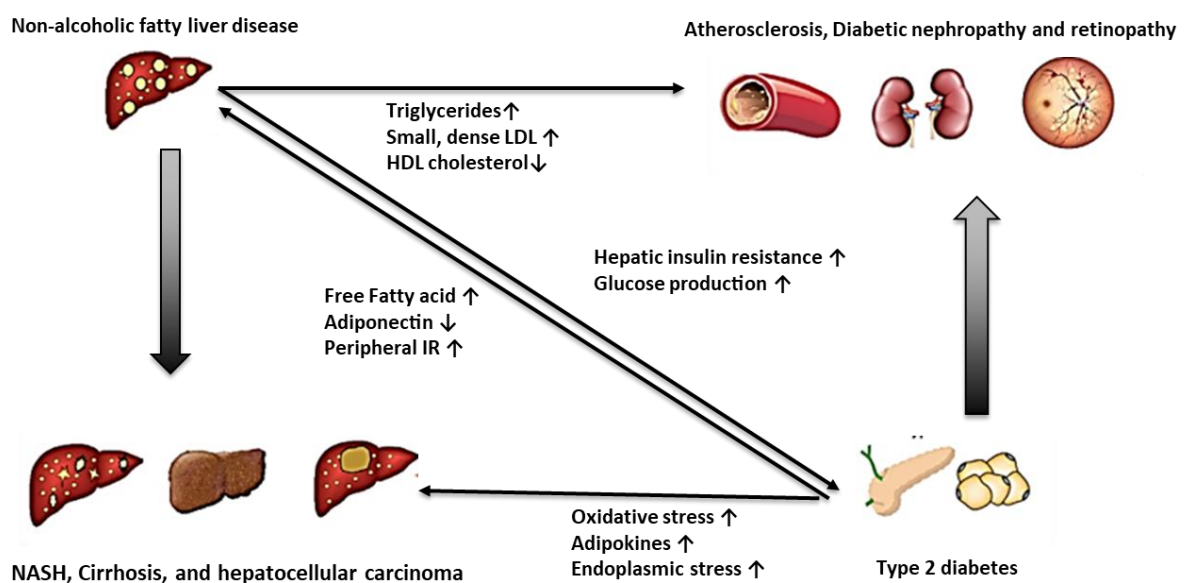


Figure 3. Relationship between type 2 diabetes and non-alcoholic fatty liver disease (Xia *et al.*, 2019). NAFLD participates in the development of diabetes through glucose production and insulin resistance leading to complications such as nephropathy and retinopathy. In addition, diabetes aggravates NAFLD, resulting in more severe complications such as NASH, cirrhosis, and hepatocellular carcinoma.

1.5. Carbohydrate digestion

Carbohydrates are the most abundant class of biological molecules, and are an essential component of all living organisms and a significant dietary component (Voet and Voet, 2011). Monosaccharides are the basic units of carbohydrates such as starch in plants and glycogen in humans (Campbell *et al.*, 2018). Monosaccharides (such as glucose, fructose, galactose) bind together through glycosidic linkage to form carbohydrates.

There are different sources of carbohydrates in the food, such as starchy vegetables, dried beans, rice, milk, and grains. The American Diabetes Association has classified the top three known sources of carbohydrates in diets as starch, sugar, and fibre.

Specific enzymes hydrolyse dietary complex carbohydrates into monosaccharide monomers before entry into the appropriate cells for energy or storage (Adefegha *et al.*, 2010). The two primary enzymes responsible for the hydrolysis of carbohydrates in the digestive tract (Bhandari *et al.*, 2008). These enzymes are α -amylase and α -glucosidase found in the intestinal lumen and brush-border of the intestinal mucosa, respectively and they work in conjunction (Martin and Montgomery, 1996). Figures 4 and 5 below show the 3D structures of the both α -amylase and α -glucosidase and their mechanisms of action in the hydrolysis of carbohydrates.

α -Amylase (α -1,4-glucan-4-glucanohydrolase, EC 3.2.1.1) is found in saliva and pancreatic juice. It is responsible for the hydrolysis of α -1,4 glycosidic linkage of complex carbohydrates from the diet to generate oligosaccharides and disaccharides (Adefegha and Oboh, 2012) (Kato *et al.*, 2017). Saliva amylase starts the hydrolysis of dietary carbohydrates, and pancreatic amylase continues the digestion in the small intestine (Smith and Morton, 2001).

α -Glucosidase (intestinal maltase-glucoamylase, EC 3.2.1.20) is a glycosylase found in the brush border of small intestine (Zhang *et al.*, 2015). It hydrolyses the α -1,4 glycosidic linkage of oligosaccharides and disaccharides. α -Amylase hydrolyses complex carbohydrates into oligosaccharides and disaccharides, which are then hydrolysed into monosaccharides by α -glucosidase (Ozougwu and Akuba, 2018).

Pharmacologically both enzymes are important targets, as enzyme inhibition will delay glucose absorption and consequently reduce the development of hyperglycaemia after a meal in T2DM patients. In addition, in individuals with prediabetes, inhibition of these enzymes may delay or prevent the onset of disease. One of the known inhibitors of these enzymes is acarbose, this drug is an oligosaccharide analogue that reduces postprandial blood glucose by competitively inhibiting both α -amylase and α -glucosidase, the inhibitory action of the inhibitor leads to the prevention of the metabolism and absorption of dietary carbohydrates (Clissold and Edwards, 1988).

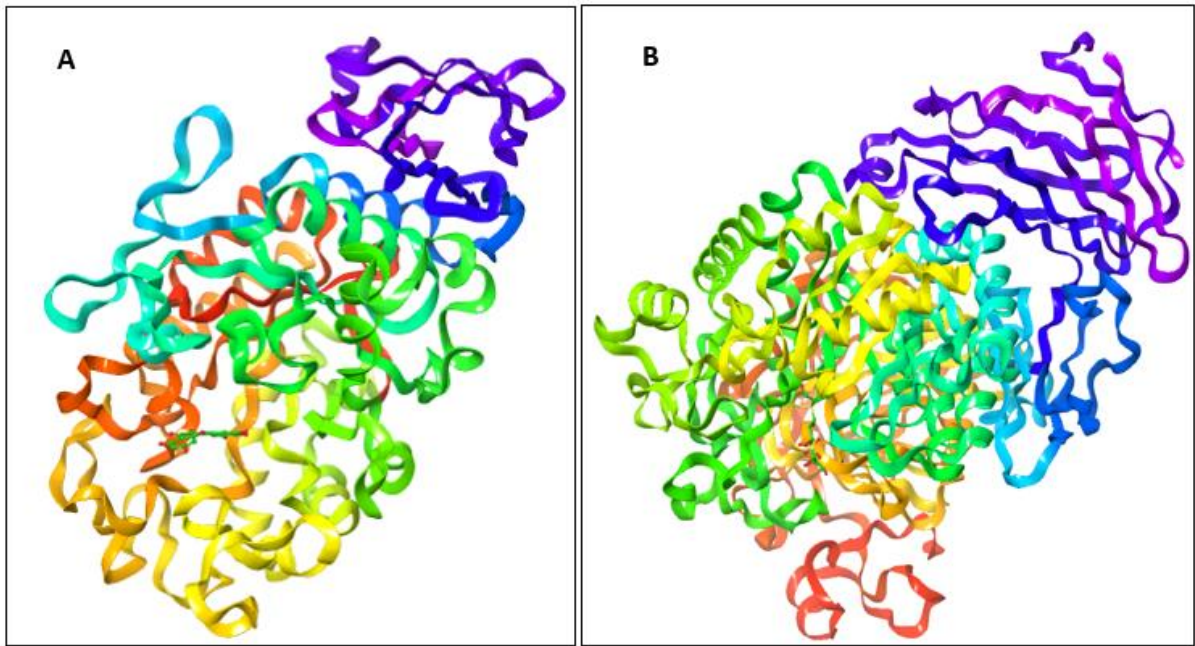


Figure 4. Three-dimensional structures of α -amylase (A) with PDB ID 4GQR and α -glucosidase (B) with PDB ID 3L4Y. The structures were compiled using Maestro 12.9 from Schrödinger and accessed from RCSB protein data bank.

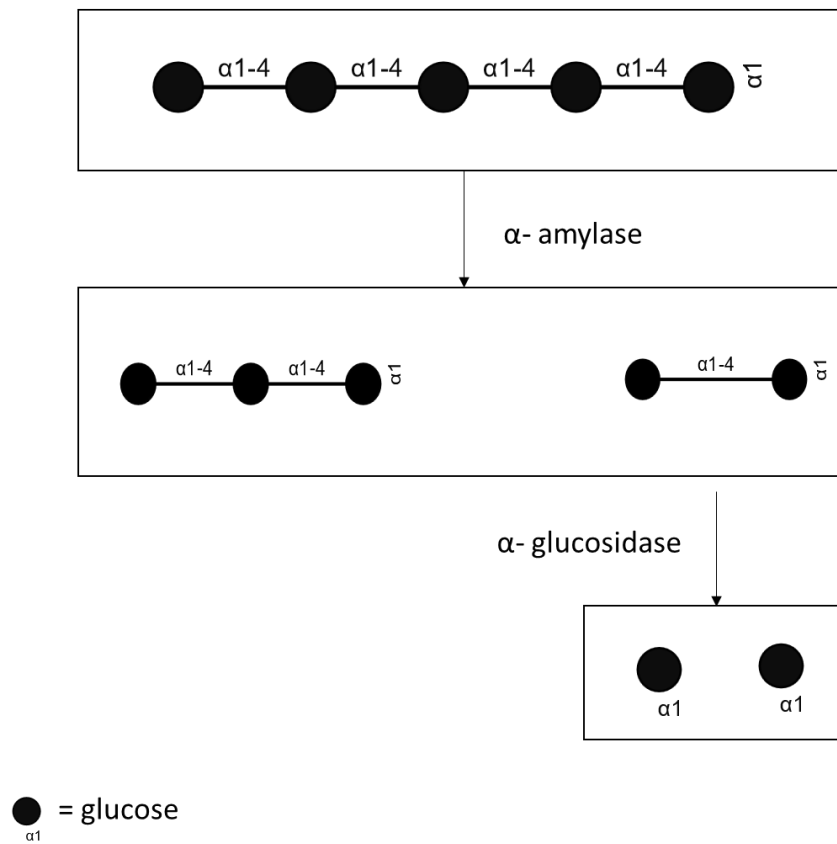


Figure 5. Mechanism of α -amylase and α -glucosidase on carbohydrates to yield glucose.

1.5.1. Insulin mediated glucose uptake in tissue

Insulin is an endocrine hormone secreted by pancreatic beta cells and released into the bloodstream in response to high blood glucose levels (Voet and Voet, 2011). Its primary function is to stimulate glucose uptake and storage in muscle, liver, and adipose cells (Voet and Voet, 2011). It is also involved in lipid metabolism.

Pancreatic beta cells release insulin into the bloodstream, and insulin binds to and activates insulin receptor, a heterotetrameric $\alpha_2\beta_2$ complex found on the surface of the cells that need insulin (Pessin and Saltiel, 2000). The binding of insulin to the receptor activates phosphatidylinositol-3-kinase (PI3k) and leads to multiple events, such as phosphorylation events, protein-protein interactions, and the production of secondary messengers (Meerza *et al.*, 2013). Some of the secondary messengers bind to phosphoinositide-dependent kinase 1 (PDK1). One of the known substrates of PDK is the protein kinase B (PKB), which plays an essential role by linking insulin-stimulated glucose transporter (GLUT4) to the insulin signalling pathway (Saini, 2010). Once GLUT-4 is activated, it moves to the cell's surface and transports glucose from the bloodstream into the cell, as shown in Figure 6. Therefore, in muscle and adipose cells, transportation of blood glucose into the cell depends on the translocation of insulin-stimulated GLUT-4 on the cell surface (Pessin and Saltiel, 2000).

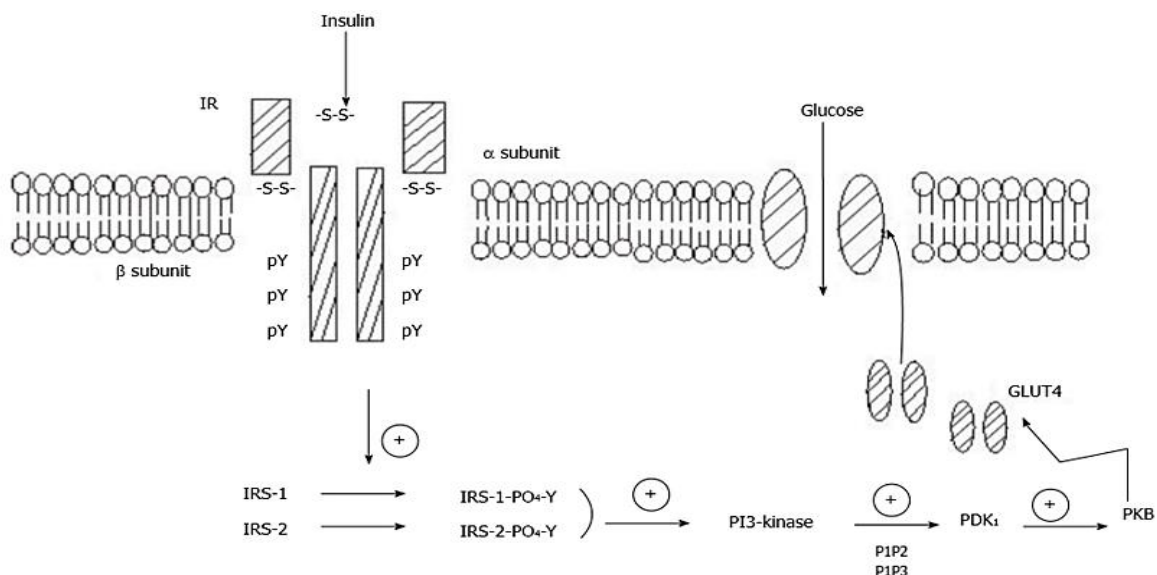


Figure 6. Insulin signalling pathway showing insulin binding to the insulin receptor leading to the activation of glucose transporter 4. pY: phosphorylated tyrosine; IR: insulin receptor; IRS: insulin receptor substrate; PIP2: phosphatidylinositol-3,4-bisphosphate; PIP3: phosphatidylinositol3,4,5-trisphosphate. Adapted from (Saini, 2010)

When body tissues have reduced sensitivity to the action of insulin, it leads to insulin resistance which is an inadequate biological response to insulin, independent of whether insulin is administered exogenously or endogenously (Goldstein, 2002) (Meerza *et al.*, 2013). For patients with insulin resistance, normal insulin concentrations could not complete the insulin signalling pathway shown in Figure 6, preventing the translocation of GLUT-4 on the cell surface.

The liver plays an important role in glucose metabolism, it reduces changes in glycemia by storing glucose as glycogen in the feeding state during modest hyperglycemia or by releasing glucose during the fasted state (Moore *et al.*, 2012) (Hwang *et al.*, 1995). In normal individuals, the liver helps to dispose of dietary carbohydrates and limits postprandial hyperglycemia through hepatic glucose uptake and production. This process depends on many factors, including the concentration of glucose in circulation, insulin, and neural mediators such as norepinephrine (Moore *et al.*, 2012). As the liver is important in the storage and production of glucose when necessary, alteration of these processes may contribute to postprandial hyperglycemia in diabetes patients (Hwang *et al.*, 1995).

Insulin resistance reduces the ability of insulin to complete the signalling pathway in Figure 6, hence affecting the process of storage of glucose by the liver. Studies have shown that lipid accumulation in non-adipocyte tissues such as muscle and liver might be a responsible for the development of insulin resistance leading to T2DM (Hana *et al.*, 2020). A strong relationship has been observed between lipid accumulation and insulin resistance where lipids compete with glucose for substrate oxidation in tissue, and increased plasma fatty acid concentrations are linked with insulin resistance, obesity and T2DM (Hana *et al.*, 2020, Shulman, 2000, Griffin *et al.*, 1999, Reaven *et al.*, 1988).

1.6. Treatment of diabetes mellitus

Diabetes mellitus is a growing problem worldwide; patients are treated with oral and subcutaneous medications. Antidiabetic drugs aim to maintain the concentration of blood glucose close to normal ranging between 3.5 and 5.5 mmol/L, to delay complications linked to diabetes and to prevent the symptoms of hyperglycemia (Güemes *et al.*, 2016). However, choosing a specific treatment depends on the physiological effects, side effects, and cost (Turner *et al.*, 2016). Common drugs used for the treatment of T2DM have several targets (Figure 7).

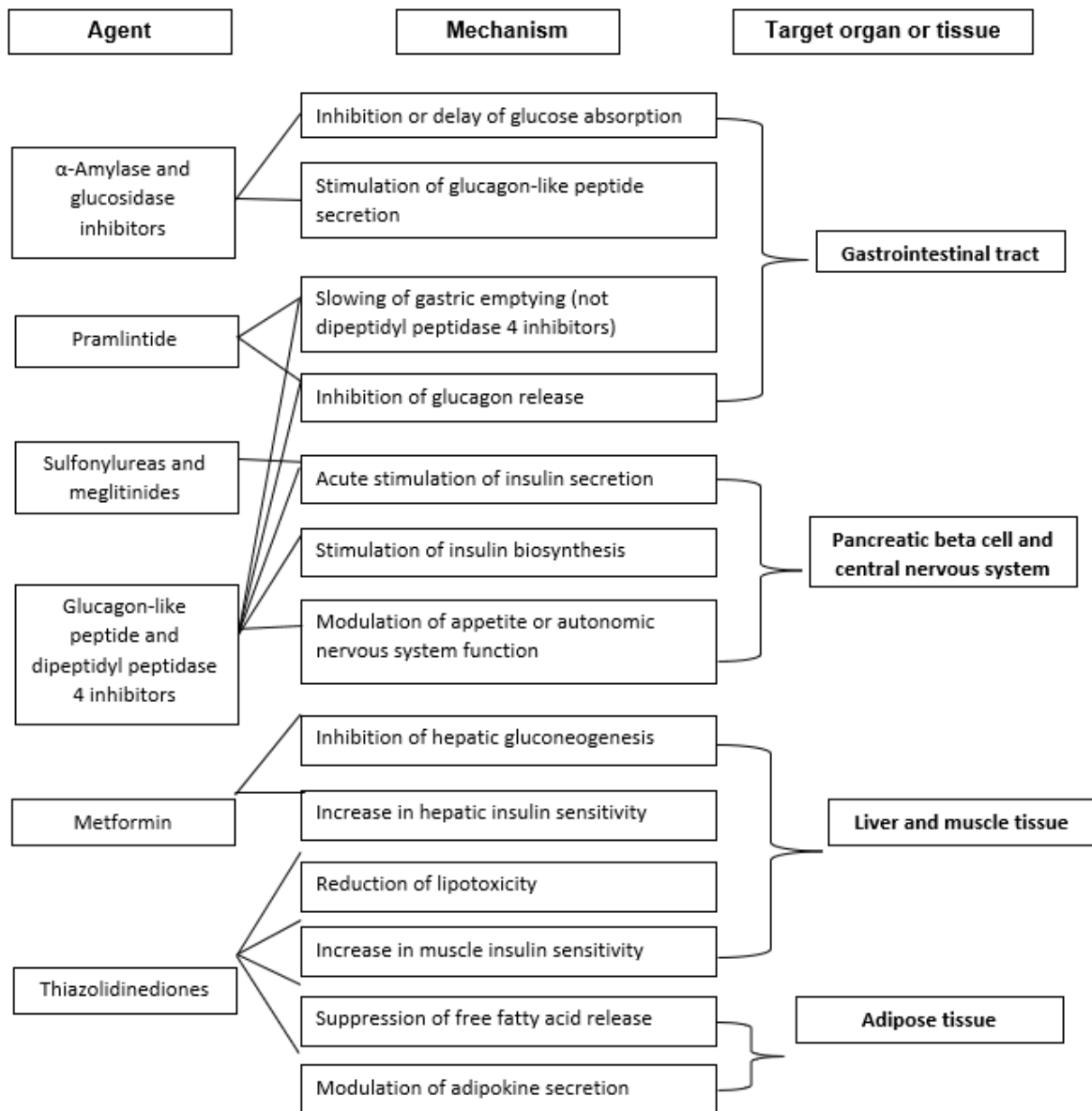


Figure 7. Mechanism of action of glucose-lowering drugs in humans and their respective target organs or tissues (Heine *et al.*, 2006)

Some drugs minimize glucose absorption by inhibiting carbohydrate hydrolysing enzymes, such as α -glucosidase and α -amylase. These inhibitors are acarbose, phaseolamine, miglitol, and voglibose (Kahn *et al.*, 2014, Jayaraj *et al.*, 2013). Meglitinide, sulfonylurea, and sulfonylurea derivatives treat insulin deficiency by increasing insulin secretion from pancreatic beta cells (Turner *et al.*, 2016). Other drugs, such as thiazolidinedione antidiabetics (pioglitazone and rosiglitazone) improve insulin sensitivity by increasing glucose utilization in skeletal muscles and adipose tissue (Kahn *et al.*, 2014, Turner *et al.*, 2016). Many of these drugs have more than one target; for example, acarbose is an α -glucosidase inhibitor and

stimulates the secretion of glucagon-like peptide, while metformin inhibits hepatic gluconeogenesis, increases hepatic insulin sensitivity, and reduces lipotoxicity (DeLeon *et al.*, 2002, Foretz *et al.*, 2010).

The drugs listed in Figure 7 are orally administered, but some patients also require exogenous insulin. Examples of exogenous insulin treatments are rapid, short, intermediate, and long-acting insulin (Kahn *et al.*, 2014). Insulin is injected using insulin syringes, insulin pens, and insulin pumps (Polonsky, 2012). In addition, the use of glucose monitoring devices is necessary to prevent hypoglycemia and these devices are used in combination with insulin injections.

Although all these drugs are currently in use and commercially available, searching for new potential treatments is still essential due to cost, drug interactions and side effects, such as headache, abdominal pain, vomiting, fatigue, dizziness, flatulence and diarrhea (Turner *et al.*, 2016, Proença *et al.*, 2019).

1.7. *Nutritional and medicinal values of plants*

There are two significant sources of food: animal and plant-based food, with most of the food coming from plants. Examples of plant-based food in our everyday diet include fruits, leaves, roots, seeds, and crops. Plant-based foods are important sources of carbohydrate, vitamins, and minerals.

The importance of plants is not limited to their nutritional benefits, but often also have medicinal advantages. Remembering Hippocrates (460 – 370 BC) with his statement: “Let food be your medicine and medicine your food” (Witkamp and van Norren, 2018). In search of medicinal drugs to treat diseases, humans search for possible solutions in nature (Petrovska, 2012). Many people in various countries rely on traditional medicine by using plants/herbs to treat several diseases (Emeka *et al.*, 2018). In addition, the use of plant-based food is associated with a reduced risk of several diseases, including diabetes, cancer, CVD and hypertension (Adelakun *et al.*, 2018, Adams and Standridge, 2006).

Plants are sources of bioactive compounds and secondary metabolites that have shown significant benefits in medicine. The different compounds found in plants are alkaloids, phenolics, flavonoids, tannins and steroids, which have been shown to have some therapeutic

effects against a variety of diseases (Murevanhema *et al.*, 2018) and several have served as lead compounds for drug development.

Some medicinal plants/herbs have been investigated for their ability to help in the management of T2DM and have shown anti-diabetic properties by enzyme inhibition, minimizing insulin resistance, or increasing insulin sensitivity (Pereira *et al.*, 2019, Christensen *et al.*, 2009, Khacheba *et al.*, 2014).

Table 2. Examples of herbs and spices and their origin in plants (El-Sayed and Youssef, 2019).

Part of Plants	Herbs and Spices
Leaves	Basil, Oregano, Bay leaf, Thyme, Mint, Sage, Curry leaf, Tarragon, Marjoram
Bark	Cinnamon, Cassia
Fruits, berries	Clove, Chilli, Black pepper, Allspice,
Bulbs	Onion, Garlic, Leek
Root	Ginger, Turmeric
Seed	Ajowan, Aniseed, Caraway, Coriander, Dill, Fennel, Celery, Fenugreek, Mustard

As shown in Table 2, herbs and spices are derived from different parts of plants, and are used in our diet to add flavour and to enhance the taste of foods (El-Sayed and Youssef, 2019). Herbs and spices are commercially available and have been reported to have therapeutic properties such as antimicrobial, antihypertension, anti-inflammatory, and antidiabetic effects (Srinivasan, 2005, Naimi *et al.*, 2017, Pereira *et al.*, 2019). Several studies have shown that phenolic and flavonoid compounds commonly found in medicinal plants might be responsible for the antidiabetic effects and unlike some commercially available drugs, may cause fewer side effects (Adelakun *et al.*, 2018, Naimi *et al.*, 2017, Xu, 2010). Table 3 lists some common compounds found in some herbs and spices and a short description of each is provided.

Table 3. Common compounds and antidiabetic effects thereof in some herbs and spices

Compounds	Description	Reference
Catechins	Green tea (<i>Camelia sinensis</i>) is a widely consumed beverage in the world and the identified health benefits are increasing and related to a large number of catechins with the major component being epigallocatechin (EGCG). Potent inhibition of α -glucosidase by EGCG and ECG identifies both as potential antidiabetic compounds.	(Higdon and Frei, 2003) (Moore <i>et al.</i> , 2009) (Yang <i>et al.</i> , 2019) (Li <i>et al.</i> , 2010) (Musial <i>et al.</i> , 2020)
Curcumin	The polyphenol, curcumin is found in turmeric (<i>Curcuma longa</i>) and curry powder (<i>Murraya koenigii</i>). In addition to its culinary use, it is also used in medicine and cosmetics. Inhibition of cellular signalling pathways and regulation of gene transcription contributes to the anti-cancer and anti-inflammatory properties.	(Goel <i>et al.</i> , 2008) (Sharma <i>et al.</i> , 2005)
18α-Glycyrrhetic acid	Glycyrrhetic acid, a pentacyclic triterpenoid is a bioactive metabolite of <i>Glycyrrhiza glabra</i> ; isolated from the roots also known as liquorice. The medicinal properties of extracts are anti-inflammatory, anti-bacterial, anti-viral, and promotes healing of ulcers wounds.	(Zígolo <i>et al.</i> , 2018) (Esmaili <i>et al.</i> , 2010)
Quercetin	Quercetin, a flavonoid is abundantly present in almost all herbs and spices and vegetables and fruits, including food products and cosmetics. It can transform into many derivatives, with anti-inflammatory, antioxidant, antibacterial, and anticarcinogenic properties. Antidiabetic effects are related to the inhibition of carbohydrate hydrolysing enzymes, often used as a positive control for α -glucosidase inhibition.	(Lesjak <i>et al.</i> , 2018) (Andres <i>et al.</i> , 2018) (Lee <i>et al.</i> , 2019)
Rosmarinic acid	Rosmarinic acid, a phenolic acid found in herbs and spices is the most abundant in peppermint (<i>Mentha piperita</i>) and rosemary (<i>Salvia rosmarinus</i>). The multitude of health benefits include anti-inflammatory, anti-mutagen, anti-bacterial, anti-viral, and there are claims that it has anti-diabetic properties.	(Petersen and Simmonds, 2003) (Petersen, 2013) (Ngo <i>et al.</i> , 2018)

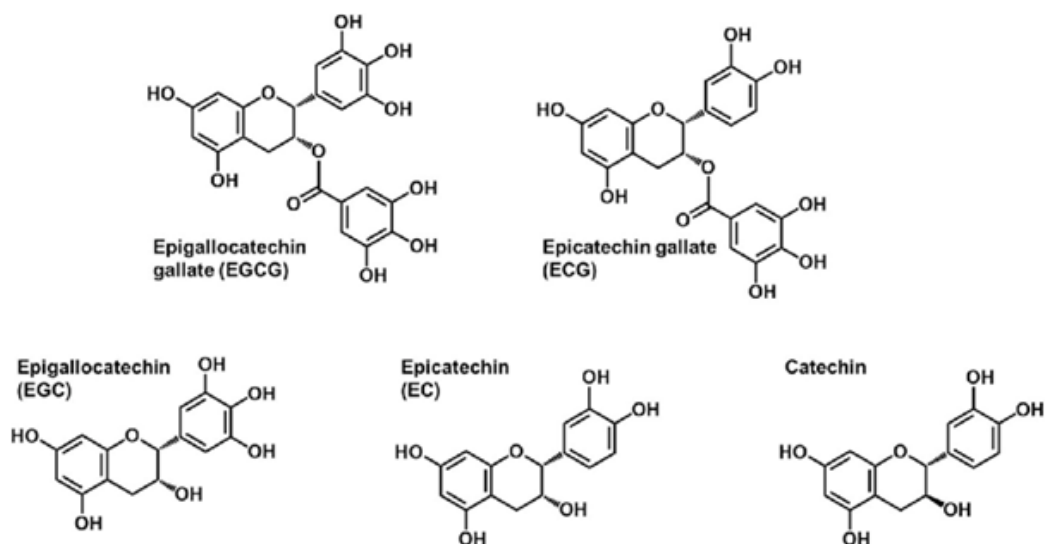


Figure 8. The structure of the catechins found in green tea. All are derivatives of the main structure of catechin with some additional functional groups (Musial et al., 2020)

1.8. Strategies for identifying new antidiabetic plant derived molecules.

Traditional methods for identifying plants with antidiabetic activity involve preparing a plant extract and then screening the extract for activity. This is followed by methodologies such as chromatography and mass spectrometry to isolate and characterise the compounds present, followed by the testing of each compound for activity using *in vitro* and *in vivo* methodologies. This hit and miss approach can be time consuming and expensive.

The development of virtual screening or *in silico* analysis and subsequent *in vitro* investigation in a defined biological system followed by *in vivo* studies effectively reduces time and costs. The strategies used are presented in Table 4 and related to identifying antidiabetic targets will be described in greater detail.

Table 4. Strategies to identify new antidiabetic compounds

Disease targets			
<i>In silico</i>	Defined biological systems	<i>In vitro</i> cellular models	<i>In vivo</i> animal models
Virtual screening of diabetic targets including enzymes and receptors	Confirmation of virtual screening results using identified targets such as enzymes or receptors.	In complex cellular systems measure the consequence of inhibition.	Testing in an <i>in vivo</i> diabetic animal model
Toxicity			
Virtual screening of ADME properties	-----	Measure the effects on cell functioning.	Measure blood levels of the compound and cellular and tissue markers of toxicity.

1.9. Virtual screening

Virtual screening is also called *in silico* analysis and involves using software to screen, evaluate, predict, and analyse compounds or data prior to *in vitro* and *in vivo* analysis (Ekins *et al.*, 2007). It includes several databases, structural relationships, similarity in searching, machine learning, and pharmacophores. This technique is now widely used in drug discovery because it provides an inexpensive and rapid alternative for initial new drug discovery. There are two approaches through which virtual screening assists in drug discovery (Hamza *et al.*, 2012).

The first approach is ligand-based design, and it uses the similarity between the ligand and known drugs to predict the activity of the ligand. The second approach is structure-based drug design, which is also known as ligand docking and uses the structure of the protein and the ligand to predict the binding affinities and modes of ligand binding to the protein of interest (Hamza *et al.*, 2012).

1.9.1. Chemical structure

Many formats are used to enable the computers to recognize the chemical structure of compounds. The most widely known formats are MOL, SDF, and Simplified Molecular Input Line Entry System (SMILES). The chemical structure can be obtained in any of the above formats in chemical databases such as PubChem (www.pubchem.ncbi.nlm.nih.gov/), ChemSpider (www.chemspider.com/), or eMolecules (www.emolecules.com/).

The MOL format represents compounds in a graph connection table. SDF is a version of MOL used for multiple compounds, and SMILES provides a linear notation to represent chemical compounds using fixed alphabet terms and other characters (Hirohara *et al.*, 2018, O'Boyle, 2012).

SMILES is currently widely used as a standard representation of chemical compounds. It is composed of a set of atomic symbols using the alphabet and a set of SMILES original symbols such as “=” and “#” for double bonds and triple bonds, respectively (Hirohara *et al.*, 2018). SMILES can provide both the chirality and stereochemistry of compounds; it is also easy to read, learn and write, making it the best format to use (O'Boyle, 2012). The structure of a protein can be obtained from the Protein Data Bank (PDB) using an identifier code called PDB

ID; such as for pancreatic α -amylase (PDB ID: 4GQR) and intestinal α -glucosidase (PDB ID: 3L4Y) (Berman *et al.*, 2000).

1.9.2. Ligand docking - scoring function

There are many tools available for ligand dockings, such as AutoDock vina and Glide, however, they differ in the scoring functions used. The scoring function evaluates docking by measuring the ability to generate and recognize different poses of the ligand when interacting with the protein of interest (Jain, 2006).

AutoDock uses the empirical scoring functions, where a database is composed of reliable binding geometry and known binding affinity of ligand-protein complexes (Eldridge *et al.*, 1997). Glide uses the empirical Chemscore function, and analyses every position of the ligand in the active site of the target protein, it generates grids to represent each pose of the ligand (Friesner *et al.*, 2004). In this project, Maestro, a Schrodinger software that uses Glide for ligand docking was used. The different poses of the ligand generated in Glide undergo a series of filters to evaluate their interaction with the target protein. The filter tests are performed in the following order: special fit of the ligand to the active site; examination of the ligand-protein interactions using a grid-based method; evaluation and minimization of the grid approximation to the unbound ligand-protein interactions; scoring energy minimized poses; and finally ranking the poses by using glide score (Eldridge *et al.*, 1997).

Glide score is relative to the difference in Gibbs free energy (ΔG) between the free protein and ligand-protein complex. A more negative ΔG indicates stability and a favourable reaction. Therefore, a good ligand should have a more negative score to indicate good binding affinity. ΔG is the combination of interactions such hydrogen bonds, lipophilicity, van der Waals interactions, polar interactions in the active site, metal-ligation interactions, and rotatable bonds among the protein, ligand, and solvent (Jain, 2006).

There are three forms of Glide: High-Throughput Virtual Screening (HTVS), Standard-Precision (SP), and Extra-Precision (XP). Glide HTVS reduces the number of intermediate conformations and the thoroughness of the refinement and sampling; glide SP is softer and adept at identifying ligands with a propensity to bind the active site; and glide XP performs extensive sampling and is efficient in removing false negatives (Friesner *et al.*, 2004).

1.9.3. ADMET properties

It is essential to predict the absorption, distribution, metabolism, excretion, and toxicity (ADMET) properties of promising compounds because, despite the remarkable efficiency of compounds as therapeutic agents during *in vitro* studies, many of the identified compounds have failed to reach the market due to their side effects and poor ADMET profiles (Kola and Landis, 2004). Therefore, an early prediction of ADMET properties is necessary to reduce expenses, increase the rate of drug discovery, and minimize the failure rate in clinical trials.

There are tools available that provide methods to determine the physicochemical properties and predict the pharmacokinetics and toxicity properties of compounds. For example, software such as Schrodinger provides tools that can be used to predict the properties of compounds using QikProp, and it relies on several databases based on the structural similarity to known drugs (Ioakimidis *et al.*, 2008).

Some online free tools, such as pkCSM (<http://biosig.unimelb.edu.au/pkcsm/>) are available, and it uses a series of databases and machine learning based on learning patterns to build predictive models (Pires *et al.*, 2015).

These tools calculate the rule of five for oral drugs described by Lipinski for physicochemical properties, including molecular weight, lipophilicity, hydrogen bond donors, and hydrogen bond acceptor (Lipinski, 2004). Table 5 describes some of the pharmacokinetic and toxicity properties that these tools can predict.

Table 5. Examples of ADMET properties predicted by different tools (Schrodinger, 2012)

Properties	Description
Water solubility	Solubility of the compound in water.
Intestinal absorption	Proportion of compound to be absorbed through the human small intestine.
P-glycoprotein inhibitors	If the compound is likely to inhibit P-glycoprotein.
HERG inhibitors	Principal causes for acquiring long QT syndrome – compound likely to inhibit HERG K ⁺ channels.
Hepatotoxicity	If the compound is likely to disrupt the normal function of the liver.
#Stars	The number of property values that fall outside the 95% range of similar values for known drugs.

1.10. Kinetic studies

The findings of virtual screening need to be confirmed using defined biological systems, and for enzyme targets, it is essential to investigate the kinetics of inhibition.

Enzyme assays are performed to determine enzyme activity; to study temperature and pH effects; and to determine constants such as inhibitory constant (K_i), the Michaelis constant (K_m), maximum velocity (V_{max}) (Wilson and Walker, 2010), and the inhibitory concentration where the response of the enzyme is halved (IC_{50}).

From the measured absorbance, the Beer-Lambert law is used to determine the concentration of the product and the associated enzyme activity. The data are used to plot both the Michaelis-Menten and Lineweaver-Burk plot.

$$\text{Enzyme activity} = \frac{\text{Concentration}}{\text{Time}}$$

$$\epsilon \times c \times d = A \quad \text{Beer-Lambert law}$$

A = Absorbance of the sample

c = Concentration (M)

ϵ = Molar absorption coefficient or molar extinction coefficient ($M^{-1} \text{ cm}^{-1}$)

d = Path length (cm)

After obtaining the enzyme activity using the Beer-Lambert equation, subsequent kinetic studies help to elucidate the enzyme mechanism by determining the constants, which are critical in analysing the effect of inhibitors.

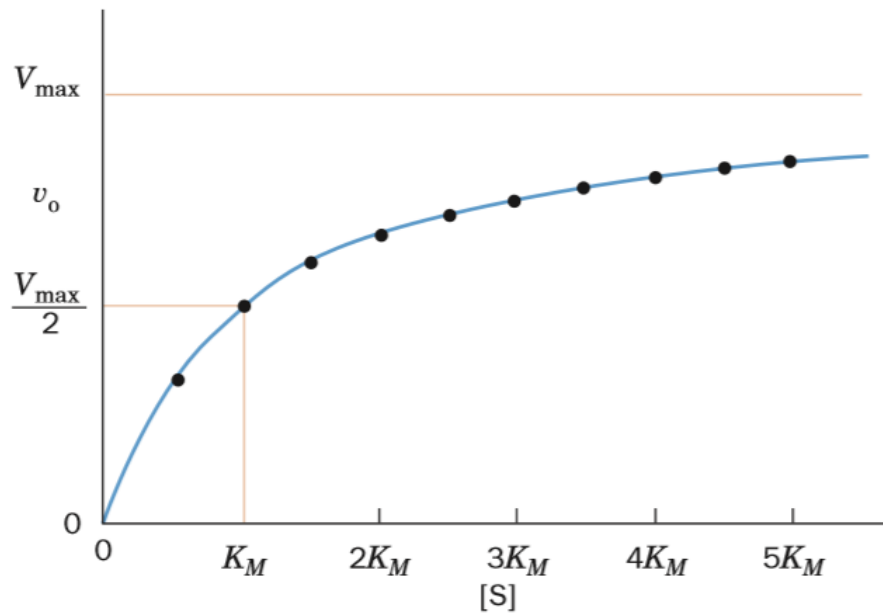


Figure 9. Michaelis-Menten plot of velocity against substrate concentrations shows the K_m and V_{max} and yields the Michaelis-Menten equation. (Voet and Voet, 2011)

$$V = \frac{V_{max} [S]}{K_m + [S]}$$

V = Initial rate or activity

V_{max} = maximum velocity

$[S]$ = Substrate concentration

K_m = Michaelis constant

Using the Michaelis-Menten curve, it is challenging to measure V at high $[S]$. Therefore, a linear transformation of the Michaelis-Menten curve called the Lineweaver-Burk plot is used to more accurately measure the kinetic constants (Wilson and Walker, 2010). The Lineweaver-Burk plot is also used to determine the type of inhibition during enzyme inhibition by comparing the uninhibited to the inhibited plot. Each of which corresponds to how the inhibitor interacts with the enzyme (see Figure 10).

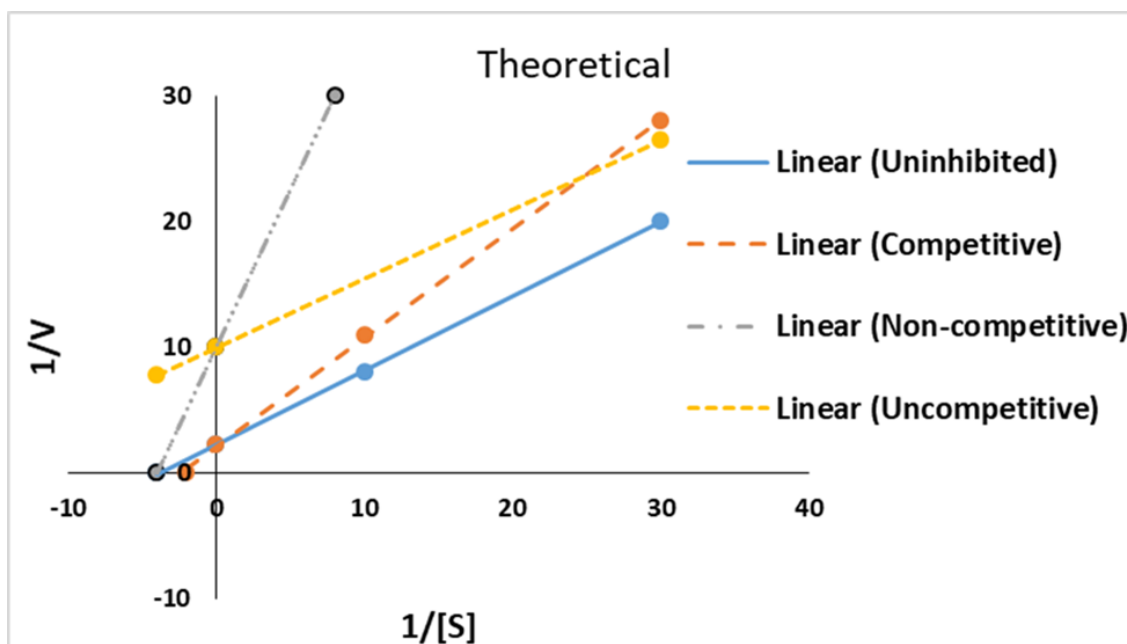


Figure 10. Lineweaver-Burk plot of different types of inhibition. This plot, together with the Lineweaver-Burk plot, is used to determine kinetic constants and types of inhibition.

The straight-line equation obtained from the Lineweaver-Burk plot is used to calculate the constants. Below is the Lineweaver-Burk equation showing the linear transformation of Michaelis-Menten.

$$\frac{1}{V} = \frac{K_m}{V_{max}} \frac{1}{[S]} + \frac{1}{V_{max}}$$

$1/V_{max}$ = y-intercept

K_m/V_{max} = Slope of the straight line

The inhibitory constant K_i is obtained by a secondary plot using data from Lineweaver-Burk plots. The K_i of compounds is calculated by using varying inhibitor concentrations $[I]$ of the inhibitor with a constant substrate concentration to plot the slope or intercept of the Lineweaver-Burk plot as a function of $[I]$.

1.11. *In vitro* and *in vivo* models

The next level of evaluation in the confirmation of activity observed in biological systems is the use of *in vitro* cellular models. This usually involves the use of cell lines that are representative of the affected tissue, and for T2DM this includes the use of liver, pancreatic, muscle cell lines. Initial evaluation is the determination of cytotoxicity in a cellular environment. This is followed by specific *in vitro* cell models that mimic aspects of disease,

such as insulin resistance and NAFLD, as used in the present study. A limitation of such studies is that aspects of disease are studied in isolation, especially for T2DM which is a disease involving several different tissues, such as the liver, muscle, and pancreas. Animal models such as rats or mice can be used to investigate these aspects, including toxicity and ADMET of candidate compounds. These models have some issues linked to the complexity and differences of species, the expression level, and functional activity should be considered (Tang and Prueksaritanont, 2010).

In vivo animal models involved in the study of T2DM include rats and rabbits that mimic T2DM in humans (Chatzigeorgiou *et al.*, 2009), and rodents are preferred because of their small size and availability. *In vivo studies* include the chemical induction of DM prior to treatment with the studied drugs/chemicals (Dewangan *et al.*, 2017). The study is dependent on the dose administered and the route of administration.

Finally, after evaluating *in vitro* and *in vivo* cytotoxicity and cellular models, the evaluation of identified compounds in clinical trials involving patients with T2DM is the final level of testing.

1.12. Aims

This study aimed to:

- To assess the *in silico* and *in vitro* antidiabetic activities of compounds commonly found in commercially available herbs and spices.
- To investigate the effects of herbal compounds on cellular glucose uptake and hepatic lipid accumulation.
- To assess the *in vitro* antidiabetic activities of five green tea brands and analyse the differences related to the levels of EGCG, ECG and quinic acid.

1.13. Null hypothesis

The null hypotheses were:

- Null hypothesis 1: There is no significant difference in the K_i values between promising compounds and acarbose at the 95% confidence level.
- Null hypothesis 2: There is no significant difference in the glucose uptake activity between promising compounds and insulin at the 95% confidence level.
- Null hypothesis 3: There is no significant difference in oleic acid (OA) induced lipid accumulation between promising compounds and metformin at the 95% confidence level.

1.14. Objectives

The objectives of this study were:

- To determine docking scores for α -amylase and α -glucosidase and the ADMET properties of these compounds using docking simulations.
- To select compounds with docking scores and properties relative to the known enzyme inhibitor, acarbose.
- To determine the biological inhibitory effect of promising compounds against α -amylase and α -glucosidase using DNSA and pNPG assays, respectively.
- Kinetic studies to determine K_i , IC_{50} , and types of inhibition of the promising compounds.
- To determine IC_{50} of the promising compounds in the Caco-2, HepG2 and C2C12 cell lines using the SRB assay.
- To determine the effect of promising compounds on glucose uptake in selected cells with the 2-NBDG assay.

- To determine the effect of promising compounds on OA induced hepatic lipid accumulation using Oil Red O (ORO) staining.
- To identify herbs and spices with high concentrations of the promising compounds.
- In the second part of this study, we quantified the concentrations of EGCG, epicatechin gallate, and quinic acid in the five green tea brands (*Camellia sinensis*) using UHPLC-MS.
- To determine the inhibitory effect of the green tea brands against α -amylase and α -glucosidase using the DNSA and pNPG assays, respectively.
- To perform metabolomics on the five green tea brands using metaboAnalyst.

Materials and methods

1.15. Materials

- Chemicals

Sodium phosphate monobasic and dibasic were obtained from Sigma Aldrich (Missouri, USA). Starch from potato and pNPG was used as substrate and were obtained from Sigma Aldrich (Missouri, USA). Acarbose, curcumin, DMSO, 18 α -GA, quercetin, quinic acid, rosmarinic acid, oleic acid (OA), Oil red O (ORO), nerolidol and all UPLC-MS standards were purchased from Sigma Aldrich (Missouri, USA), and 2-NBDG was obtained from ThermoFisher Scientific (Massachusetts, USA). Both α -glucosidase (EC 3.2.1.20) from *Saccharomyces cerevisiae* and porcine pancreatic α -amylase (EC 3.2.1.1) were obtained from Sigma Aldrich (Missouri, USA). Potassium sodium tartrate tetrahydrate, DNSA, maltose monohydrate, p-nitrophenol, Dulbecco's Modified Eagle Medium (DMEM), and SRB were purchased from Sigma Aldrich (Missouri, USA). C2C12 myotubes (American Type Culture Collection [ATCC] CRL-1772) and HepG2 hepatocarcinoma cells (ATCC HB-8065) were obtained from the ATCC. Caco-2 human colon adenocarcinoma cells (CCAC-FL) were obtained from CELLONEX Separation Scientific (Johannesburg, South Africa). Dilmah, Eve's, Five Roses, Livewell, and Tetley green teas were purchased from a local store.

- Instruments

The instrumentation used was a heating block from Scientific (Johannesburg, RSA) and a pH meter from Jenway (Staffordshire, UK) were used to incubate at a specific temperature and to adjust the pH of the buffers and solutions. The SpectraMax paradigm from Molecular Devices (California, USA), Maestro v12-6, canvas from Schrodinger (New-York, USA), and ChemSketch from ACD/Labs (Toronto, Canada) were used to measure the absorbance, perform docking and computer simulations, and to draw chemical structures, respectively (Bhachoo and Beuming, 2017, Spessard, 1998). MetaboAnalyst 5.0 (Ontario, Canada) was used for metabolomics analysis (www.metaboanalyst.ca/). A Waters Synapt G2 Quadrupole time-of-flight mass spectrometer connected to a Waters Acquity ultra-performance liquid chromatography from Waters (Massachusetts, USA) was used for high-resolution UPLC-MS analysis.

1.16. Methods

1.16.1. Selection of compounds

Compounds selected and used in this project went through about three selection processes before being identified. The first was to confirm the antidiabetic properties of 1070 compounds present in 30 commercially available herbs and spices (Pereira *et al.*, 2019). Then, herbs and spices with either or both α -glucosidase and α -amylase inhibitory activities were identified. The most abundant compounds in selected commercially herbs and spices were then evaluated for their affinity to bind both enzymes using docking scores from AutoDock (DIA-DB). The docking scores were then compared to the those obtained from Maestro v12-6 (Schrodinger, 2015).

The scores are compared to a known inhibitor, acarbose, the current gold standard drug for the treatment of T2DM. Compounds with an affinity better than or similar to acarbose were selected for further analysis. A total of four compounds with docking scores more negative or similar to acarbose were selected, and two compounds with docking scores more positive than acarbose were selected as negative controls to compare *in silico* with *in vitro* studies. The compounds selected were curcumin, 18 α -GA, quercetin and rosmarinic acid as promising compounds, with nerolidol and quinic acid as negative controls.

1.16.2. Computer simulation

- Ligand preparation

Chemical structures of the compounds were imported from canvas to Maestro and with SMILES obtained from PubChem. The LigPrep function in Maestro was used to prepare 3D structures from 2D structures, pre-process the structures, and generate multiple poses from each structure (Vijayakumar *et al.*, 2018). This function ensured that the structures were ready for docking.

- Protein preparation

The crystal structures of the enzymes were downloaded to Maestro from the PDB (www.rscb.org) using the respective PDB IDs for pancreatic α -amylase (4GQR) and intestinal α -glucosidase (3L4Y) (Berman *et al.*, 2000).

The protein preparation wizard in Maestro was used to prepare enzymes for molecular docking. All cofactors and water molecules were removed, and the structures were optimized. This wizard resolved structural issues and made the structures suitable for docking (structural-based virtual screening).

- Molecular docking

The grid file and the ligand file are needed to run a docking job. The grid file was generated using the receptor grid generation tool in Maestro, keeping the default parameters. The tool was used to represent the active site of the proteins.

Protein docking was performed using glide HTVS, and the prepared ligands were docked against the generated grid file of intestinal α -glucosidase and pancreatic α -amylase enzyme complex. Maestro was also used to illustrate the binding interactions between the compounds and the active site of the enzymes.

The docking score is relative to the ΔG of the protein-compound interaction; a low, more negative score indicates stability, thus strong binding affinity of the compound to the receptor protein. Interactions in the protein-compound complex contribute to the estimation of ΔG , including hydrophobic interactions and hydrogen bonds (Eldridge *et al.*, 1997, Friesner *et al.*, 2004).

- Physicochemical properties

Selected compounds were further analysed using Schrodinger's canvas program and the online tool pkCSM to obtain pharmacokinetic and toxicity properties. The SMILES notations of the compounds were imported to pkCSM to calculate the physicochemical properties by using a series of databases and machine learning based on patterns to build predictive models (Pires *et al.*, 2015). This is based on pattern recognition and algorithm to link similarities such between known compounds and possible potential drugs.

1.16.3. Preparation of reagents

Stock solutions of the inhibitors were prepared by dissolving the compounds in DMSO to a final concentration of 50 mM. Then, the respective buffers were used to prepare the required concentration for each assay.

Phosphate buffer was prepared and used to dilute the compounds for the α -glucosidase inhibition assay. A 100 mM phosphate buffer was prepared using equal concentrations of sodium phosphate monobasic and sodium phosphate dibasic in deionized distilled water, and the pH was adjusted to 6.9.

A para-nitrophenol solution was prepared by dissolving 0.0139 g para-nitrophenol in 100 mL of deionized distilled water (ddH₂O) to prepare a 1 mM solution used to make a standard curve and determine the molar absorption coefficient. A pNPG solution was prepared by dissolving 0.07531 g pNPG in 5 mL ddH₂O to make a 5 mM solution. Intestinal α -glucosidase from *Saccharomyces cerevisiae* (0.2 U/mL) was prepared in phosphate buffer (100 mM, pH 6.9).

A sodium phosphate buffer containing NaCl was prepared and used to prepare other reagents for the α -amylase inhibition assay. A 20 mM phosphate buffer with 6.7 mM NaCl pH 6.9 was prepared by dissolving 0.7098 g NaH₂PO₄, 0.5999 g Na₂HPO₄ and 0.1957 g NaCl in 500 mL ddH₂O.

A maltose solution was prepared by dissolving 0.02 g maltose monohydrate in 10 mL phosphate buffer (20 mM pH 6.9) to prepare a 5.6 mM solution. The colorimetric reagent was prepared by dissolving 0.4380 g DNSA in 20 mL ddH₂O to make a 96 mM solution and 12 g potassium sodium tartrate tetrahydrate dissolved in 8 mL of a 2 M NaOH to make the colour reagent. A 2% (20 mg/mL) starch solution was prepared by dissolving 0.50 g potato starch powder in 25 mL of phosphate buffer (20 mM pH 6.9) and then the solution was heated with constant stirring to facilitate solubility. Finally, the α -amylase solution was prepared by dissolving 3 mg porcine pancreatic α -amylase (10 U/mg) in 15 mL phosphate buffer (20 mM pH 6.9) to make a final solution of 2 U/mL.

For the cell culture studies all cells were cultured at 37°C under an atmosphere with 5% CO₂, and were maintained in DMEM with 5% FCS, non-essential amino acids, NaHCO₃, 25 mM dextrose and 1% penicillin/streptomycin (DMEM/FCS). All compounds were initially dissolved in DMSO to make a stock concentration of 40 mM. Then, the stock solutions were further diluted with DMEM to the respective concentrations for the SRB assay. For the glucose uptake assay, the compounds were diluted with glucose-free DMEM containing nonessential amino acids, NaHCO₃ and 1% penicillin/streptomycin (Glc-free-DMEM). Finally, for hepatic lipid

accumulation, the compounds were diluted with PBS containing 9.23 g of FTA hemagglutination buffer in 1L ddH₂O at pH 7.2. The ORO stock solution was prepared (0.5% in 60% isopropanol) and dissolved in a 50°C water bath for 15 minutes.

1.16.4. α -Glucosidase inhibition assay

The *in vitro* ability of the promising compounds to inhibit α -glucosidase was assessed using a colorimetric pNPG assay, where pNPG acts as a substrate and the absorbance of the coloured product is measured spectrometrically. Therefore, the enzyme activity is proportional to the colour of the solution, the darker the solution is, the greater the activity. The addition of an inhibitor such as acarbose can minimize the binding of pNPG to the catalytic site of the enzyme and reduce the amount of product generated.

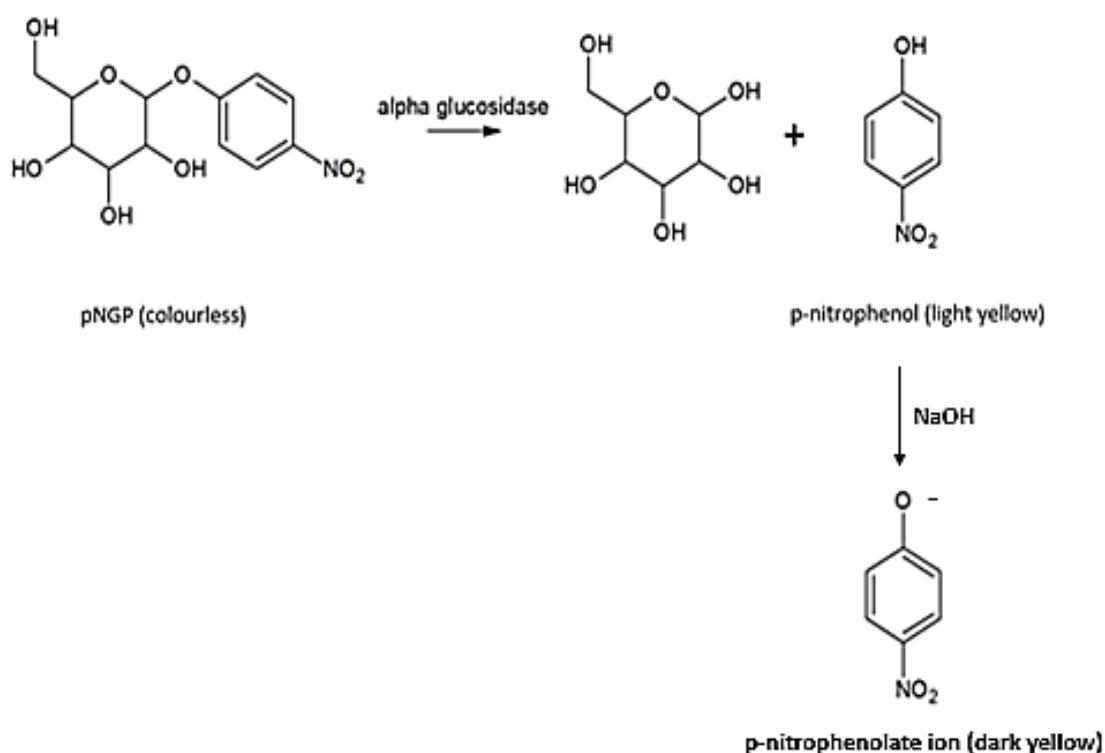


Figure 11. The reaction of the substrate pNPG with α -glucosidase to yield glucose and p-nitrophenol. Glucosidase breaks the α -glucopyranoside linkage of colourless pNPG, releasing a light-yellow p-nitrophenol and D-glucose.

- Kinetics of α -glucosidase inhibition

Working directly in a 96 well microplate, 50 μ L of 0.2 U/mL in phosphate buffer (100 mM, pH 6.9) and 100 μ L of the compound or acarbose (0 to 8 mM) were preincubated at 37°C for

10 min before adding 50 μL of pNPG at different concentrations (0, 0.3, 0.6, 0.8, 1.25, 2.5 and 4 mM) in phosphate buffer (100 mM, pH 6.9). Next, the reaction was incubated at 37°C for 30 min before adding 50 μL of a 1 M NaOH solution. The addition of the base led to the deprotonation of p-nitrophenol, which becomes basic and generates a dark yellow colour that can be read at 405 nm. When the experiment was performed without inhibitor, buffer was added to ensure that all final volumes were the same. The enzyme activity was determined as described in section 1.10. The initial velocity was calculated from the enzyme activity, and Lineweaver-Burk plots were generated by plotting inverse velocity against inverse pNPG concentration at different concentrations of the inhibitor. The straight lines were used to determine the K_i values by generating a secondary plot of the slope of the straight lines against inhibitor concentrations.

- Inhibition of α -glucosidase by tea samples

In a 96 well microplate, 50 μL of 0.2 U/mL the enzyme in phosphate buffer (100 mM, pH 6.9) and 100 μL of varying concentrations of tea 0.00001 - 1% w/v were preincubated at 37°C for 10 min before adding 50 μL of 2 mM pNPG in phosphate buffer (100 mM, pH 6.9). The reaction was incubated at 37°C for 30 min before adding 50 μL of a 1 M NaOH solution. Subsequently, the absorbance was measured at 405 nm. The negative control consisted of the same amount of buffer instead of inhibitor. The *in vitro* inhibitory activity of α -glucosidase by the tea samples was measured by determining the IC_{50} of each tea brand using the formula below to obtain the percentage inhibition.

$$\%inhibition = \frac{(Abs. \textit{negative} - Abs. \textit{sample})}{Abs. \textit{negative}} \times 100\%$$

1.16.5. α -Amylase inhibition assay

This assay screens the action of α -amylase with starch as the substrate. In this assay, the colour reagent, DNSA is reduced to 3-amino-5-nitrosalicylic acid, an orange-red product by reducing the sugar maltose. The presence of the inhibitor reduces the amount of maltose released from starch by preventing the interaction between starch and the catalytic site of the enzyme. Therefore, a decrease in the amount of maltose that reacts with DNSA and subsequently the amount of 3-amino-5-nitrosalicylic acid will be lower, decreasing the amount of measured enzyme activity.

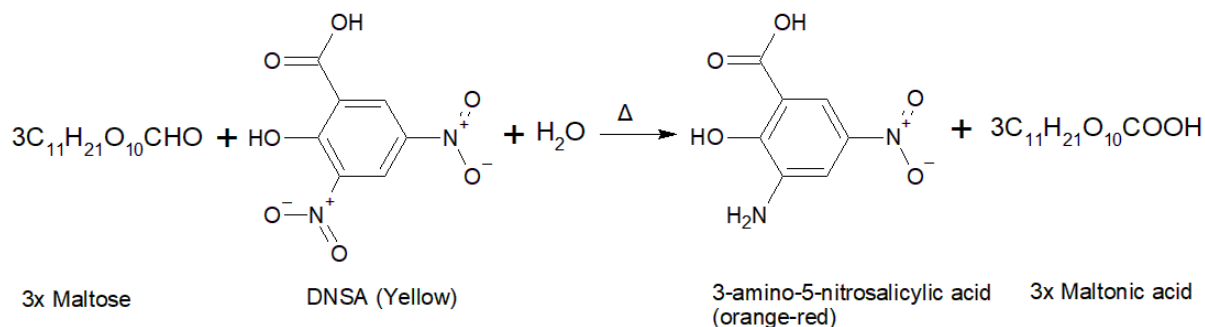


Figure 12. The reaction of the colour reagent DNSA with the reducing sugar maltose produced from the hydrolysis of starch by α -amylase. This reaction results in an orange-red solution.

- Kinetics of α -amylase inhibition

To evaluate the amount of maltose released and to assess the inhibitory activity of the compounds against α -amylase the following procedure was followed. In different Eppendorf tubes, 100 μL of the inhibitor (0 to 1.5 mM) was mixed with 100 μL α -amylase (2 U/mL) and preincubated at approximately 25°C for 10 min before adding 100 μL of starch (0, 2, 4, 5, 6, 8, 9 and 10 mg/mL). After incubation at approximately 25°C for 10 min, 100 μL of DNSA colour reagent was added. After 10 min incubation at 85°C on a heating block, the solution was cooled and diluted with ddH₂O before transferring a 200 μL volume to a 96 well plate and the absorbance was measured at 540 nm.

- Inhibition of α -amylase by tea samples

In different Eppendorf tubes, 100 μL of varying concentrations of the tea sample 0.1 - 10% (w/v) was mixed with 100 μL of 2 U/mL α -amylase in phosphate buffer (20 mM pH 6.8) and was preincubated at approximately 25°C for 10 min. Then 100 μL of a 2% (w/v) potato starch solution was added and the solution was incubated at approximately 25°C for 10 min before adding 100 μL of the 96 mM DNSA colour reagent. After a further 10 min incubation at 85°C on a heating block, the solution was cooled and diluted with distilled ddH₂O before a 200 μL volume was transferred to a 96 well plate, and the absorbance was then measured at 540 nm. The negative control was an equal amount of the solvent instead of the tea sample. The *in vitro* inhibitory activity of α -amylase by the tea samples was measured by determining the IC₅₀ of each tea brand using the formula below to obtain the percentage inhibition.

$$\%inhibition = \frac{(Abs. \textit{negative} - Abs. \textit{sample})}{Abs. \textit{negative}} \times 100\%$$

1.16.6. Cytotoxicity

It is essential to perform cell cytotoxicity and proliferation assays to screen the response of a cell to the promising compounds (Adan *et al.*, 2016). Several assays can be used to determine the *in vitro* cytotoxicity and commonly used assays are the 3-(4,5-dimethylthiazol-2-yl)-2,5-diphenyltetrazolium bromide (MTT), the neutral red uptake assay, and the SRB assay.

In the SRB assay, the cellular protein content (Orellana and Kasinski, 2016) is determined. SRB is a bright-pink dye that has two sulfonic groups on its structure that bind to basic amino residues of cellular proteins (Vichai and Kirtikara, 2006, Adan *et al.*, 2016). It is important to determine cytotoxicity in more than one cell line due to the differences in metabolism and sensitivity. In this study three cell lines, the Caco2 adenocarcinoma, the HepG2 hepatocarcinoma and C2C12 myotube cells were used to represent the site of absorption, metabolism, and insulin target tissue.

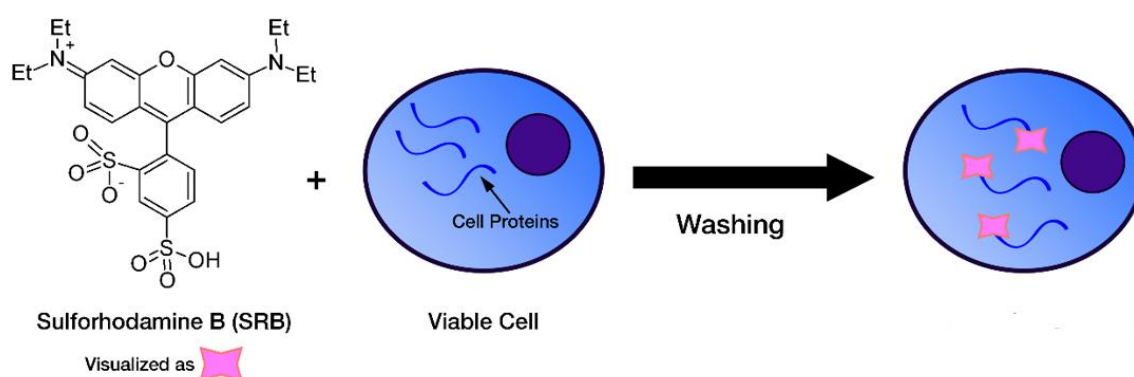


Figure 13. Chemical reaction of SRB with the cell protein content. (www.cephamls.com)

SRB assay was performed by the method used by (Vichai and Kirtikara, 2006), with slight modifications. In a 96 wells plate, a 100 μL cell suspension representing 1×10^5 cells was added to every well and then was incubated overnight at 37°C with 5% CO_2 to allow cell attachment. Different concentrations (0.01, 0.1, 1, 10 and 100 μM) of the compounds in a volume of 100 μL were added, and then the plate was incubated at 37°C with 5% CO_2 for 72 hours. Wells containing only cells and media were used as the negative control. Saponin was used as the positive control, and wells containing only media were used as blanks. After the 72 hours incubation period, the cells were fixed with 50 μL of 50% (w/v) trichloroacetic acid

solution and incubated overnight at 4°C. The plates were then washed with water and dried in an oven overnight before adding 100 µL of 0.057% w/v SRB solution. After incubation for 30 min, the wells were washed with 1% v/v acetic acid and then dried overnight in an oven. Once dry, 200 µL Tris buffer (10 mM, pH 10.5) was added to each well, followed by gentle shaking at 550 rpm for an hour. The absorbance of the extracted dye was measured at 540 nm, and the IC₅₀ representing the concentration that induces 50% cell death was calculated for each compound.

1.16.7. Glucose uptake assay

Glucose is the primary energy source for many tissues, and the ability of the selected compounds to promote glucose uptake was evaluated in the HepG2 cells, where uptake is GLUT4 mediated. This will identify compounds with insulin mimetic properties. Many different assays can be used to evaluate glucose uptake including radioactive, fluorescence, luminescence and absorbance assays (Kanwal *et al.*, 2012).

In the 2-NBDG assay, 2-NBDG is a fluorescent glucose analogue (O'Neil *et al.*, 2005, Yamada *et al.*, 2000) that provides a direct and rapid method to measure glucose uptake in single living cells.

The assay was carried out according to (Zou *et al.*, 2005) and (Theerakittayakorn and Bunprasert, 2011) with some modifications. HepG2 cells were plated at a density of 1.0×10^5 cells per well in DMEM/FCS in 96 well plates followed by a 24-hour incubation at 37 °C with 5% CO₂. The DMEM/FCS was removed and replaced by a Glc-free-DMEM containing 2.5% FCS (Glc-free-DMEM/FCS) and incubated overnight. Cells were treated with the promising compounds at a concentration range of 1 to 10 µM, 1 nM to 100 nM insulin and 1 to 10 µM metformin for 45 min. Then, 80 µM 2-NBDG was added for 1 hour. Insulin and metformin were the positive controls, and the negative control was Glc-free-DMEM/FCS at the same volume as the added compounds. The reaction was stopped by washing the monolayer twice with cold PBS. A final volume of 100 µL cold PBS was added to each well, and the fluorescence was measured at excitation and emission wavelengths of 460 nm and 544 nm, respectively. The data was expressed as relative fluorescence units.

1.16.8. Hepatic lipid accumulation

Excess fat accumulation can cause NAFLD, linked with obesity, insulin resistance, and T2DM. In the HepG2 cell line exposure to OA led to the accumulation of intracellular droplets of lipids that could be observed with ORO staining, and subsequent extraction of ORO allows the quantification of lipid accumulation.

The experiment was carried out according to (Huang *et al.*, 2018, Theerakittayakorn and Bunprasert, 2011) with some modifications. HepG2 cells were seeded on 96 well plate at a density of 5×10^4 cells per well and incubated overnight for attachment. The cells were then treated with the compounds and 1 mM OA for 48 hours before fixing the cells with 2% formalin for 30 minutes at 37°C. The medium was discarded, and then 100 μ L of the ORO working solution (ratio 3:2 of 0.5% ORO dissolved in H₂O) was added and incubated for 1 hour at room temperature. The staining solution was removed, and the plate was washed with tap water until the water was clear. Then, the plate was blotted dry. Microscopic images were taken to visualize ORO-stained lipid droplets in the HepG2 cells. Then, the lipids were extracted with 100 μ L of 60% isopropanol solution and the absorbance was measured at 405 nm. The results are expressed as the percentage lipid accumulation relative to HepG2 cells exposed only to OA using the formula below:

$$\% \text{ lipid accumulation} = \frac{(\text{Abs. test sample})}{(\text{Abs. oleic acid only})} \times 100\%$$

1.16.9. Herbs/spices dose-related to acarbose dose

Online databases such as Phenol-Explorer and previous studies were used to find the amount of each compound in several herbs and spices (Neveu *et al.*, 2010). The herb or spice with the highest amount of the compound (mg of compound /100 g of the herb) was used to calculate the dose of each herb related to the dose of acarbose taken per meal, which is 50 mg. Glycyrrhizin is the main bioactive compound in Liquorice, and it is hydrolysed to produce 18 α -GA; hence the dosage of glycyrrhizin is presented instead (Tian *et al.*, 2008, Li *et al.*, 2014).

1.16.10. Identification, profiling, and metabolomics of compounds in green tea

Tea is an important beverage that is cost-effective and a readily available source of compounds that have reported antidiabetic effects such as: epicatechin gallate, and EGCG (Yang *et al.*, 2019, Li *et al.*, 2010). In this study, UPLC-MS was used to quantify the amount of

30 different metabolites in five different brands of green tea. The green tea brands were Dilmah, Eve's, Five Roses, Livewell, and Tetley. For the purpose of this study, the focus was the levels of epicatechin gallate, EGCG, and quinic acid that were quantified.

- Green tea extraction and standards preparation

The contents of the green tea bags were ground to a powder, and then 0.25 g of the powder was weighed into a 2 mL Eppendorf tube. A volume of 1.6 mL of 50% methanol/1% formic acid in water solution was added. The tubes were vortexed for 1 min before extracting the samples in an ultrasonic bath for one hour. The tubes were then centrifuged at 12 100 g for 5 min. The supernatants were diluted 10x with extraction buffer. The diluted solutions were then transferred into 1.5 mL glass vials for analysis.

The standards were prepared as a cocktail; the cocktail was composed of 12 compounds: catechin, caffeic acid, chlorogenic acid, p-coumaric acid, epicatechin, epicatechin-3-O-gallate, epigallocatechin, EGCG, quercetin, quinic acid, rosmarinic acid, and rutin. The cocktail was prepared by adding 10 μ L of a 1 mg/mL standard solution in acetonitrile (70%) of each compound to a total volume of 120 μ L.

- Liquid Chromatography-Mass spectrometry (LC-MS) analysis

The LC-MS is a method that separates mixtures into each specific component based on their physical and chemical properties. This method also assists in identifying the components of the mixtures through the detection of peaks based on the mass spectrum (Korfmacher, 2005). In this study, the samples were sent at the Central Analytical Facilities at Stellenbosch University for analysis.

The column eluate was first passed through a Photodiode Array (PDA) detector with a wavelength range of 230 to 650 nm before mass spectrometry. This process allowed simultaneous collection of UV and MS spectra. Electrospray ionization was used in negative mode with a cone voltage of 15 V, desolvation temperature of 275 $^{\circ}$ C, and desolvation gas at 650 L/h, and the rest of the MS settings were optimized for the best resolution and sensitivity. Data were acquired by scanning the mass-to-charge 150 to 1500 mass-to-charge ratios in resolution and MSE modes. In MSE mode, two channels of mass spectrometry data were acquired at low collision energy (4 V) and at a collision ramp (40 – 100 V) to obtain fragments.

Leucine enkephalin was used as the reference mass to accurately determine the mass, and the instrument was calibrated with sodium formate. Separation was achieved on a Waters HSS T3, 2.1 x 100 mm, 1.7 μ m column. An injection volume of 2 μ L was used, and the mobile phase used consisted of 0.1% formic acid as solvent A and acetonitrile containing 0.1% formic acid as solvent B. The gradient started at 100% solvent A for 1 minute and changed to 28% solvent B over 22 minutes in a linear way. Then it was changed to 40% solvent B over 50 seconds and a wash step of 1.5 minutes at 100% solvent B, followed by re-equilibration to the initial conditions for 4 minutes. The flow rate was 0.3 mL/min, and the column temperature was maintained at 55°C. Data were processed using Mass Lynx for quantitative analysis; MSDIAL and MSFINDER can be used for unsupervised data processing (RIKEN Centre for Sustainable Resource Science: Metabolome Informatics Research Team, Kanagawa, Japan) (Lai *et al.*, 2018, Tsugawa *et al.*, 2015).

1.17. Statistical analysis

All experiments were performed in triplicate with at least three independent repeats, and the results are expressed as the mean \pm standard error of the mean (SEM). Excel from Windows 10 was used to analyse the data before exportation to other software for further analysis. The IC₅₀ of the compounds was calculated using GraphPad Prism version 8.3.0 (San Diego, California, USA). Kinetic parameters of the compounds were calculated on Excel from Windows 10, and the graphs were generated using R Studio and Python 3.9. (Delaware, USA) on virtual studio code from Microsoft (Redmond, Washington, USA). The K_i values were obtained from the Lineweaver-Burk plot and by plotting secondary plots, and the data were analysed with a one-sided unpaired Student's t-test. Significance was considered at $p < 0.05$ and is indicated either with * or a different letter of the English alphabet. Multivariate analysis was performed using the online tool MetaboAnalyst 5.0 (www.metaboanalyst.ca/), and statistical analysis (one factor) and default settings were used on the analysed data obtained from the Central Analytical Facilities at Stellenbosch University.

Results

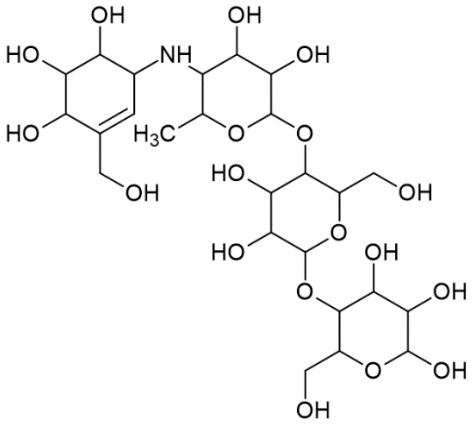
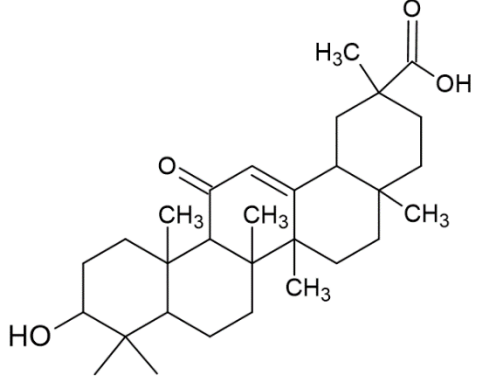
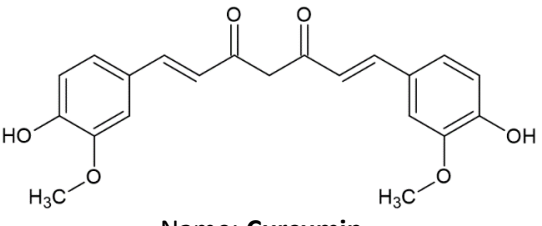
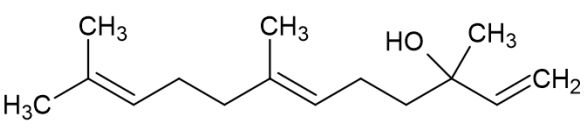
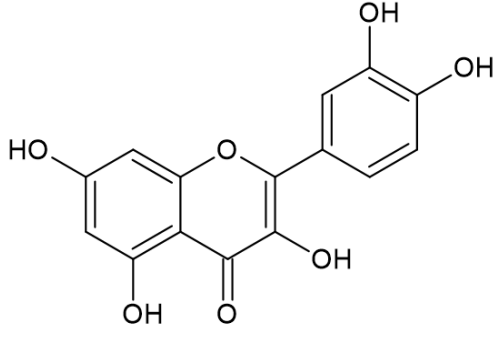
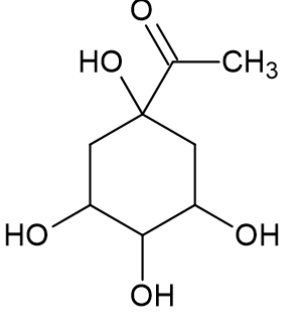
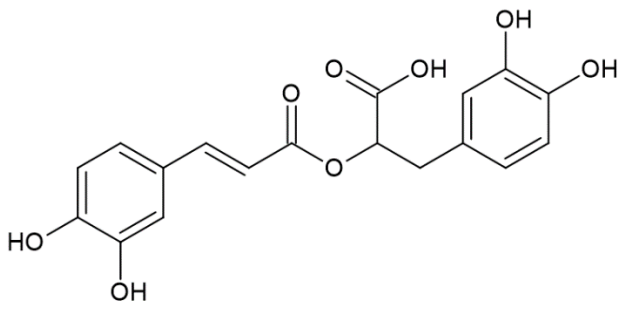
1.18. *In silico* studies

1.18.1. Chemical structures of selected compounds

Many herbs and spices such as Oregano, Turmeric, Rosemary, and Liquorice are known to have antidiabetic activity (Pereira *et al.*, 2019, El-Sayed and Youssef, 2019). These effects were attributed to the inhibition of carbohydrate hydrolysing enzymes and/or insulin action and/or other modes of action. Compounds that were the most abundant in these herbs and spices were selected and these compounds were curcumin, 18 α -GA, quercetin and rosmarinic acid with nerolidol and quinic acid as negative controls based on the docking scores.

The chemical structures of these compounds are drawn from SMILES using ChemSketch and are presented in Table 6.

Table 6. The structures of the compounds used in this study

 <p>The structure shows a complex polycyclic molecule with multiple hydroxyl groups and a methyl group, characteristic of a saccharide.</p> <p>Name: Acarbose Structure: Saccharide</p>	 <p>The structure is a complex triterpenoid with multiple fused rings, several methyl groups, and a carboxylic acid group.</p> <p>Name: 18α-glycyrrhetic acid Structure: Triterpenoid</p>
 <p>The structure features two phenolic rings connected by a heptadienone chain, with methoxy and hydroxyl substituents.</p> <p>Name: Curcumin Structure: Polyphenol</p>	 <p>The structure is a long-chain terpene with three methyl groups and a terminal vinyl group.</p> <p>Name: Nerolidol Structure: Terpene</p>
 <p>The structure is a flavonoid with a central chromone ring system and multiple hydroxyl groups on the phenyl rings.</p> <p>Name: Quercetin Structure: Polyphenol flavonoid</p>	 <p>The structure is a cyclohexane ring with three hydroxyl groups and an acetyl group.</p> <p>Name: Quinic acid Structure: Cyclitol</p>
 <p>The structure is a phenolic acid consisting of two hydroxyphenyl rings linked by a propionic acid chain.</p> <p>Name: Rosmarinic acid Structure: Phenolic acid</p>	

1.18.2. Molecular docking

For molecular docking studies, the PDB structures of intestinal α -glucosidase (PDB ID: 3LY4) from *Saccharomyces cerevisiae* and the human pancreatic α -amylase complex (PDB ID: 4GQR) were used. Docking was performed using glide scoring functions in Maestro, and the docking scores were then compared to those obtained from DIA-DB using the AutoDock vina algorithm. Maestro was used to prepare the protein structures as well as the different compounds that were used.

The compounds, including acarbose the positive control, were docked in the active site of both α -glucosidase (Figure 14) and α -amylase (Figure 15), and the docking scores and interactions were generated with hydrogen bonding being the major interaction (see annexure A). Compounds with scores more negative than acarbose were considered to be potential inhibitors of α -glucosidase and α -amylase.

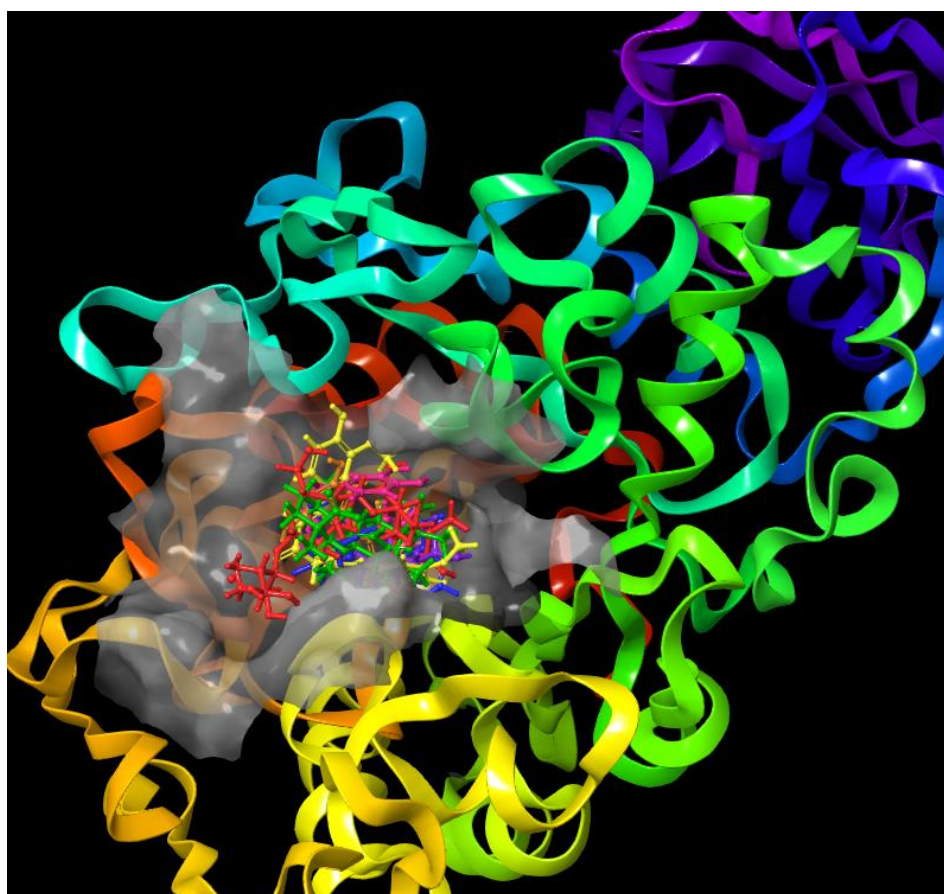


Figure 14. Representation of the compounds on the active side of α -amylase. This shows that all the compounds were docked in the same binding site in the enzyme pocket. The following colours represent the compounds: red (acarbose), yellow (curcumin), green (18 α -GA), blue (nerolidol), orange (quercetin), purple (quinic acid) and pink (rosmarinic acid).

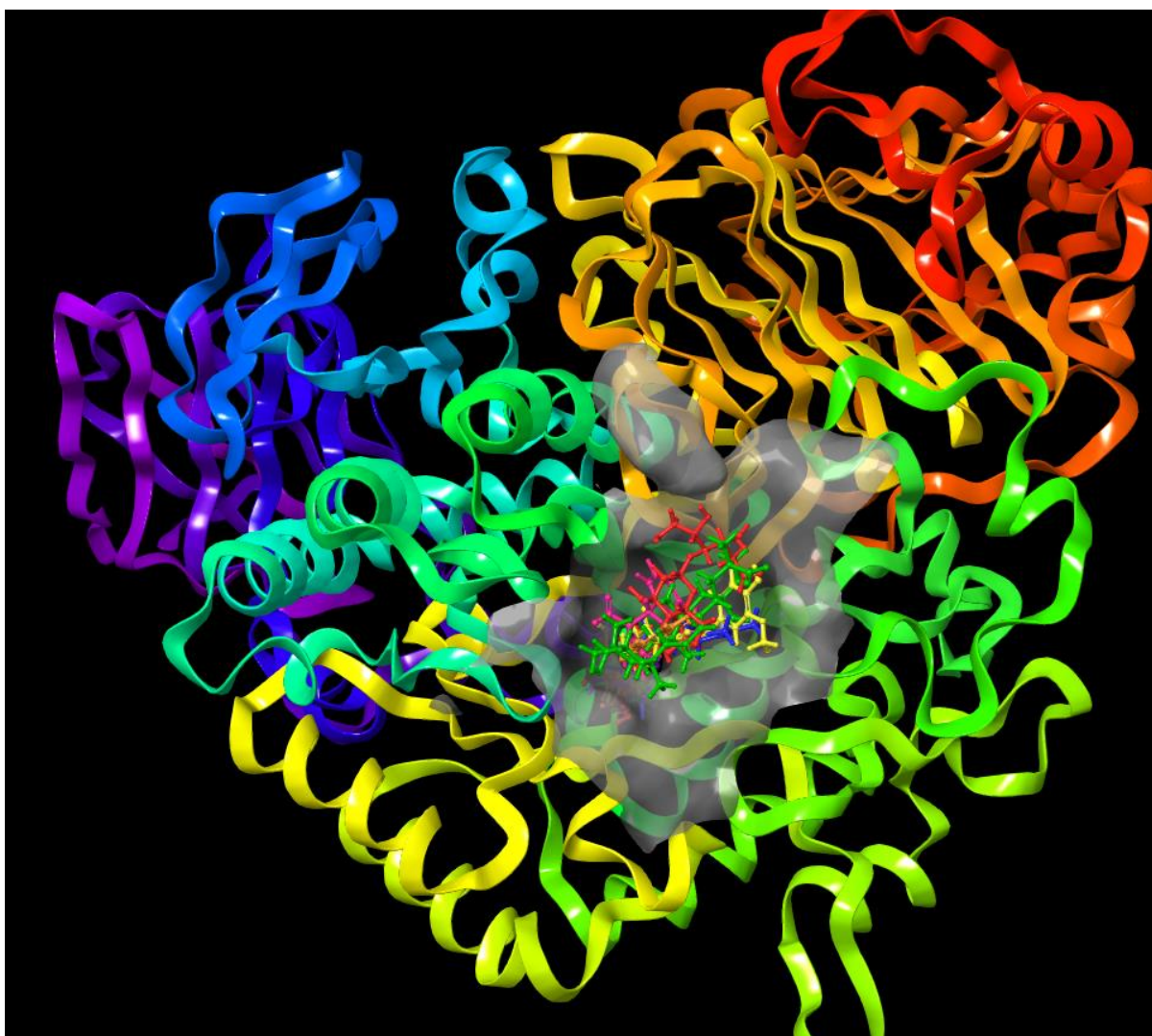


Figure 15. Representation of the compounds on the active side of α -glucosidase. This shows that all the compounds were docked in the same binding site in the enzyme pocket. The following colours represent the compounds: red (acarbose), yellow (curcumin), green (18 α -GA), blue (nerolidol), orange (quercetin), purple (quinic acid) and pink (rosmarinic acid).

From Table 7, curcumin, quercetin and rosmarinic acid had more negative scores than acarbose for α -glucosidase with both Maestro and DIA-DB. These compounds were identified as promising compounds for further biological enzyme inhibition studies. On the other hand, nerolidol had a more positive score than acarbose in α -glucosidase for both Maestro and DIA-DB; hence, it was used as a negative control for enzyme inhibition studies.

Table 7. Docking scores of compounds docked to α -glucosidase

Compound	Docking score (Kcal/mol)	
	Glide	AutoDock
Quinic acid	-4.7	-4.5
Quercetin	-4.6	-7.2
Rosmarinic acid	-4.1	-7.3
Curcumin	-3.3	-7.5
Acarbose	-3.1	-6.5
18 α -GA	-2.1	-7.4
Nerolidol	0.4	-5.9

Table 8. Docking scores of compounds docked to α -amylase

Compound	Docking score (Kcal/mol)	
	Glide	AutoDock
Acarbose	-6.5	-7.5
Quercetin	-6.5	-8.1
Curcumin	-6.3	-8.2
Rosmarinic acid	-6.0	-8.3
Quinic acid	-5.2	-5.4
18 α -GA	-4.1	-9.8
Nerolidol	-2.5	-5.9

From Table 8, quercetin, curcumin and rosmarinic acid have similar scores to acarbose for Glide and more negative scores than acarbose for AutoDock vina. This identified quercetin, curcumin and rosmarinic acid as promising compounds for biological study of α -amylase inhibition. Nerolidol had more positive scores than acarbose for both Glide and AutoDock vina, and consequently, it was used as a negative control for the inhibition of α -amylase.

In contrast to the Glide data, 18 α -GA had a more negative score than acarbose for both α -glucosidase and pancreatic α -amylase with AutoDock vina, and consequently, was also a promising compound of both enzymes. Quinic acid had a more positive score than acarbose in the inhibition of both enzymes in DIA-DB, in contrast to Maestro; indicating that it may be a poor enzyme inhibitor.

Table 9. Spearman's and Pearson's correlation coefficients between Glide and AutoDock vina

	Spearman's coefficient ρ	Pearson's coefficient r
α -Amylase	0.51	0.57
α -Glucosidase	0.46	0.31

Correlation studies between Glide and AutoDock vina were conducted by plotting a graph of Glide against AutoDock vina docking scores. This graph was crucial in determining the relationship between the two methods. The R^2 values represent the scattering of points around the straight line (Figure 16). The docking scores of quinic acid in α -glucosidase and 18 α -GA in α -amylase were removed due to the undue influence in determining the R^2 values. Spearman and Pearson's correlation coefficients were used to determine the relationship between the two algorithms; positive coefficients were obtained for the two algorithms in α -amylase and α -glucosidase (Table 9). A positive coefficient between 0 and 1 indicates a positive relationship between the algorithm in predicting the affinity of the compounds for α -amylase and α -glucosidase.

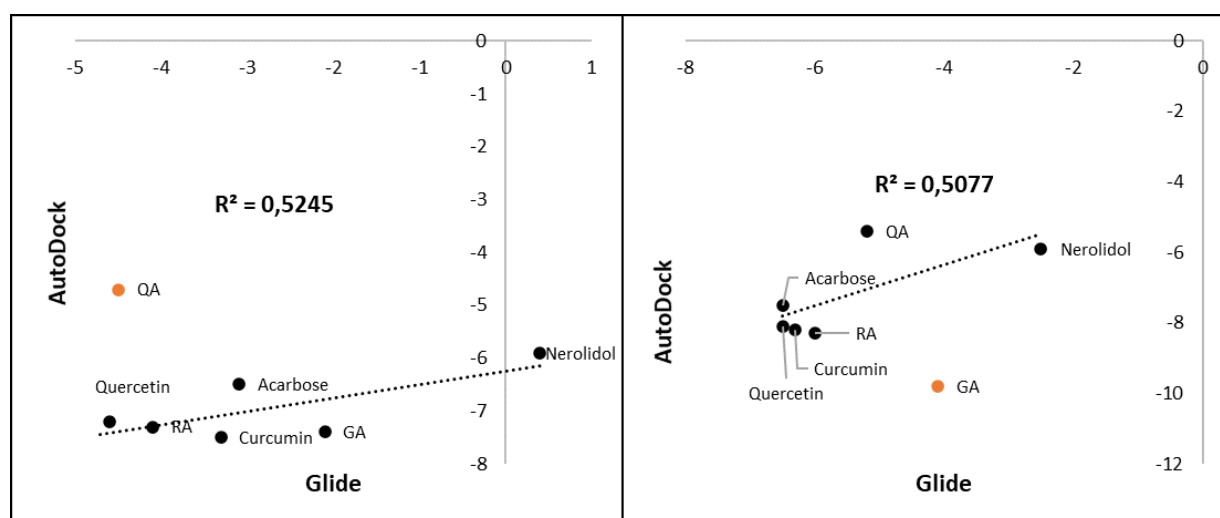


Figure 16. The relationship between the Glide and AutoDock docking scores against alpha-glucosidase (Left) and alpha-amylase (Right).

Ligand interactions were observed in the binding pocket of the enzymes using Maestro. In addition, compounds with more interactions with the binding pocket had a more negative docking score, which suggests better affinity.

Curcumin, 18 α -GA, quercetin, and rosmarinic acid were identified as promising compounds for further analysis based on the positive *in silico* enzyme docking interactions for both docking algorithms. In contrast, nerolidol and quinic acid were identified as negative controls due to poor inhibition of both enzymes *in silico*.

1.18.3. ADMET proprieties

The ADMET properties of selected compounds were obtained using Canvas a Schrödinger software and pkCSM', and the properties of each compound were compared to acarbose, a gold standard antidiabetic drug.

Table 10. Predicted toxicity properties of selected compounds

	HERG inhibitor	#Stars	Bioavailability score	Lipinski #violation
Acarbose	No	13	0.17	3
Curcumin	No	0	0.55	0
18 α -GA	No	0	0.85	1
Nerolidol	No	2	0.55	0
Quercetin	No	0	0.55	0
Quinic acid	No	0	0.56	0
Rosmarinic acid	No	2	0.56	0

From Table 10, all compounds have a higher bioavailability score than acarbose, indicating that they are absorbed and enter the systemic circulatory system. In addition, all the compounds, including acarbose, do not cause hepatotoxicity or are inhibitors of the HERG potassium channel. The promising compounds did not violate the Lipinski rules compared to acarbose, which violated three of the Lipinski rules. Acarbose had more stars, suggesting that acarbose is less drug-like than compounds with fewer #stars.

1.19. *In vitro* enzyme inhibition

The ability of the compounds to inhibit the enzymes was assessed by determining their K_i values compared to acarbose, the positive control. A lower value indicates more potent enzymatic inhibition.

The inhibitory constant of each compound was determined using kinetic assays by analysing the double reciprocal Lineweaver-Burk plots (see Annexure B). The inhibition potential was evaluated, and K_i values were compared using secondary plots generated from the slope of the Lineweaver-Burk plots against inhibitor concentration. For each compound, the types of inhibition were compared by calculating the critical kinetic parameters K_m and V_{max} , and by using the template in Figure 10 above (see section 1.10) compared to the plots in annexure B for each compound in the inhibition of both α -amylase and α -glucosidase.

For α -glucosidase inhibition in Table 11, there was a significant difference ($p < 0.05$) between the K_i value of acarbose and those of 18 α -GA, curcumin, and quercetin. These values were also significantly lower ($p < 0.05$) than acarbose, suggesting more potent inhibition of α -glucosidase. Only rosmarinic acid had a K_i value not significantly different ($p > 0.05$) to acarbose and can also be considered a potential inhibitor of the enzyme. The remaining two compounds, nerolidol and quinic acid, had K_i values significantly higher ($p < 0.05$) than acarbose, indicating weaker inhibition of α -glucosidase. The type of inhibition differed. Acarbose, nerolidol and quinic acid exhibited a competitive type of inhibition in which these compounds compete with the substrate pNPG to bind to the active site of α -glucosidase. In contrast, 18 α -GA exhibited a non-competitive type of inhibition where binding is at a site other than the active site and does not compete with the substrate, pNPG. Curcumin, quercetin and rosmarinic acid exhibited mixed-type inhibition, a mixture of competitive and non-competitive inhibition.

For α -amylase inhibition (Table 12), there was a significant difference ($p < 0.05$) between the K_i value of acarbose and the compounds evaluated. The K_i value of acarbose was significantly lower ($p < 0.05$), indicating potent inhibition of α -amylase. Of the compounds evaluated curcumin had the second-lowest K_i value for the inhibition of α -amylase, indicating that it is a more potent inhibitor than the other compounds, except acarbose. The mode of inhibition for acarbose, curcumin, 18 α -GA, rosmarinic acid, and quinic acid exhibited mixed-type inhibition. Inhibition by quercetin was competitive, while nerolidol type of inhibition was uncompetitive.

Table 11. K_i values and types of inhibition of α -glucosidase by the selected compounds.

Compound	Type of inhibition	$K_i \pm \text{SEM}$ (μM)
18 α -GA	Non-competitive	27 ± 4^b
Curcumin	Mixed	33 ± 2^b
Quercetin	Mixed	45 ± 6^b
Rosmarinic acid	Mixed	94 ± 13^a
Acarbose	Competitive	130 ± 10^a
Nerolidol	Competitive	1075 ± 132^c
Quinic acid	Competitive	2642 ± 394^c

Mean values with different letters are significantly different ($p < 0.05$) ($n = 3$)

Table 12. K_i values and types of inhibition of α -amylase by the selected compounds.

Compound	Type of inhibition	$K_i \pm \text{SEM}$ (μM)
Acarbose	Mixed	31 ± 4
Curcumin	Mixed	154 ± 17^a
Quercetin	Competitive	465 ± 61^a
18 α -glycyrrhetic acid	Mixed	723 ± 180^a
Rosmarinic acid	Mixed	1082 ± 216^a
Quinic acid	Mixed	2948 ± 169^a
Nerolidol	Uncompetitive	3044 ± 100^a

^aMean values significantly different to acarbose ($p < 0.05$) ($n = 3$)

1.20. Relationship between Docking scores and K_i

Correlation studies between docking scores and K_i were conducted by plotting a graph of Docking scores (Glide and AutoDock) against the K_i value of each compound.

Spearman's and Pearson's correlation coefficients were used to determine the relationship between the two studies. Positive coefficients were obtained for both α -amylase and α -glucosidase. A positive coefficient between 0 and 1 indicates a positive relationship between the *in vitro* and *in silico* study of the inhibition of α -amylase and α -glucosidase. A positive relationship between the two approaches with positive Spearman's and Pearson's correlation

coefficients was obtained (Tables 13 and 14). The K_i value of quinic acid was not included when plotting the graph of Glide scores vs. K_i value of each compound because it had a significant influence on the line, but it was included when plotting the regression line of AutoDock.

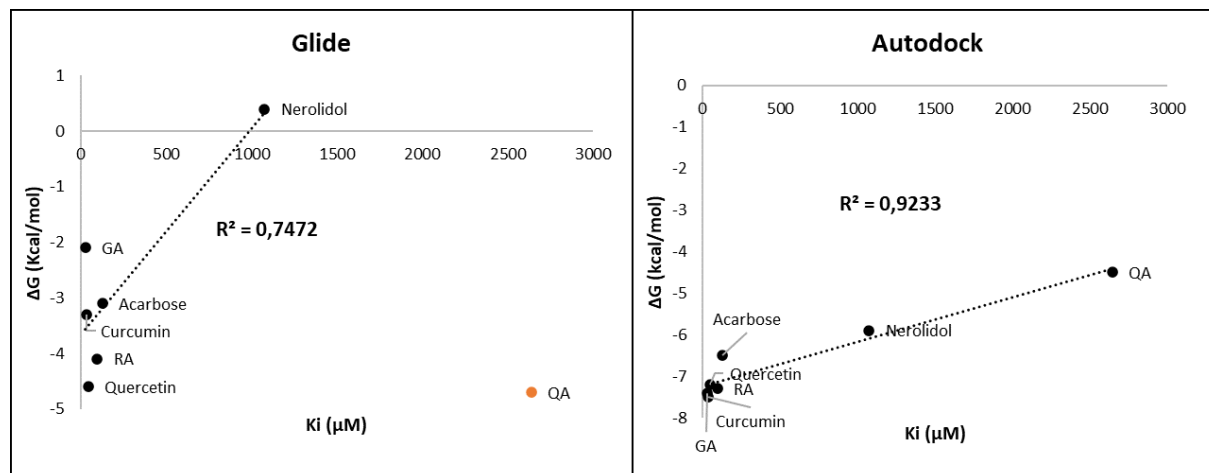


Figure 17. Graphs showing the relationship between the docking scores Glide (Left) and AutoDock (Right) against the K_i of each compound for α -glucosidase.

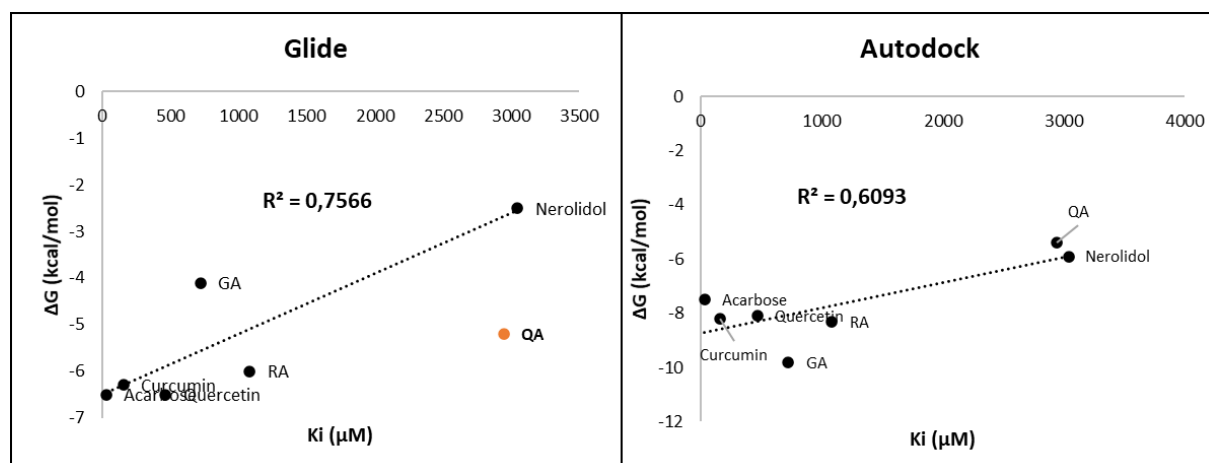


Figure 18. Graphs showing the relationship between the docking scores Glide (Left) and AutoDock (Right) against the K_i of each compound for α -amylase.

Spearman's and Pearson's coefficients were positive in the relationship between *in silico* and *in vitro* studies for the inhibition of α -glucosidase when using both AutoDock and Glide docking scores. However, when comparing AutoDock scores with K_i values, coefficient values were higher than the Glide docking scores (Table 13).

Table 13. Spearman's and Pearson's correlation coefficients between *in vitro* and *in silico* studies for α -glucosidase

	Spearman's coefficient ρ	Pearson's coefficient r
AutoDock	0.93	0.93
Glide	0.43	0.26

Spearman's and Pearson's coefficients were positive for the relationship between *in silico* and *in vitro* studies for the inhibition of α -amylase when using both AutoDock and Glide docking scores. However, unlike in the inhibition of α -glucosidase, coefficient values when comparing Glide scores with K_i values were higher than those of AutoDock docking scores (Table 14).

Table 14. Spearman's and Pearson's correlation coefficients between *in vitro* and *in silico* studies for α -amylase

	Spearman's coefficient ρ	Pearson's coefficient r
AutoDock	0.32	0.32
Glide	0.62	0.88

1.21. *In vitro* cytotoxicity

Cytotoxicity was tested against C2C12 myotubes, HepG2 hepatocarcinoma, and Caco2 adenocarcinoma cells. Glucose uptake in the C2C12 and HepG2 cell lines occurs via the GLUT-4 transporter; therefore, the concentration range used for the evaluation of toxicity included the concentration used for the glucose uptake studies. Caco2 adenocarcinoma cells represent cells of the human intestine and represent the site of α -amylase and α -glucosidase activity.

Table 15. IC_{50} of selected compounds on C2C12 cells (Mean \pm SEM)

Compound	C2C12 IC_{50} (μ M)
18 α -GA	24 \pm 1*
Acarbose	60 \pm 15
Rosmarinic acid	81 \pm 17
Quercetin	87 \pm 20
Curcumin	> 100*
Quinic acid	> 100*
Nerolidol	> 100*

18 α -GA had the lowest IC₅₀ and showed significant cytotoxicity in the C2C12 and HepG2 cell lines, with values significantly lower ($p < 0.05$) than acarbose. In C2C12 cells, rosmarinic acid and quercetin had IC₅₀ not significantly ($p > 0.05$) different to acarbose while all other compounds have shown limited cytotoxicity where concentrations up to 100 μ M did not induce 50% cell death (Table 15). The cytotoxicity of rosmarinic acid and quercetin was similar to that of acarbose in the C2C12 cell line. No IC₅₀ value could be determined for curcumin, quinic acid and nerolidol, indicating the lack of toxicity at concentrations as high as 100 μ M.

In the HepG2 cell line, 18 α -GA, curcumin, and quercetin had significantly lower ($p < 0.05$) IC₅₀ values than acarbose (Table 16). In contrast, no cytotoxicity in this cell line was observed for rosmarinic acid, acarbose, quinic acid and nerolidol at concentrations up to 100 μ M (Table 16).

Table 16. IC₅₀ of selected compounds on HepG2 cells (Mean \pm SEM)

Compound	HepG2 IC₅₀ (μM)
18 α -GA	28 \pm 8*
Curcumin	41 \pm 2*
Quercetin	54 \pm 2*
Rosmarinic acid	> 100
Acarbose	> 100
Quinic acid	> 100
Nerolidol	> 100

In the Caco2 cell line, the IC₅₀ of curcumin and rosmarinic acid was significantly less than the IC₅₀ of acarbose. Quercetin, nerolidol, acarbose, quinic acid and 18 α -GA were not cytotoxic at any of the concentrations evaluated (Table 17).

Table 17. IC_{50} of selected compounds on Caco2 cells (Mean \pm SEM)

Compound	Caco2 IC_{50} (μ M)
Curcumin	15 \pm 1*
Rosmarinic acid	83 \pm 3*
Quercetin	> 100
Nerolidol	> 100
Acarbose	> 100
Quinic acid	> 100
18 α -GA	> 100

1.22. *In vitro* glucose uptake

Glucose uptake was evaluated in C2C12 and HepG2 cells using the 2-NBDG uptake assay. 2-NBDG is a fluorescent analogue of glucose that is taken up by these cell lines via the GLUT4 transporter. Insulin and metformin were used as controls. For both compounds there was no significant increase in 2-NBDG uptake in C2C12 cells was observed at 25 and 50 nM insulin and 1, 10 and 100 μ M metformin. For all, no significant difference was observed ($p > 0.05$) when compared with the control at all concentrations evaluated (Figures 19 and 20).

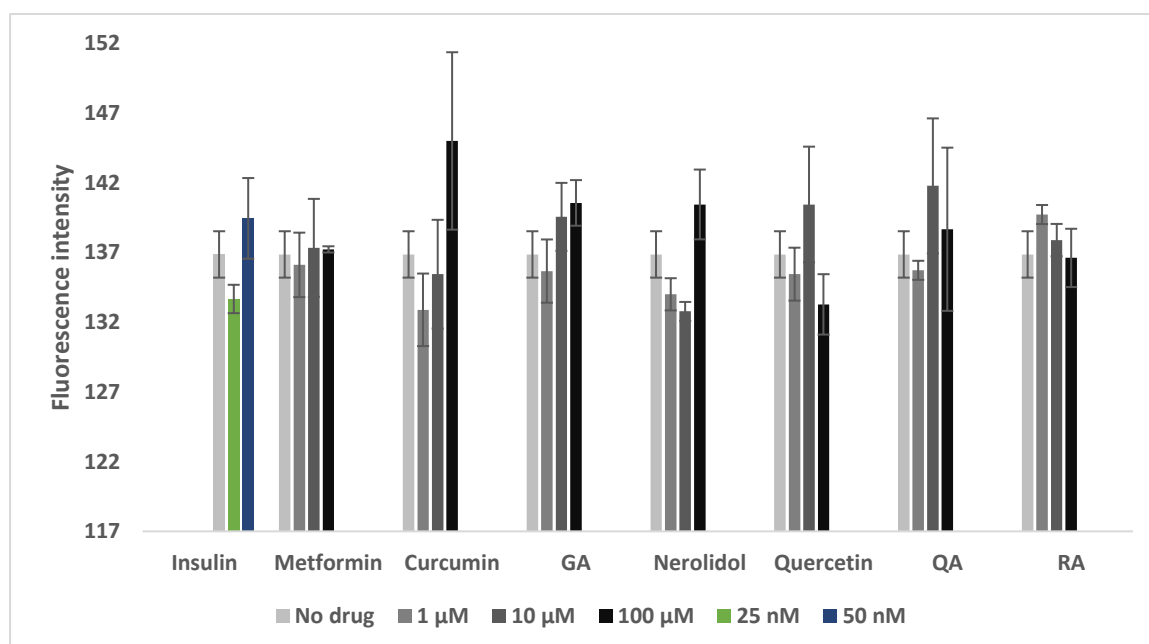


Figure 19. Glucose uptake by C2C12 cells. C2C12 cells were exposed for 1h to 80 μ M 2-NBDG as control (No drug added) or 2-NBDG with 25 nM – 100 μ M of the following compounds, insulin, curcumin, 18 α -GA (GA), metformin, nerolidol, quinic acid (QA), quercetin and rosmarinic acid (RA) in different concentrations. (Mean \pm SEM) ($n = 3$).

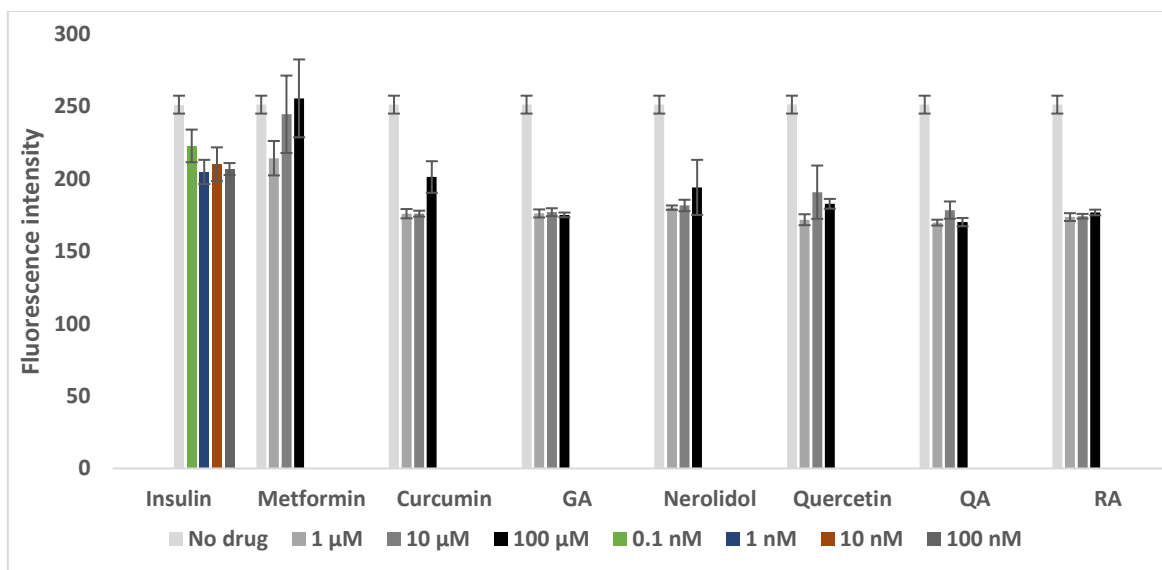


Figure 20. Glucose uptake by HepG2 cells. HepG2 cells were exposed for 1h to 80 μM 2-NBDG as control (No drug added) or 2-NBDG with 0.1 nM – 100 μM of the following compounds, insulin, curcumin, 18α-GA (GA), metformin, nerolidol, quinic acid (QA), quercetin and rosmarinic acid (RA). (Mean ± SEM) (n = 3).

In HepG2 cells, there was no significant change ($p > 0.05$) in 2-NBDG uptake at any of the evaluated concentrations of insulin and metformin. In contrast the uptake of 2-NBDG was significantly reduced for all concentrations of the compounds evaluated ($p < 0.05$).

1.23. Hepatic lipid accumulation

Oleic acid induces lipid droplet accumulation in HepG2 cells, treatment with the compounds were compared to the control with OA added and the vehicle control (DMSO) with no OA added after 48 hours exposure.

Quantification of lipid droplets after treatment with metformin at 1 and 10 μM caused a significant decrease in lipid accumulation. At 1 μM, treatment with curcumin, quercetin, and quinic acid caused a significant decrease in lipid accumulation. At 10 μM, all compounds except curcumin caused a significant decrease in lipid accumulation. Metformin and quercetin showed a significant dose dependent decrease in lipid accumulation. Rosmarinic acid at 10 μM induced the greatest decrease in lipid droplet accumulation compared with the other compounds.

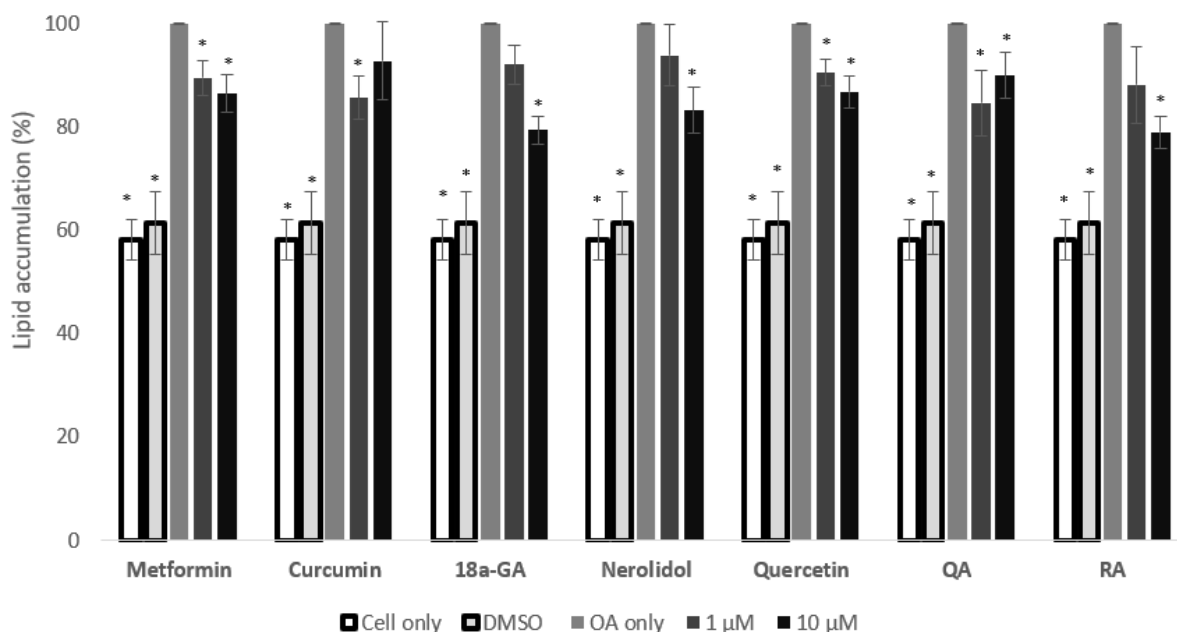


Figure 21. Lipid accumulation in HepG2 cells. Cells were exposed for 48 hrs to oleic acid (OA) only or a combination of OA and 1 – 10 μ M of the following compounds metformin, curcumin, 18 α -GA, (GA), nerolidol, quercetin, quinic acid (QA) and rosmarinic acid (RA). Data are represented as Mean \pm SEM. * $p < 0.05$ compared to OA only treatment.

Microscopic images (Figure 22) show the lack of ORO staining for the control, cells only and the DMSO vehicle control which contrasts with the red staining observed for cells exposed to OA. Although some staining was observed for all cells exposed to OA in combination with the tested compounds the intensity of staining was reduced and was confirmed following the extraction of ORO (Figure 21).

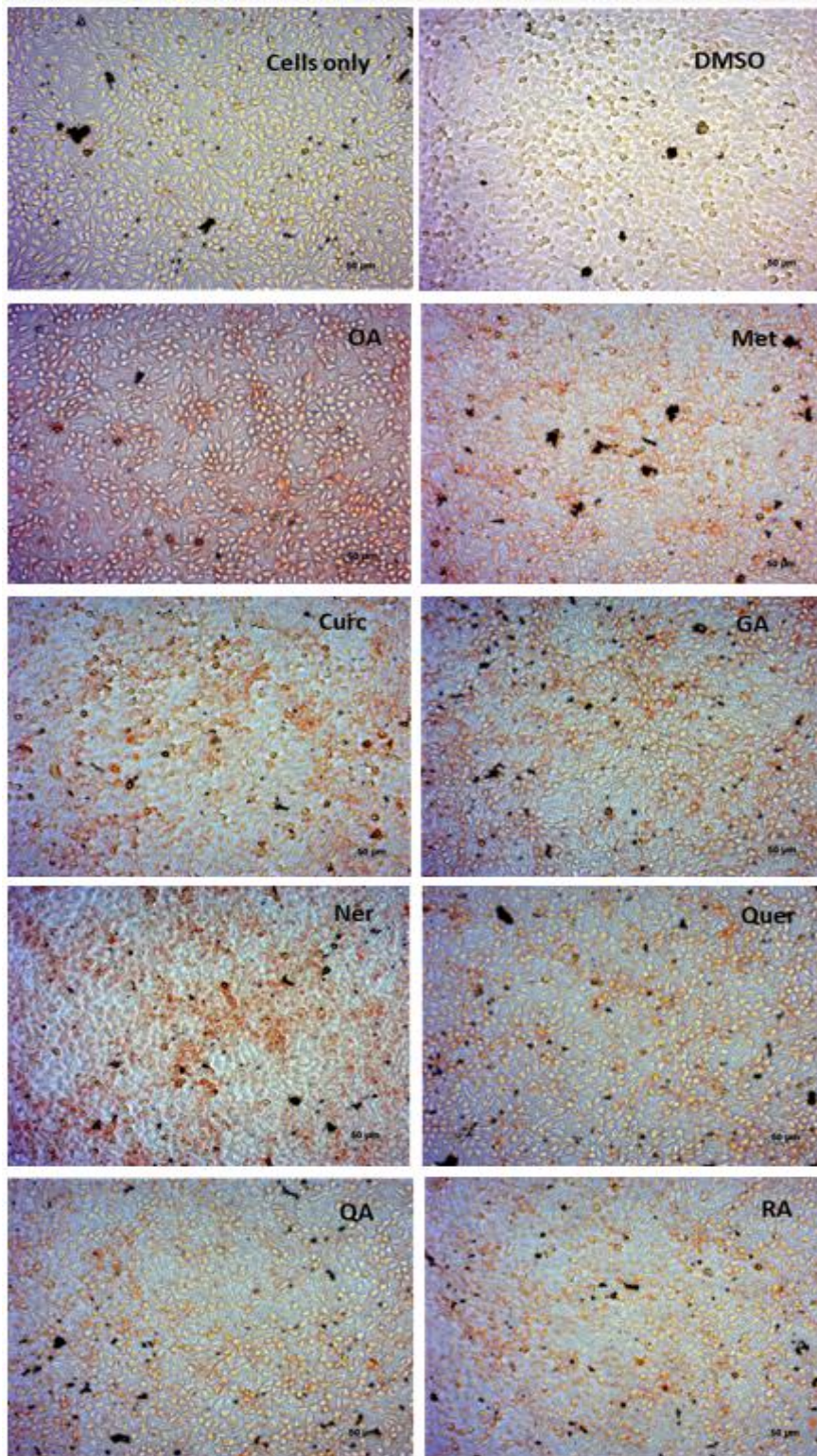


Figure 22. Light microscopy images showing the accumulation of lipids in HepG2 cells after staining with Oil Red O. The controls were HepG2 cells alone, exposed to DMSO, (vehicle control), oleic acid (OA) (positive control) and 10 μ M of metformin (Met), curcumin (Curc), 18 α -GA (GA), nerolidol (Ner), quercetin (Quer), quinic acid (QA) and rosmarinic acid (RA).

1.24. Herbs/spices dose-related to acarbose dose

The herbs and spices with the highest contents of curcumin, glycyrrhizin, quercetin, quinic acid and rosmarinic acid were identified (Table 18). Curcumin and rosmarinic acid which are potent inhibitors of α -glucosidase and reduced hepatic lipid accumulation, were present in Turmeric as well as Peppermint and Rosemary, respectively. These results indicate that these herbs have antidiabetic properties. Quercetin and quinic acid are present in green tea (Table 19). The levels of these compounds and two known antidiabetic compounds, ECG and EGCG were determined in five brands of green tea.

Table 18 is showing a small amount of Turmeric, 1.3 g dry weight may be required to match the dose of acarbose per meal. Green tea, Peppermint and Rosemary have also shown small amount, 1.9, 1.6, and 1.8 g dry weight, respectively. This relates to the moles of selected compounds to approximately match the moles in the dose of acarbose per meal.

Table 18. Herb/spice dosage required relative to acarbose

Compound	Herb or spice (Species)	Amount in herb/spice (mg/100 g)	Amount (g) of herb relative to acarbose per meal
Curcumin	Turmeric (<i>Curcuma longa</i>)	2213	1.3
	Curry powder (<i>Murraya koenigii</i>)	285	10.0
Epicatechin gallate	Green tea (<i>Camelia sinensis</i>)	1256	2.7
Epigallocatechin gallate	Green tea (<i>Camelia sinensis</i>)	3000	1.2
Glycyrrhizin	Liquorice (<i>Glycyrrhiza glabra</i>)	239*	27.0
Quercetin	Oregano (<i>Lippia graveleones</i>)	42	56.0
	Green tea (<i>Camelia sinensis</i>)	2.77	845
Quinic acid	Green tea (<i>Camelia sinensis</i>)	795	1.9
Rosmarinic acid	Peppermint (<i>Mentha piperita</i>)	1620	1.6
	Rosemary (<i>Salvia rosmarinus</i>)	1534	1.8

*(Tian *et al.*, 2008)

1.25. LC/MS and metabolomic analysis on green tea

1.25.1. Identification of the peaks in the teas

LC/MS was used to identify the different compounds in five different tea brands: Dilmah, Eve's, Five Roses, Livewell and Tetley. Twelve compounds were used as standards to be identified in *Camellia sinensis* green tea brands. The retention time and m/z ratio of the standards were identified, and these data are presented in Table 19 and Figure 23.

Table 19. Peaks of standards according to the mass spectra from the negative ion mode.

Name	Molecular mass (Da)	m/z ratio	Retention time (min)
Caffeic acid	180.042255	179.04	12.89
Catechin	290.079041	289.07	11.78
Chlorogenic acid	354.095093	353.09	12.11
p-Coumaric acid	164.047348	163.04	15.73
Epicatechin	290.079041	289.07	13.89
Epicatechin-3-O-gallate	442.089996	441.08	17.40
Epigallocatechin	306.073944	305.07	11.05
Epigallocatechin gallate	458.084900	457.07	14.08
Quercetin	302.053223	301.04	24.20
Quinic acid	192.063385	191.06	1.860
Rosmarinic acid	360.084503	359.07	20.07
Rutin	610.153381	609.15	17.54

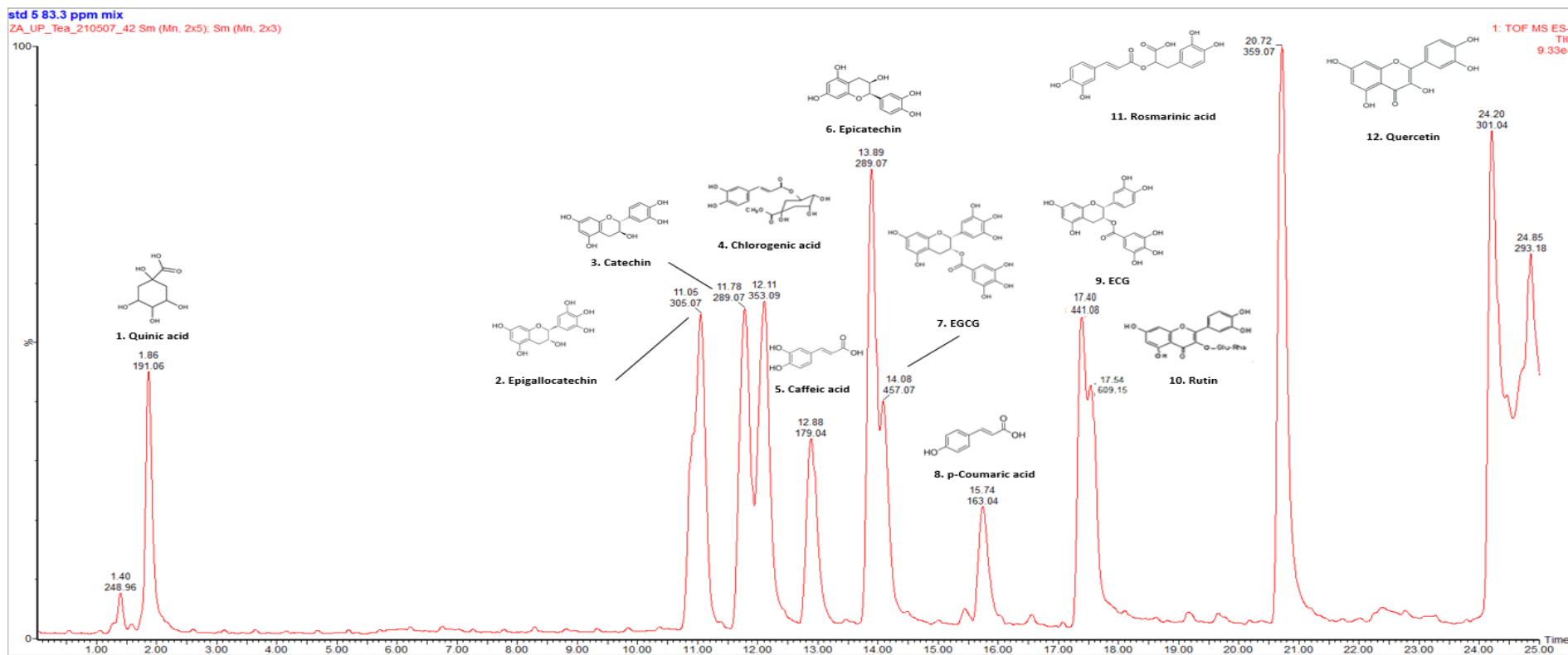


Figure 23. Chromatogram of the standards cocktail in ESI negative. The chromatograms show the retention time and the m/z ratio of the 12 standards.

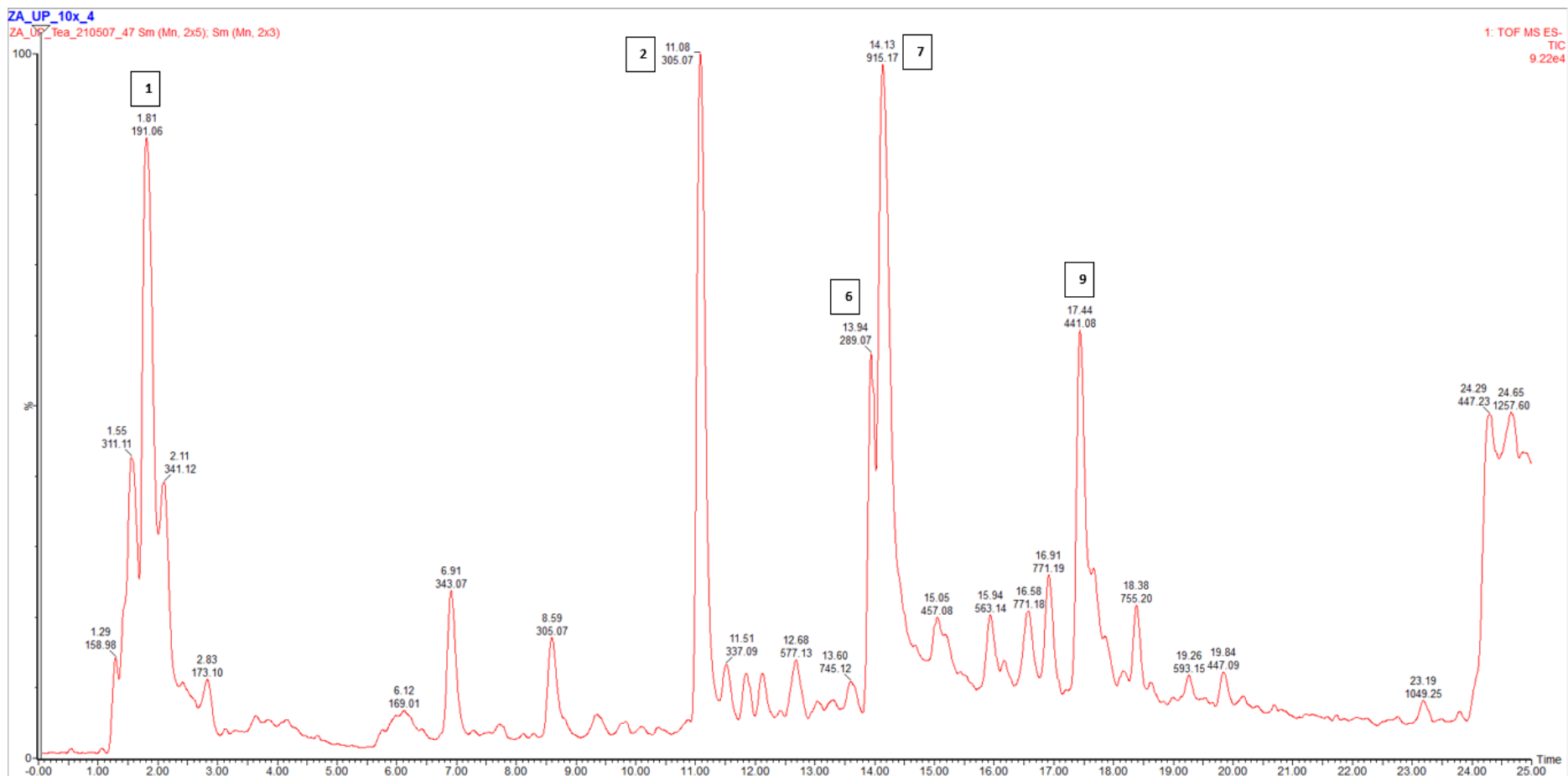


Figure 24. Chromatogram of the green tea in ESI negative. The chromatograms show the retention time and the m/z ratio of the compounds in the green tea compared to the standards in Figure 23. The number corresponds to the compound in Figure 23.

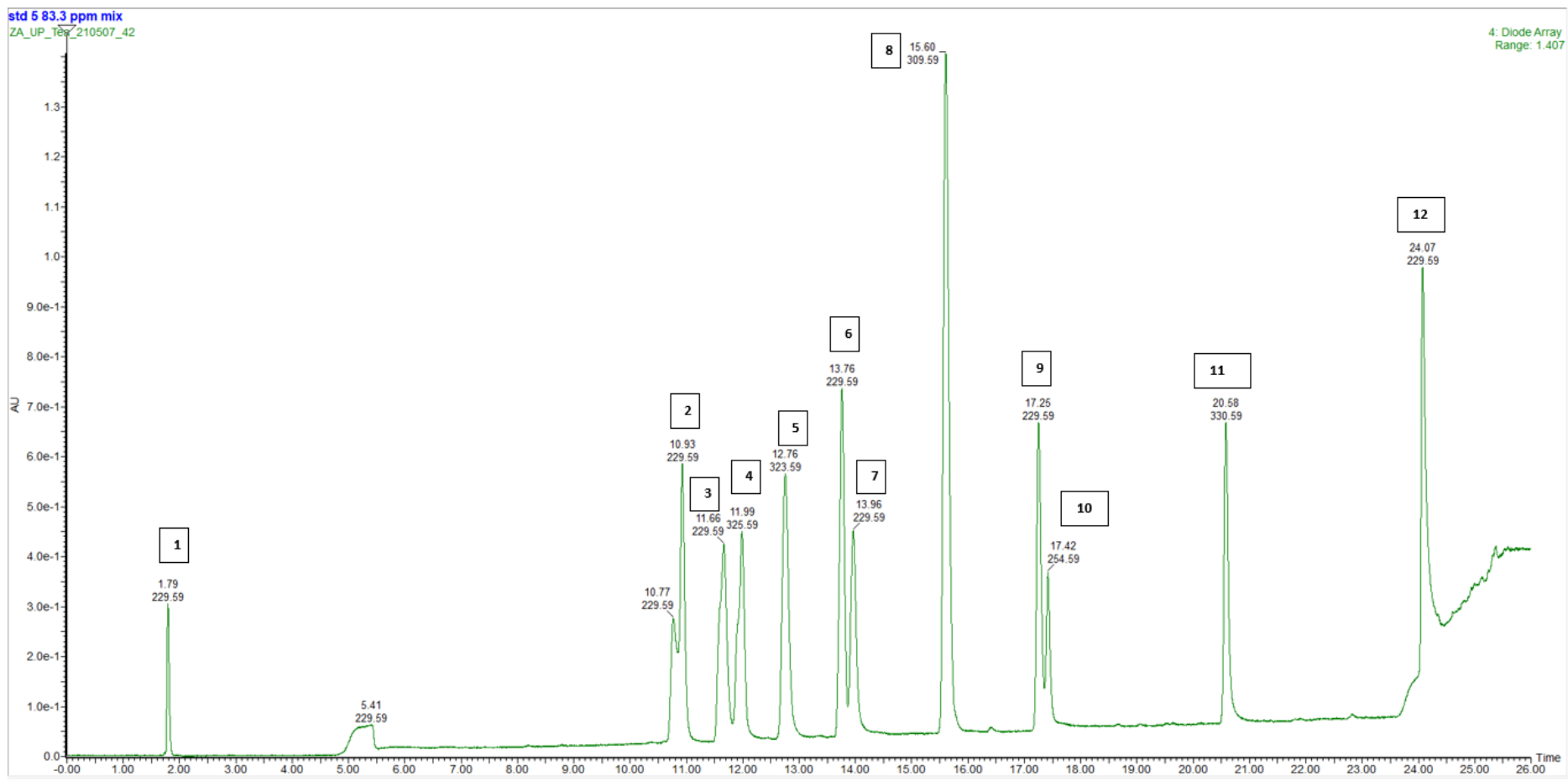


Figure 25. UV/Vis spectrum of the standards. It is used to identify standards in green tea that are only visible with UV/Vis. The top and bottom values represent the retention time and the wavelength respectively.

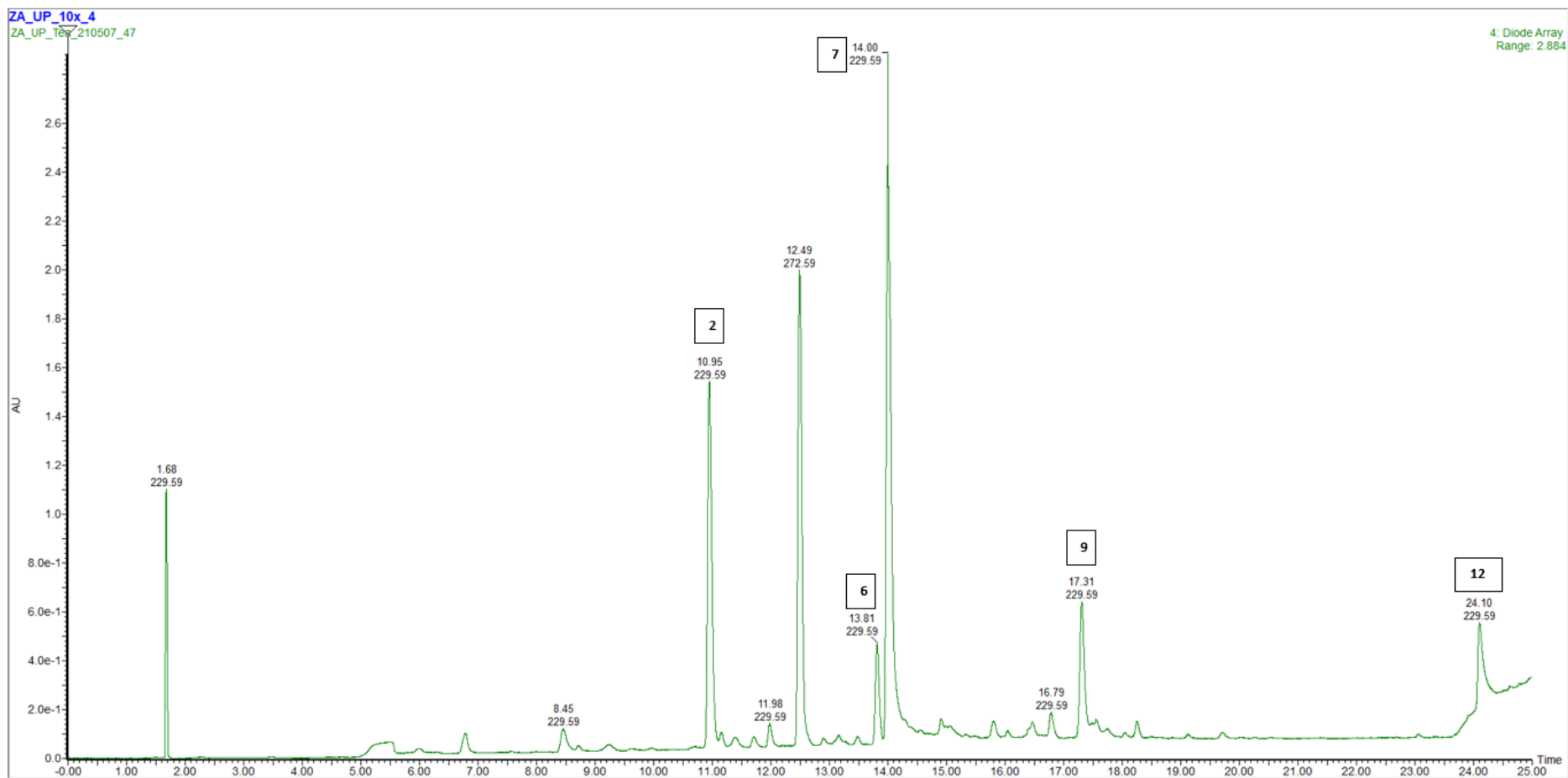


Figure 26. UV/Vis spectra of the green tea. It is used to identify standards from Figure 25 that are only visible with UV/Vis. The number corresponds to the compound in Figure 23. The top and bottom values below each compound represent the retention time and the wavelength respectively.

In Figures 23 and 24, when comparing the chromatogram of the standards to that of the green tea samples in ESI negative, five standards were identified based on their respective retention times. The identified standards were: quinic acid (Peak 1), epigallocatechin (Peak 2), epicatechin (Peak 6), EGCG (Peak 7) and ECG (Peak 9). The same standards were also identified based on the UV/Vis spectrum of the standards compared with the spectrum for green tea (Figures 25 and 26).

From the 12 standards, only the peaks of catechin, epicatechin, ECG, epigallocatechin, EGCG and quinic acid were identified in the five tea brands based on their retention times and m/z ratios as indicated in Table 19. The peak areas of the identified standard are shown in Table 20. In addition, seven unidentified peaks (labelled UP1 – UP7) were selected based on their presence in the chromatograms of the five teas. Their retention times, m/z ratios and peak areas were determined (Table 21 and Table 22).

Table 20. Average peak areas of the identified standards in the tea chromatograms

	Dilmah	Eve's	Five Roses	Livewell	Tetley
Catechin	2328.15	1672.79	804.91	882.76	951.45
Epicatechin	14464.52	8315.60	6343.48	6043.74	6051.43
*ECG	15109.45	13511.51	10000.06	8968.80	8360.31
Epigallocatechin	21144.23	15311.82	15331.98	15571.49	13797.43
*EGCG	22070.77	24035.29	20819.63	19754.86	21180.79
Quinic acid	13758.07	13935.07	16738.70	16257.02	16881.81

*Epicatechin gallate **Epigallocatechin gallate

Table 21. Retention times and m/z ratios of the unidentified peaks (UP)

	Retention time (min)	m/z ratio
UP1	2.10	341.11
UP2	2.81	173.09
UP3	6.09	169.01
UP4	6.90	343.07
UP5	8.60	305.07
UP6	16.92	771.19
UP7	18.37	755.2

UP: Unidentified peaks

Table 22. Average peak areas of the unidentified peaks (UP) in the tea chromatograms

	Dilmah	Eve's	Five Roses	Livewell	Tetley
UP1	2127.77	2788.89	9020.37	7998.25	9184.54
UP2	1012.86	1708.82	1009.24	1273.29	1529.14
UP3	1161.35	1123.33	1296.63	1365.79	1105.62
UP4	4233.63	4697.76	2568.99	2919.58	3231.52
UP5	6234.90	2498.56	1992.38	2169.4	2403.18
UP6	1520.60	2038.74	2330.1	2219.74	2208.09
UP7	466.763	1833.37	1419.7	1418.46	1406.39

1.25.2. Quantification of metabolites in green tea

Quinic acid, epicatechin gallate, and EGCG were identified and quantified in the five green tea brands based on their retention times, and m/z ratios (Table 19 and Figure 23).

From Table 23, Dilmah had a higher mean %w/w dry weight of quinic acid and ECG than the other green tea brands. No significant difference was observed in the mean %w/w dry weight of ECG in Dilmah, Eve's, and Five Roses. However, Eve's had a significantly higher mean %w/w dry weight of EGCG than the other green tea brands.

Livewell and Tetley had significantly lower mean %w/w dry weights of quinic acid and ECG, while Tetley had a significantly lower mean %w/w dry weight of EGCG.

Table 23. Quantification of quinic acid, epicatechin gallate and epigallocatechin gallate in the 5 tea brands. Values presented as (Mean \pm SEM) % w/w dry weight

	Quinic acid	Epigallocatechin gallate	Epicatechin gallate
Dilmah	0.80 \pm 0.01 ^a	2.85 \pm 0.04 ^a	1.26 \pm 0.01 ^a
Eve's	0.50 \pm 0.02 ^b	3.00 \pm 0.05 ^b	1.18 \pm 0.01 ^a
Five Roses	0.30 \pm 0.01 ^c	2.76 \pm 0.02 ^a	1.01 \pm 0.01 ^a
Livewell	0.42 \pm 0.01 ^d	2.85 \pm 0.05 ^a	0.93 \pm 0.01 ^b
Tetley	0.41 \pm 0.01 ^d	2.68 \pm 0.04 ^c	0.92 \pm 0.01 ^b
Average	0.49 \pm 0.01	2.82 \pm 0.04	1.06 \pm 0.01

Mean values with different letters are significantly different ($p < 0.05$) (n = 6)

1.25.3. Inhibition of α -amylase and α -glucosidase by green tea

The DNSA and pNPG assays were used to determine the inhibition of both enzymes by the five green tea brands. A lower IC₅₀ value indicated potent inhibition.

Table 24. IC_{50} of the green tea brands for the inhibition of α -amylase and α -glucosidase (Mean \pm SEM)

	α -Amylase (mg/mL)	α -Glucosidase (mg/mL)
Dilmah	19 \pm 4 ^a	0.98 \pm 0.02 ^a
Eve's	33 \pm 1 ^b	1.30 \pm 0.01 ^b
Five Roses	25 \pm 2 ^a	1.70 \pm 0.01 ^c
Livewell	23 \pm 2 ^a	0.26 \pm 0.01 ^d
Tetley	31 \pm 3 ^b	0.44 \pm 0.01 ^e

Mean values with different letters are significantly different ($p < 0.05$) ($n = 3$)

From Table 24, Dilmah and Livewell had lower IC_{50} values for α -amylase and α -glucosidase, respectively. However, no significant differences were observed in the IC_{50} values of Dilmah, Five Roses, and Livewell in the inhibition of α -amylase. The IC_{50} for Tetley was significantly higher than that of the other tea brands. For α -glucosidase, inhibition, Livewell had the lowest IC_{50} and Eve's tea the highest.

Dilmah and Livewell brands are more effective inhibitors of both enzymes and are used to perform multivariate analysis; Eve's and Five Roses tea can be considered to be weaker inhibitors compared to the other tea brands.

1.25.4. Correlation between peak areas in green tea brands and enzyme inhibition by green tea brands

Spearman and Pearson's correlation coefficients were used to determine the relationship between the identified peak areas in the chromatograms and the inhibition of α -amylase and α -glucosidase by the five tea brands. The relationship between peak areas and enzyme inhibition was determined for the identified standards in Table 20 and the unidentified peaks (UP) in Table 22.

Table 25. Spearman's and Pearson's correlation coefficients between peak areas of the identified standards and α -amylase inhibition by the green tea brands

	Spearman's coefficient ρ	Pearson's coefficient r
Catechin	0.1	0.1
Epicatechin	0.1	0.1
ECG	0.3	0.3
Epigallocatechin	0.3	0.3
EGCG	-0.1	-0.1
Quinic acid	0.3	0.3

Catechin, epicatechin, ECG, epigallocatechin and quinic acid had a positive correlation coefficient, suggesting a positive correlation between the peak areas of these compounds in the five green teas and the inhibition of α -amylase by the five green tea brands (Table 25). Among the five standards with positive correlation, ECG, epigallocatechin and quinic acid correlated best with enzyme inhibition.

Table 26. Spearman's and Pearson's correlation coefficients between peak areas of the identified standards and α -glucosidase inhibition by the green tea brands

	Spearman's coefficient ρ	Pearson's coefficient r
Catechin	0.1	0.1
Epicatechin	-0.6	-0.6
ECG	-0.5	-0.6
Epigallocatechin	-0.5	-0.5
EGCG	0	0
Quinic acid	0.2	0.2

Catechin and quinic acid had a positive correlation coefficient when comparing the peak areas and the inhibition of α -glucosidase by the five green tea brands (Table 26). Quinic acid correlated best with enzyme inhibition, with a correlation coefficient of 0.2 compared to 0.1 for catechin.

Table 27. Spearman's and Pearson's correlation coefficients between the peak areas of the unidentified peaks (UP) and α -amylase inhibition by the green tea brands

	Spearman's coefficient ρ	Pearson's coefficient r
UP1	-0.4	-0.4
UP2	-0.7	-0.7
UP3	0.6	0.6
UP4	-0.3	-0.3
UP5	0.1	0.1
UP6	-0.1	-0.1
UP7	-0.7	-0.7

Unidentified peaks UP3 and UP5 had a positive correlation with correlation coefficients of 0.6 and 0.1, respectively, when comparing the peak areas and the inhibition of α -amylase by the five green tea brands. UP3 correlated better with enzyme inhibition than UP5 (Table 27).

Comparing the peak areas and the inhibition of α -glucosidase by the five green tea brands, unidentified peaks UP1, UP2, UP3 and UP5 had positive correlation with UP2 having the best positive correlation coefficient of 0.3 (Table 28).

Table 28. Spearman's and Pearson's correlation coefficients between the peak areas of the unidentified peaks (UP) and α -glucosidase inhibition by the green tea brands

	Spearman's coefficient ρ	Pearson's coefficient r
UP1	0.1	0.1
UP2	0.3	0.3
UP3	0.1	0.1
UP4	0	0
UP5	0.1	0.1
UP6	-0.1	-0.1
UP7	-0.5	-0.5

Compounds belonging to UP3 and UP5 have a positive correlation between their peak areas and inhibition of α -amylase and α -glucosidase with UP3 having a better correlation than the identified standards for the inhibition of α -amylase.

Table 29. Details on UP3 and UP5 according to the obtained mass spectra

	Retention time (min)	m/z ratio	Proposed formula	Fragment ions	Tentatively identified compounds	Reference
UP3	6.09	169.01	C ₇ H ₆ O ₅	125	Gallic acid	(Lin <i>et al.</i> , 2008) (Jin <i>et al.</i> , 2019)
UP5	8.60	305.07	C ₁₅ H ₁₄ O ₇	125, 179	Gallocatechin	(Jin <i>et al.</i> , 2019)

www.pubchem.ncbi.nlm.nih.gov/ and www.genome.jp/kegg/compound/

The compounds UP3 and UP5 were tentatively identified as gallic acid and gallocatechin respectively (Table 29). Figures 27 and 28 show the fragment ions of the two proposed compounds. The KEGG pathway website was used to determine the different compounds with the proposed molecular formula and PubChem, and previous studies revealed ms/ms fragments that corresponded to those observed in the present study.

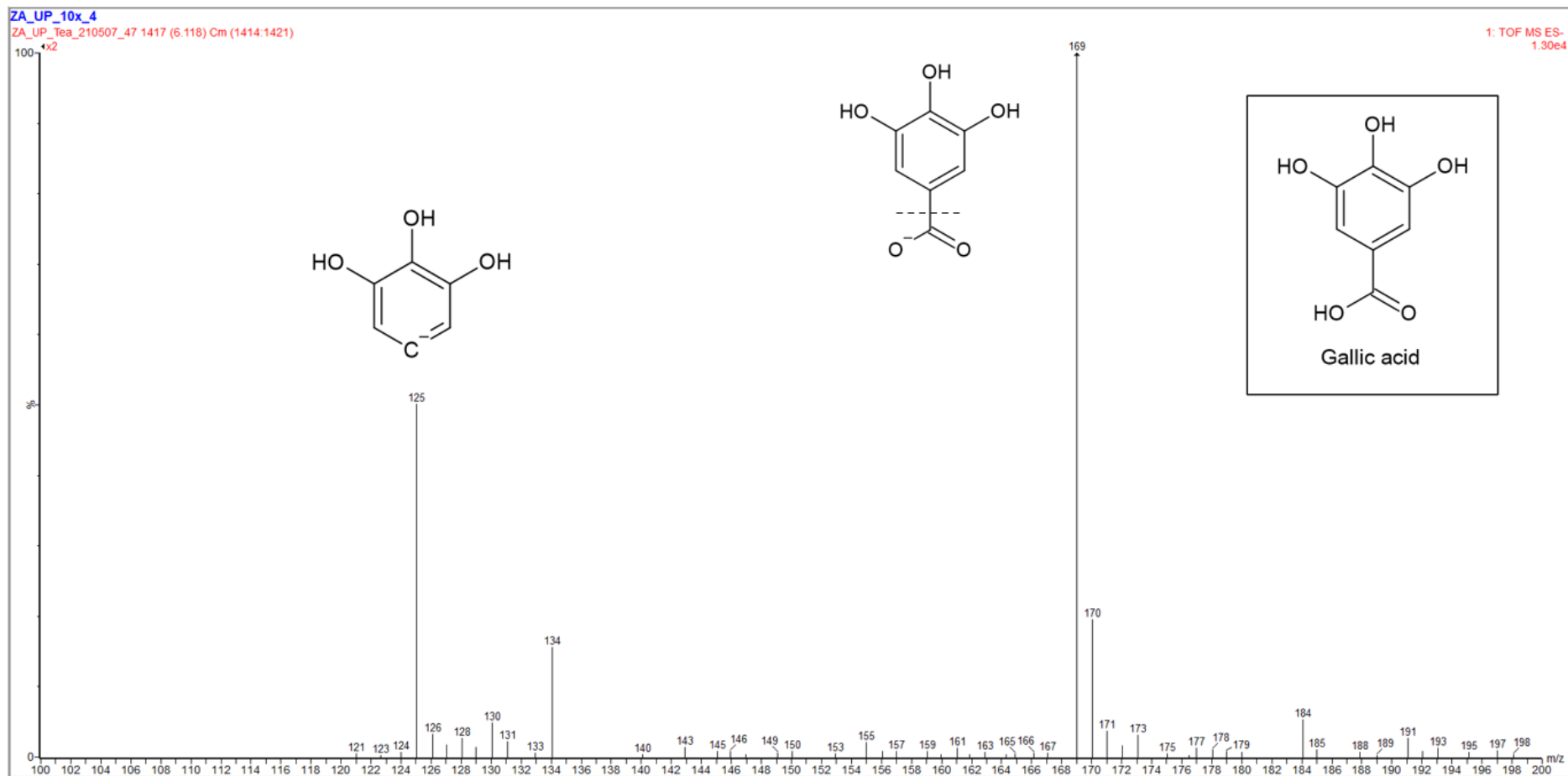


Figure 27. Molecular structures and *ms/ms* fragment ions of the proposed compound UP3.

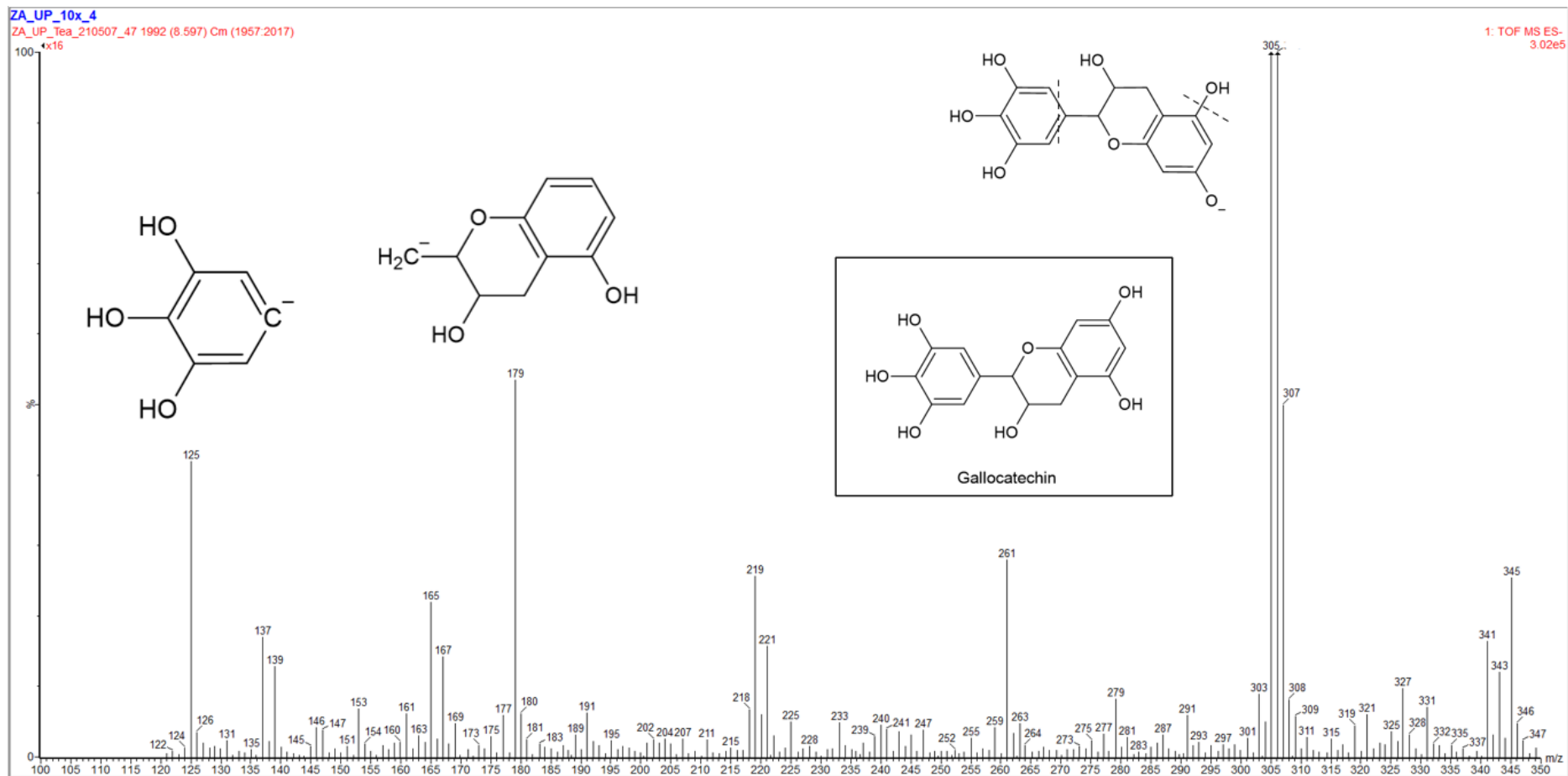


Figure 28. Molecular structures and m_s/m_s fragment ions of the proposed compound UP5

1.25.5. Multivariate data analysis

PCA and OPLSDA were performed to evaluate the variability between the five green tea brands. Samples with similarities are clustered together, and samples with fewer similarities are separated.

On the PCA score plot (Figure 30A), Dilmah and Eve's green teas were separated from the other tea brands. Five Roses, Livewell, and Tetley clustered together. In the separation, PC1 and PC2 were 87.3% and 4.7%, respectively.

The OPLSDA (Figure 30B) showed more differences in the metabolite content, where there was further separation between the clustered tea brands in the PCA. Five Roses seem to show a slight separation, while Livewell and Tetley remain slightly more clustered.

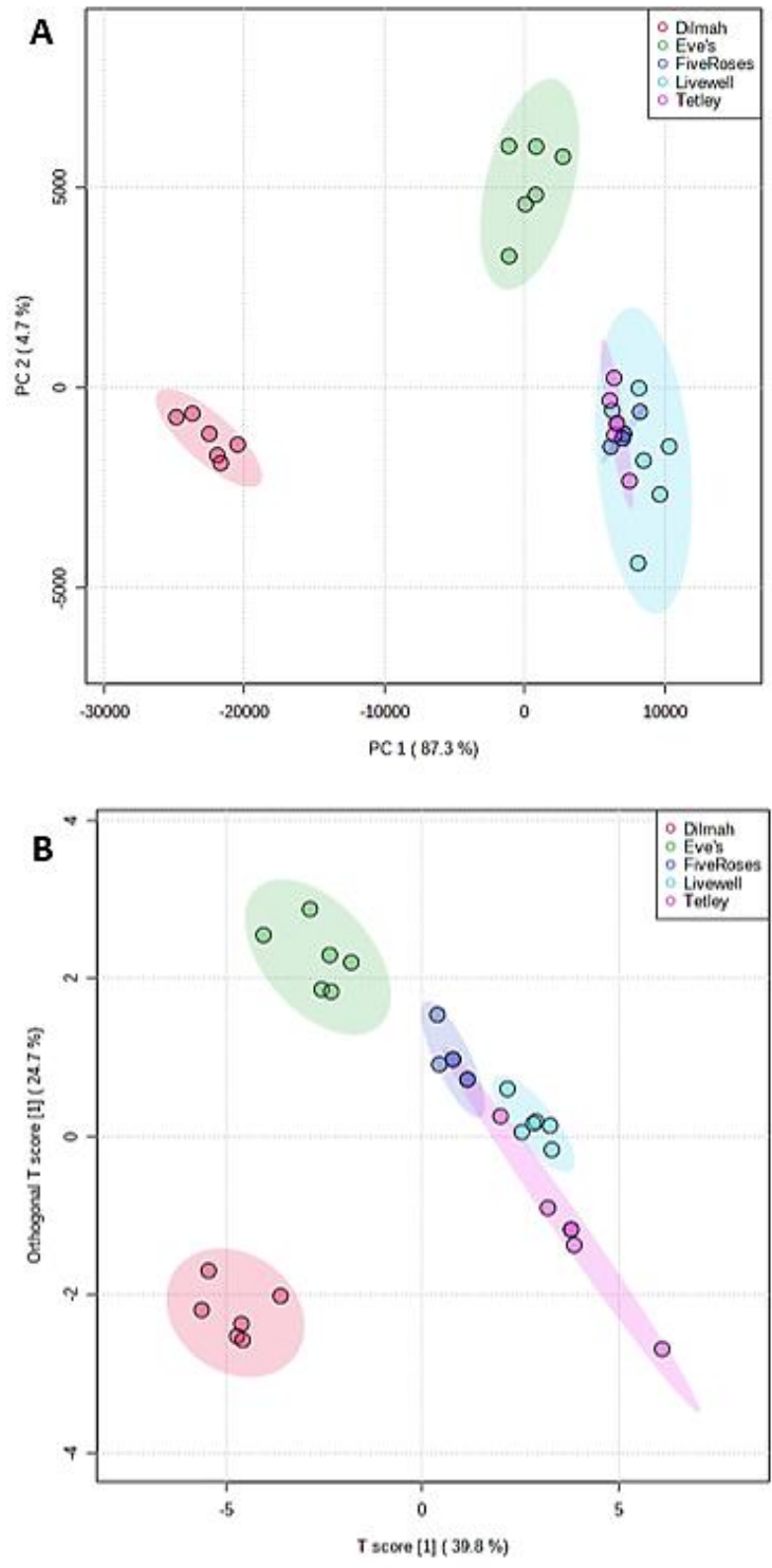


Figure 29. PCA (A) and OPLS-DA (B) score plots of the metabolite content of the five green tea brands.

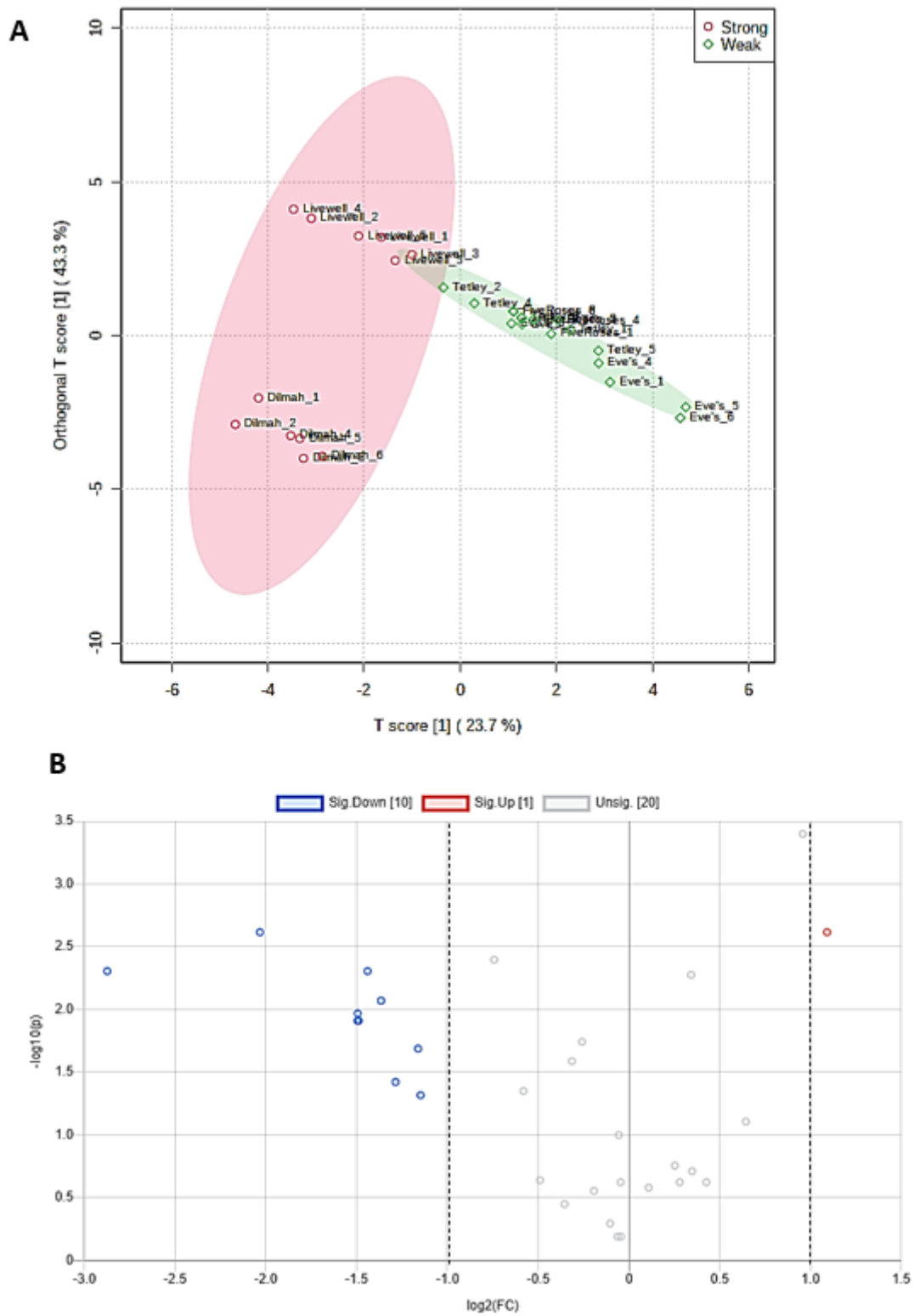


Figure 30. OPLS-DA (A) and volcano plot diagram (B) of α -amylase and α -glucosidase inhibition by the five green tea brands.

In the OPLS-DA in Figure 31A, the stronger inhibitors tea brands such as Dilmah and Livewell were located on the left side of the confidence interval, and the weaker inhibitors such as Five Roses and Eve's tea brands were on the right side of the confidence interval. The principal component T score [1] was 23.7%, and the orthogonal T score [1] in the OSC process was 43.3%. The volcano map in Figure 21B shows that 31 metabolites (see Table 1D in Annexure D) were detected and screened; 20 of the metabolites were not significantly changed, 11 metabolites were significantly changed where 10 metabolites were downregulated, and one metabolite was upregulated. Significantly changed metabolites accounted for approximately 35.5% of the total metabolites detected; this indicates a significant change in metabolites between strong (Dilmah and Eve's) and weak (Livewell and Tetley) inhibitors.

Discussion

1.26. *In silico* studies

In silico studies were performed before any biological studies to predict the binding abilities of the herbal compounds in the active site of α -amylase and α -glucosidase were undertaken. It was also used to predict the physiochemical, pharmacokinetic, and toxicity properties of the compounds.

In silico studies were used as a step in the selection of the compounds to be used. Compounds were selected based on the docking scores compared with a drug known to inhibit these enzymes, acarbose. The compounds were docked in the active site of α -amylase and α -glucosidase. The docking scores of the compounds were obtained using Maestro and AutoDock vina. Maestro is a Schrödinger software that uses the Glide scoring function; this scoring function analyses the different interactions in the ligand-protein complex and minimizes any steric clashes to generate docking scores (Friesner *et al.*, 2004). AutoDock vina uses the empirical scoring function that focuses on simple contact terms, the contribution of lipophilic and metal-ligand interactions in the ligand-protein complex to estimate the Gibbs free binding energy between the ligand and the protein (Eldridge *et al.*, 1997). The scores from AutoDock vina were obtained from the DIA-DB (<https://bio-hpc.eu/software/dia-db/>). The compounds interact with the amino acid in the enzyme's catalytic site to generate binding energy where a more negative binding energy indicates a spontaneous interaction and a stronger affinity between the ligand and protein, thus more potent inhibition.

The scores were used to select seven compounds, including acarbose. These were four compounds with an affinity better or similar than acarbose and two compounds with an affinity lower than acarbose.

For α -glucosidase *in silico* inhibition (Table 7), the order of affinity was as follow: quinic acid > quercetin > rosmarinic acid > curcumin > acarbose > 18 α -GA > nerolidol when docked with Glide; and curcumin > 18 α -GA > rosmarinic acid > quercetin > acarbose > nerolidol > quinic acid when docked with AutoDock vina. Similar to these findings Jhong *et al.* (Jhong *et al.*, 2015), reported a higher *in silico* binding affinity to α -glucosidase for curcumin with docking scores more negative than acarbose. However, they used PDB ID 2ZE0 while we used PDB ID 3L4Y, and the authors used AutoDock for their scoring function. A study by Tolmie *et al.* (Tolmie *et al.*, 2021) reported that rosmarinic acid has a higher *in silico* binding affinity to α -glucosidase than acarbose, and as in the present study, the same PDB ID and the glide scoring function were used.

For pancreatic α -amylase *in silico* inhibition (Table 8), the order of affinity was as follow: acarbose > quercetin > curcumin > rosmarinic acid > quinic acid > 18 α -GA > nerolidol when docked with Glide; and 18 α -GA > rosmarinic acid > curcumin > quercetin > acarbose > nerolidol > quinic acid when docked with AutoDock vina. Compared to acarbose, curcumin, 18 α -GA, quercetin, and rosmarinic acid are considered potential inhibitors of α -amylase and α -glucosidase. Nerolidol was considered to be a weak inhibitor of both enzymes, and quinic acid had different affinities when comparing the two docking algorithms.

A positive correlation was observed between the two docking algorithms with a R² value slightly higher than 0.5; although this can be interpreted as a positive correlation, it can be interpreted as a low effect on the prediction (Lewis-Beck and Skalaban, 1990, Moore and Kirkland, 2007). These results were used as motivation to perform *in vitro* enzyme inhibition to further investigate the potential inhibitory activities of these compounds against pancreatic α -amylase and α -glucosidase.

For systemic applications, it is important to determine the ADMET properties of the compounds. This was generated *in silico* using Schrödinger software known as QikProp and an online free tool, pkCSM. These programs help predict the ADMET properties of the compounds. In Table 10, all compounds, including acarbose, were predicted not to be

hepatotoxic and had no HERG potassium (K^+) channel inhibition. Potential cardiotoxicity was also evaluated, and this involved the prediction of effects on the KCNH2 channel, as it takes part in the electrical activity of the heart and modulates some cellular functions of the nervous system. In the heart, an inhibition or blockage of this channel may result in a disorder called long Q-T syndrome (LQTS) (Aronov, 2005, Hedley *et al.*, 2009, Ntie-Kang, 2013).

A bioavailability score close to 1, indicates that these drugs are absorbed into the circulation before reaching their target (Ntie-Kang, 2013). The bioavailability of the compounds was assessed and compared to acarbose, which mediates its effect in the gastrointestinal tract and had a lower bioavailability score of 0.17. 18 α -GA had the highest bioavailability score of 0.85. Curcumin, nerolidol, quercetin, quinic acid, and rosmarinic acid had a bioavailability score of 0.5, showing that almost half of these compounds are absorbed into the circulation. This is of importance if there are multiple targets such as the inhibition of α -amylase and α -glucosidase, as well as systemic targets.

The #stars are an indication of the drug-likeness of the compounds. Canvas QikProp uses approximately 20 descriptors to determine the drug-likeness of the compounds. The #stars indicates the number of descriptors significantly different from known drugs' 95% value range (Schrodinger, 2012). Findings were that the selected compounds are more drug-like than acarbose having more #stars than all compounds.

The Lipinski rule of five is used to determine the parameters associated with 90% of orally administered drugs that have passed the phase II clinical stage trial (Lipinski *et al.*, 1997, Lipinski, 2004). The results from Table 6 show that acarbose violated three rules; 18 α -GA violated one rule, while the remaining compounds did not violate the rule of five. However, Lipinski has also stated that some of the orally active drugs may lie outside of the rule of five and can still be used, mainly because these drugs are substrates of naturally occurring targets, and the rule of five does not guarantee that the compound is drug-like (Lipinski *et al.*, 1997, Lipinski, 2004).

1.27. *In vitro* enzyme inhibition

α -Amylase and α -glucosidase are necessary critical enzymes in the digestion of dietary carbohydrates. These enzymes are among the therapeutic targets in T2DM, and inhibition of

these enzymes reduces the increase in postprandial blood level glucose by delaying hydrolysis and absorption of carbohydrates (Nguyen and Le, 2012, Tiwari *et al.*, 2014).

Acarbose, voglibose, and miglitol are currently commercially available inhibitors of these enzymes in clinical use, but these inhibitors cause some side effects such as abdominal stress diarrhea, flatulence, and other gastrointestinal effects (Wang *et al.*, 2016). Therefore, it is important to find new inhibitors that are readily available, cost-effective, and possibly have fewer side effects. Dietary intervention based on plant derived products that can contribute to reducing hyperglycaemia can also reduce the required dosage of these drugs thereby reducing side effects.

Two values are commonly used parameters to compare the potency of inhibitors. The first is the constant inhibition value, K_i which is the equilibrium constant of the dissociation of the inhibitor-enzyme complex; the second value is the IC_{50} which is the inhibitor concentration that reduces the rate of the enzyme-catalysed reaction by half (Burlingham and Widlanski, 2003). Data are commonly reported using either or both, where a smaller value/s denotes a higher binding affinity, thus more potent inhibition.

The increasing order of the K_i values in the inhibition of α -glucosidase was as follows: 18α -GA < curcumin < quercetin < rosmarinic acid < acarbose < nerolidol < quinic acid (Table 11). The compounds, 18α -GA, curcumin, and quercetin showed stronger *in vitro* inhibition of α -glucosidase than acarbose, the positive control, with K_i values significantly lower ($p < 0.05$) than acarbose. In contrast, the efficacy of rosmarinic acid was similar to that of acarbose for the inhibition of α -glucosidase with a K_i value not significantly different ($p > 0.05$) from that of acarbose. Jhong *et al.* (Jhong *et al.*, 2015) also reported more potent inhibition of α -glucosidase by curcumin and quercetin compared to acarbose. In this study, the IC_{50} values were used for comparison, with the IC_{50} values of curcumin and quercetin being lower than that of acarbose. No data have previously been reported for the inhibition of α -glucosidase by 18α -GA, although, Ko *et al.* (Ko *et al.*, 2007) reported some antidiabetic properties for 18α -GA related to insulin-stimulated glucose uptake in adipocytes.

None of the selected compounds showed stronger *in vitro* inhibition of pancreatic α -amylase than acarbose, with the K_i value of acarbose being significantly lower than that of the selected compounds. The increasing order of K_i values was as follows (Table 12) acarbose < curcumin

< quercetin < 18 α -GA < rosmarinic acid < quinic acid < nerolidol, where a lower K_i indicates more potent inhibition. Of the compounds evaluated, curcumin had the most potent inhibition. Likewise Jhong *et al.* (Jhong *et al.*, 2015), showed that curcumin had more potent inhibition of pancreatic α -amylase than quercetin with the IC_{50} of curcumin being lower than that of quercetin. In the latter study, a more potent inhibition of pancreatic α -amylase by curcumin and quercetin compared with acarbose, with their IC_{50} values being lower than that of acarbose. Although some compounds showed mild inhibition of α -amylase, this may be preferred as it may help prevent excessive bacterial fermentation that can lead to adverse gastrointestinal side effects (Etxeberria *et al.*, 2012, Tolmie *et al.*, 2021).

Kinetics studies not only helped us determine the inhibitory constant; it was also used to determine the type of inhibition of the compounds. For example, acarbose is a competitive inhibitor of α -glucosidase and a mixed inhibitor of α -amylase (Kim *et al.*, 1999, Proena *et al.*, 2017). In this study, the type of inhibition of acarbose was confirmed, with competitive and mixed inhibition of α -glucosidase and α -amylase, respectively. In addition, this study also determined the type of inhibition of curcumin, 18 α -GA, quercetin, and rosmarinic acid in the inhibition of α -glucosidase and α -amylase, as seen in Tables 11 and 12. Although indicating a weaker inhibition of α -glucosidase, nerolidol and quinic acid, as competitive inhibitors, had the same mode of action as acarbose for the inhibition of α -glucosidase. Curcumin, 18 α -GA, rosmarinic acid and quinic acid being mixed inhibitors of α -amylase, these compounds had the same mode of action as acarbose for the inhibition of α -amylase.

1.28. *In vitro* cytotoxicity

The cytotoxicity of the promising compounds against C2C12, HepG2, and Caco2 cells was quantified after 48 hours exposure with the SRB assay and the IC_{50} was calculated.

Cytotoxicity in the Caco2 cells was used to predict the effect of the tested compounds in the small intestine where both carbohydrate hydrolysing enzymes are located. For curcumin and rosmarinic acid, IC_{50} values of 15 and 83 μ M, respectively could be determined while for the remaining compounds at the highest concentration of 100 μ M, a 50% toxicity could not be determined. A study by (Şueki *et al.*, 2019) showed that Caco2 cells are more resistant to curcumin where at 50 μ M only 16.2% toxicity was observed in Caco2 cells after 24 hours exposure.

In the C2C12 cell line, curcumin, quinic acid, and nerolidol were not toxic even at 100 μM the highest concentration used. The compounds for which the IC_{50} could be determined were $18\alpha\text{-GA} > \text{acarbose} > \text{rosmarinic acid} > \text{quercetin}$ with IC_{50} values of 24 ± 1 , 60 ± 15 , 81 ± 17 and 87 ± 20 μM , respectively. A study by (Tolmie *et al.*, 2021) reported IC_{50} values of 83 and 60 μM for rosmarinic acid and acarbose in C2C12 cells, which are similar to the findings of the present study. In another study by (Chen *et al.*, 2020) quercetin showed no toxicity in C2C12 cells at a concentration as high as 100 μM after 24 hours exposure compared to the 50% toxicity at a concentration of 87 μM in the present study after 72 hours. Toxicity is dependent on dosage, exposure time and the assay used for quantification. Increased exposure time will show a time related increase in toxicity and may account for the observed differences. Recently limited cytotoxicity of curcumin was reported even at a concentration of 100 μM (Septisetyani *et al.*, 2020).

Rosmarinic acid, acarbose, quinic acid, and nerolidol were not cytotoxic in the HepG2 cell line. The IC_{50} values for $18\alpha\text{-GA} > \text{curcumin} > \text{quercetin}$ was 28 ± 8 , 41 ± 2 , 54 ± 2 μM , respectively. This confirms the findings of (Tolmie *et al.*, 2021) who reported a lack of toxicity in the same cell line even at concentrations as high as 500 μM .

The different cell lines responded differently to the compounds and may be related to the doubling times and cellular metabolism related to cellular ADMET, with HepG2 and C2C12 cells being more sensitive. For example, for $18\alpha\text{-GA}$, an IC_{50} was obtained in the C2C12 and HepG2 cell lines but not in the CaCo-2 cell line. The highest concentrations used in the glucose uptake studies in the C2C12 and HepG2 cell lines was 100 μM , and exposure was only for 45 min, probably not sufficient to have any cytotoxic effects considering that cytotoxicity is also time dependent. Likewise, for the lipid accumulation studies, the HepG2 cells were exposed to 10 μM of the compounds for 48 hours, where these compounds would have limited toxicity. Microscopy images of HepG2 cells exposed to OA (Figure 22) and the compounds also show the lack of cellular features associated with toxicity.

1.29. *In vitro* glucose uptake

The ability of the promising compounds to stimulate glucose uptake in C2C12 and HepG2 cells was determined using the 2-NBDG assay. Both cell lines represent insulin target tissue where insulin stimulates glucose uptake through the translocation of glucose transporters. The positive controls, insulin and metformin did not increase glucose uptake in the studied cells.

Likewise, a study by (Zou *et al.*, 2005) observed no glucose uptake in HepG2 cells when treated with insulin and metformin. In contrast, anti-diabetic drugs such as rosiglitazone, glibenclamide, and chiglitazar mediated cellular glucose uptake possibly through mechanisms different from insulin (Zou *et al.*, 2005). Another study by (Park *et al.*, 2014) showed an increase in cellular glucose uptake in differentiated C2C12 cells in the presence of 100 nM insulin compared to untreated cells. No change in glucose uptake was found for the compounds investigated in this study.

A study by (Yamamoto *et al.*, 2015) identified the advantages and disadvantages of the 2-NBDG assay where the method of quantification is a major consideration with quantification of microscopic images being the method of choice rather than plate formats. In other studies (Zhang *et al.*, 2010, Kim *et al.*, 2012) measured glucose uptake in HepG2 and C2C12 cells by first inducing insulin resistance prior to adding specific drugs to evaluate subsequent glucose uptake. In contrast, in the present study, the cell lines were not insulin resistant, and rather the direct effects on glucose uptake were studied. This is an important aspect that should be included in future studies.

1.30. *Hepatic lipid accumulation*

Rosmarinic acid and 18 α -GA caused the highest decrease in hepatic lipid accumulation at 10 μ M compared with the other compounds. A study by (Balachander *et al.*, 2018) showed similar results to the present study where both rosmarinic acid and metformin significantly reduced OA induced lipid accumulation in HepG2 cells and can be considered potential compounds in the management of NAFLD. Curcumin reduced lipid accumulation in OA induced HepG2 cells after 24 hours exposure (Kang *et al.*, 2013). Likewise (Vidyashankar *et al.*, 2013, Li *et al.*, 2013) also found a reduction in hepatic OA induced lipid accumulation by quercetin, and the proposed mechanism was the enhancement of tyrosine phosphate and downregulation of the levels of sterol regulatory element-binding protein-1c (SREBP-1c).

In the present study, the promising compounds improved hepatic lipid accumulation and can be used as a potential treatment in NAFLD by decreasing OA induced lipid accumulation while also taking into consideration the bioavailability scores (Table 10). The present study confirms the findings of previous studies for curcumin, rosmarinic acid and quercetin but the beneficial effects for 18 α -GA, quinic acid and nerolidol have not yet been reported.

Furthermore, there are suggestions that the mode of action involved in the reduction of lipid accumulation may involve pathways such as: insulin signalling, lipogenic enzymes, cholesterol biosynthesis, TG biosynthesis, and fatty acid β -oxidation and should be evaluated in more detailed studies.

Several different herbs and spices can be a source of these compounds, and screening of herbs and spices identified Turmeric as a rich source of curcumin, and Rosemary as a rich source of rosmarinic acid (Table 18). An identified rich source of these bioactive molecules was green tea, where the polyphenols in green tea have been identified to contribute to the antidiabetic activity of green tea (Juśkiewicz *et al.*, 2008, Polychronopoulos *et al.*, 2008).

1.31. Qualitative and quantitative analysis of green tea

The levels of quinic acid, EGCG and ECG were determined in Dilmah, Eve's, Five Roses and Livewell green tea. Levels of quinic acid, EGCG and ECG were similar in all teas. Quinic acid and epicatechin gallate levels were the highest in Dilmah tea while the levels of ECG were the highest in Eve's tea.

In the present study the anti-diabetic effect of green tea brands related to the inhibition of α -amylase and α -glucosidase was also evaluated. Lower IC_{50} values were observed in the inhibition of α -glucosidase than α -amylase, showing that green tea is a better inhibitor of α -glucosidase. In a previous study, *Camellia sinensis* green tea was shown to be a more potent inhibitor of α -glucosidase and a less potent inhibitor of α -amylase than acarbose (Yilmazer-Musa *et al.*, 2012).

Among the five green tea brands, Dilmah and Livewell showed better inhibition of both enzymes than Eve's and Five Roses. A metabolomic approach was taken to analyse the difference between the tea brands to identify the best tea related to enzyme inhibition. PCA showed an apparent clustering of Dilmah and Eve's while the other brands clustered together. The PCA plot in Figure 25 shows that the good inhibitors clustered on the negative side, while the poor inhibitors were located on the positive side of the T score [1]. This finding was confirmed with the volcano plot in Figure 26B; 35.5% of the total metabolites were significantly different between the good and poor inhibitors.

The ability of the green tea brands to inhibit the enzymes may be linked to the metabolites that are present. The difference among them may be linked to the % w/v dry weight of the

compounds present in the green tea brands. Epigallocatechin and ECG are potent inhibitors of α -glucosidase and have been quantified in the five green tea brands (Yang *et al.*, 2019, Li *et al.*, 2010). In the present study, the levels in Dilmah tea were higher than those in the other green tea brands, which may be linked to the inhibitory activity of Dilmah. Although Eve's tea is identified as a poor inhibitor, it contains significant amounts of epigallocatechin and ECG. Two conclusions can therefore be drawn: the first is that - other metabolites may contribute to activity, and secondly although differences are statistically different the biological effects may be similar. Therefore, to address the possible role of additional metabolites, it was necessary to identify and annotate other peaks using software applications such as MSDIAL and MSFINDER. This software helps to identify metabolite differences among the green tea brands.

Using the peak areas, identified standards and unidentified selected peaks were screened for correlations with the enzyme inhibition. Unidentified peaks 3 and 5 (UP3 and UP5) showed better or similar correlations to some authentic standards, therefore, it was necessary to putatively identify the two peaks. Using previous studies as well as different databases www.pubchem.ncbi.nlm.nih.gov/ and www.genome.jp/kegg/compound/, gallic acid and galocatechin were identified as the compounds occupying UP3 and UP5, respectively. These compounds might be among the compounds that contributed to the activity of the green tea brands to inhibit α -amylase and α -glucosidase, however, an individual *in vitro* testing of these compounds in the inhibition of both α -amylase and α -glucosidase together with reviews of previous studies will help strengthen this assumption. Gallic acid showed strong inhibition of starch hydrolysing enzymes in previous studies (Limanto *et al.*, 2019, Gutierrez *et al.*, 2020) with an IC_{50} better than acarbose. Gallic acid has been reported to play a role in the quality of green tea (Le Gall *et al.*, 2004), and it has been quantified in Chinese green tea products at a concentration of 0.52 mg per 100 mg green tea (Lin *et al.*, 1998). Gallocatechin is part of the catechin family, which is known to have inhibitory activities against starch hydrolysing enzymes, and it has been reported to be present in green tea at a concentration of 0.30 mg per 100 mg green tea (Lee *et al.*, 2014). These findings may explain the positive correlations observed in the present study, and relative to the amount of gallic acid and gallocatechin in green tea, doses of 2.50 g and 7.90 g of green tea relate to the 50 mg acarbose per meal, respectively.

Lastly, it will be important to determine the biological relevance of the significant differences observed related to enzyme inhibition using a diabetic rat model such as DM induction in db/db or ob/ob mice that are extremely obese and mimic human T2DM with hyperglycemia and hyperinsulinemia as major defects (Jeong *et al.*, 2012), and it will also be important to determine the concentration of these compounds in water extracts mimicking tea consumption.

Conclusion

Based on the obtained results, the first null hypothesis is rejected for α -amylase inhibition by the promising compounds. For α -glucosidase, the first null hypothesis is rejected for 18 α -GA, curcumin, and quercetin and is not rejected for the inhibition of α -glucosidase by rosmarinic acid. There is a positive relationship between the *in vitro* and *in silico* studies for pancreatic α -amylase and intestinal α -glucosidase inhibition, this was evaluated by using correlation coefficients.

The second null hypothesis is not rejected; however, uptake studies should be undertaken in an insulin resistant model, mimicking T2DM.

The third null hypothesis is not rejected; the control, metformin and the compounds reduced OA induced lipid accumulation in HepG2 cells, and the mode of action is related to metabolic pathways linked with lipogenesis.

Curcumin, 18 α -GA, quercetin, and rosmarinic acid inhibited α -glucosidase, and decreased hepatic lipid accumulation, indicating the potential of these compounds to alleviate the prolonged hyperglycemia and potentially manage NAFLD.

Many of these compounds are found in herbs, spices, and teas which are cost-effective, easily cultivated, and readily available. For example, curcumin is found abundantly in Turmeric and EGCG in green tea and is specifically more abundant in Eve's green tea brand. Related to the levels of curcumin in Turmeric, a dose of 1.3 g relates to the 50 mg dose of acarbose per meal. For green tea, 1.2 g of green tea is required and as one teabag contains 2.5 g green tea; one cup of green tea per meal may help prevent prolonged hyperglycaemia.

In addition, green tea was also found to be a rich source of quinic acid as well as other polyphenols, such as EGCG and epicatechin, with reported anti-diabetic effects. Further

studies determined the levels of these compounds in several green tea brands with the purpose of identifying the best tea brand related to the inhibition of α -amylase and α -glucosidase activity. Analysis confirmed that green tea strongly inhibited α -glucosidase, and if consumed with a meal may prevent the development of hyperglycemia. Furthermore, synergism between compounds and other unidentified compounds may have further beneficial effect/s and future research can focus on these aspects.

References

- Adams, S. M. & Standridge, J. B. 2006. What should we eat? Evidence from observational studies. *Southern medical journal*, 99, 744-749.
- Adan, A., Kiraz, Y. & Baran, Y. 2016. Cell proliferation and cytotoxicity assays. *Current Pharmaceutical Biotechnology*, 17, 1213-1221.
- Adefegha, A., Oboh, G., Akinyemi, A. & Ademiluyi, A. 2010. Inhibitory effects of aqueous extract of two varieties of ginger on some key enzymes linked to type-2 diabetes in vitro. *Journal of Food and Nutrition Research*, 49, 14-20.
- Adefegha, S. A. & Oboh, G. 2012. Inhibition of key enzymes linked to type 2 diabetes and sodium nitroprusside-induced lipid peroxidation in rat pancreas by water extractable phytochemicals from some tropical spices. *Pharmaceutical Biology*, 50, 857-865.
- Adelakun, O. E., Bolarinwa, I. F. & Adejuyitan, J. A. 2018. Bioactive Compounds in Plants and Their Antioxidant Capacity. *Bioactive Compounds of Medicinal Plants*. Apple Academic Press, 4, 13-34.
- Andres, S., Pevny, S., Ziegenhagen, R., Bakhiya, N., Schäfer, B., Hirsch-Ernst, K. I. & Lampen, A. 2018. Safety aspects of the use of quercetin as a dietary supplement. *Molecular Nutrition and Food Research*, 62, 1700447. <https://doi.org/10.1002/mnfr.201700447>
- Aronov, A. M. 2005. Predictive in silico modeling for hERG channel blockers. *Drug Discovery Today*, 10, 149-155.
- Association, A. D. 2004. Gestational diabetes mellitus. *Diabetes Care*, 27, s88-s90.
- Association, A. D. 2014. Diagnosis and classification of diabetes mellitus. *Diabetes Care*, 37, S81-S90.
- Atkinson, M. A., Eisenbarth, G. S. & Michels, A. W. 2014. Type 1 diabetes. *The Lancet*, 383, 69-82.
- Balachander, G. J., Subramanian, S. & Ilango, K. 2018. Rosmarinic acid attenuates hepatic steatosis by modulating ER stress and autophagy in oleic acid-induced HepG2 cells. *RSC Advances*, 8, 26656-26663.
- Berman, H. M., Westbrook, J., Feng, Z., Gilliland, G., Bhat, T. N., Weissig, H., Shindyalov, I. N. & Bourne, P. E. 2000. The protein data bank. *Nucleic Acids Research*, 28, 235-242.
- Bhachoo, J. & Beuming, T. 2017. Investigating protein-peptide interactions using the Schrödinger computational suite. *Modeling Peptide-protein Interactions*, 235-254.

- Bhandari, M. R., Jong-Anurakkun, N., Hong, G. & Kawabata, J. 2008. α -Glucosidase and α -amylase inhibitory activities of Nepalese medicinal herb Pakhanbhed (*Bergenia ciliata*, Haw.). *Food Chemistry*, 106, 247-252.
- Burlingham, B. T. & Widlanski, T. S. 2003. An intuitive look at the relationship of K_i and IC_{50} : a more general use for the Dixon plot. *Journal of Chemical Education*, 80, 214-218.
- Campbell, M. K., Farrell, S. O. & McDougal, O. M. 2018. *Biochemistry*, Boston, MA, Cengage Learning.
- Cernea, S. & Dobreanu, M. 2013. Diabetes and beta cell function: from mechanisms to evaluation and clinical implications. *Biochemia Medica: Biochemia Medica*, 23, 266-280.
- Chatterjee, S., Khunti, K. & Davies, M. J. 2017. Type 2 diabetes. *The Lancet*, 389, 2239-2251.
- Chatzigeorgiou, A., Halapas, A., Kalafatakis, K. & Kamper, E. 2009. The use of animal models in the study of diabetes mellitus. *In vivo*, 23, 245-258.
- Chen, C., Yang, J.-S., Lu, C.-C., Chiu, Y.-J., Chen, H.-C., Chung, M.-I., Wu, Y.-T. & Chen, F.-A. 2020. Effect of quercetin on dexamethasone-induced C2C12 skeletal muscle cell injury. *Molecules*, 25, 3267.
- Christensen, K. B., Minet, A., Svenstrup, H., Grevsen, K., Zhang, H., Schrader, E., Rimbach, G., Wein, S., Wolffram, S. & Kristiansen, K. 2009. Identification of plant extracts with potential antidiabetic properties: effect on human peroxisome proliferator-activated receptor (PPAR), adipocyte differentiation and insulin-stimulated glucose uptake. *Phytotherapy Research: An International Journal Devoted to Pharmacological and Toxicological Evaluation of Natural Product Derivatives*, 23, 1316-1325.
- Clissold, S. P. & Edwards, C. 1988. Acarbose. *Drugs*, 35, 214-243.
- DeLeon, M. J., Chandurkar, V., Albert, S. G. & Mooradian, A. D. 2002. Glucagon-like peptide-1 response to acarbose in elderly type 2 diabetic subjects. *Diabetes Research and Clinical Practice*, 56, 101-106.
- Deshpande, A. D., Harris-Hayes, M. & Schootman, M. 2008. Epidemiology of diabetes and diabetes-related complications. *Physical Therapy*, 88, 1254-1264.
- Dewangan, H., Tiwari, R. K., Sharma, V., Shukla, S. S., Satapathy, T. & Pandey, R. 2017. Past and Future of in-vitro and in-vivo Animal Models for Diabetes: A Review. *Indian Journal of Pharmaceutical Education and Research*, 51, s522-s530.
- Egan, A. M. & Dinneen, S. F. 2019. What is diabetes? *Medicine*, 47, 1-4.

- Ekins, S., Mestres, J. & Testa, B. 2007. *In silico* pharmacology for drug discovery: applications to targets and beyond. *British Journal of Pharmacology*, 152, 21-37.
- El-Sayed, S. M. & Youssef, A. M. 2019. Potential application of herbs and spices and their effects in functional dairy products. *Heliyon*, 5, e01989.
- Eldridge, M. D., Murray, C. W., Auton, T. R., Paolini, G. V. & Mee, R. P. 1997. Empirical scoring functions: I. The development of a fast empirical scoring function to estimate the binding affinity of ligands in receptor complexes. *Journal of Computer-Aided Molecular Design*, 11, 425-445.
- Emeka, N. K., Bola, A. & Gail, M. 2018. Phytochemistry and Antifungal Activity of *Desmodium adscendens* Root Extracts. *Bioactive Compounds of Medicinal Plants*. Apple Academic Press, 1, 4-12.
- Esmaeili, S., Naghibi, F., Mosaddegh, M. & Nader, N. 2010. Determination of 18?-Glycyrrhetic Acid in *Glycyrrhiza glabra* L. Extract by HPLC. *Iranian Journal of Pharmaceutical Research*, 137-141.
- Etxeberria, U., de la Garza, A. L., Campión, J., Martínez, J. A. & Milagro, F. I. 2012. Antidiabetic effects of natural plant extracts via inhibition of carbohydrate hydrolysis enzymes with emphasis on pancreatic alpha amylase. *Expert Opinion on Therapeutic Targets*, 16, 269-297.
- Foretz, M., Hébrard, S., Leclerc, J., Zarrinpashneh, E., Soty, M., Mithieux, G., Sakamoto, K., Andreelli, F. & Viollet, B. 2010. Metformin inhibits hepatic gluconeogenesis in mice independently of the LKB1/AMPK pathway via a decrease in hepatic energy state. *The Journal of Clinical Investigation*, 120, 2355-2369.
- Friesner, R. A., Banks, J. L., Murphy, R. B., Halgren, T. A., Klicic, J. J., Mainz, D. T., Repasky, M. P., Knoll, E. H., Shelley, M. & Perry, J. K. 2004. Glide: a new approach for rapid, accurate docking and scoring. 1. Method and assessment of docking accuracy. *Journal of Medicinal Chemistry*, 47, 1739-1749.
- Goel, A., Kunnumakkara, A. B. & Aggarwal, B. B. 2008. Curcumin as "Curecumin": from kitchen to clinic. *Biochemical Pharmacology*, 75, 787-809.
- Goldstein, B. J. 2002. Insulin resistance as the core defect in type 2 diabetes mellitus. *The American journal of Cardiology*, 90, 3-10.
- Griffin, M. E., Marcucci, M. J., Cline, G. W., Bell, K., Barucci, N., Lee, D., Goodyear, L. J., Kraegen, E. W., White, M. F. & Shulman, G. I. 1999. Free fatty acid-induced insulin

- resistance is associated with activation of protein kinase C theta and alterations in the insulin signaling cascade. *Diabetes*, 48, 1270-1274.
- Güemes, M., Rahman, S. A. & Hussain, K. 2016. What is a normal blood glucose? *Archives of Disease in Childhood*, 101, 569-574.
- Gutierrez, A. S. A., Guo, J., Feng, J., Tan, L. & Kong, L. 2020. Inhibition of starch digestion by gallic acid and alkyl gallates. *Food Hydrocolloids*, 102, 105603-105630.
- Hamza, A., Wei, N.-N. & Zhan, C.-G. 2012. Ligand-based virtual screening approach using a new scoring function. *Journal of Chemical Information and Modeling*, 52, 963-974.
- Hana, C. A., Klebermass, E.-M., Balber, T., Mitterhauser, M., Quint, R., Hirtl, Y., Klimpke, A., Somloi, S., Hutz, J. & Sperr, E. 2020. Inhibition of lipid accumulation in skeletal muscle and liver cells: a protective mechanism of bilirubin against diabetes mellitus type 2. *Frontiers in Pharmacology*, 11, 636533-636547.
- Hardt, P. D., Brendel, M. D., Kloer, H. U. & Bretzel, R. G. 2008. Is pancreatic diabetes (type 3c diabetes) underdiagnosed and misdiagnosed? *Diabetes Care*, 31, S165-S169.
- Hedley, P. L., Jørgensen, P., Schlamowitz, S., Wangari, R., Moolman-Smook, J., Brink, P. A., Kanters, J. K., Corfield, V. A. & Christiansen, M. 2009. The genetic basis of long QT and short QT syndromes: a mutation update. *Human Mutation*, 30, 1486-1511.
- Heine, R., Diamant, M., Mbanya, J. & Nathan, D. 2006. Management of hyperglycaemia in type 2 diabetes: the end of recurrent failure? *British Medical Journal*, 333, 1200-1204.
- Higdon, J. V. & Frei, B. 2003. Tea catechins and polyphenols: health effects, metabolism, and antioxidant functions. *Food Science and Nutrition*, 43, 89-143.
- Hirohara, M., Saito, Y., Koda, Y., Sato, K. & Sakakibara, Y. 2018. Convolutional neural network based on SMILES representation of compounds for detecting chemical motif. *BMC Bioinformatics*, 19, 84-94.
- Huang, W.-C., Chen, Y.-L., Liu, H.-C., Wu, S.-J. & Liou, C.-J. 2018. Ginkgolide C reduced oleic acid-induced lipid accumulation in HepG2 cells. *Saudi Pharmaceutical Journal*, 26, 1178-1184.
- Hwang, J.-H., Perseghin, G., Rothman, D. L., Cline, G. W., Magnusson, I., Petersen, K. F. & Shulman, G. I. 1995. Impaired net hepatic glycogen synthesis in insulin-dependent diabetic subjects during mixed meal ingestion. A ¹³C nuclear magnetic resonance spectroscopy study. *The Journal of Clinical Investigation*, 95, 783-787.
- IDF, I. D. F. 2019. Diabetes atlas. *International Diabetes Federation*. 9 ed. Brussels.

- Ioakimidis, L., Thoukydidis, L., Mirza, A., Naeem, S. & Reynisson, J. 2008. Benchmarking the reliability of QikProp. Correlation between experimental and predicted values. *QSAR & Combinatorial Science*, 27, 445-456.
- Jain, A. N. 2006. Scoring functions for protein-ligand docking. *Current Protein and Peptide Science*, 7, 407-420.
- Jayaraj, S., Suresh, S. & Kadeppagari, R. K. 2013. Amylase inhibitors and their biomedical applications. *Starch-Stärke*, 65, 535-542.
- Jeong, S.-M., Kang, M.-J., Choi, H.-N., Kim, J.-H. & Kim, J.-I. 2012. Quercetin ameliorates hyperglycemia and dyslipidemia and improves antioxidant status in type 2 diabetic db/db mice. *Nutrition Research and Practice*, 6, 201-207.
- Jhong, C. H., Riyaphan, J., Lin, S. H., Chia, Y. C. & Weng, C. F. 2015. Screening alpha-glucosidase and alpha-amylase inhibitors from natural compounds by molecular docking in silico. *Biofactors*, 41, 242-251.
- Jin, Y., Zhao, J., Kim, E. M., Kim, K. H., Kang, S., Lee, H. & Lee, J. 2019. Comprehensive investigation of the effects of brewing conditions in sample preparation of green tea infusions. *Molecules*, 24, 1735.
- Juśkiewicz, J., Zduńczyk, Z., Jurgoński, A., Brzuzan, Ł., Godycka-Kłós, I. & Żary-Sikorska, E. 2008. Extract of green tea leaves partially attenuates streptozotocin-induced changes in antioxidant status and gastrointestinal functioning in rats. *Nutrition Research*, 28, 343-349.
- Kahn, S. E., Cooper, M. E. & Del Prato, S. 2014. Pathophysiology and treatment of type 2 diabetes: perspectives on the past, present, and future. *The Lancet*, 383, 1068-1083.
- Kang, O., Kim, S., Seo, Y., Joung, D., Mun, S., Choi, J., Lee, Y., Kang, D., Lee, H. & Kwon, D. 2013. Curcumin decreases oleic acid-induced lipid accumulation via AMPK phosphorylation in hepatocarcinoma cells. *European Review for Medical and Pharmacological Science*, 17, 2578-2586.
- Kanwal, A., Singh, S. P., Grover, P. & Banerjee, S. K. 2012. Development of a cell-based nonradioactive glucose uptake assay system for SGLT1 and SGLT2. *Analytical biochemistry*, 429, 70-75.
- Kato, C. G., Gonçalves, G. d. A., Peralta, R. A., Seixas, F. A. V., de Sá-Nakanishi, A. B., Bracht, L., Comar, J. F., Bracht, A. & Peralta, R. M. 2017. Inhibition of α -amylases by condensed

- and hydrolysable tannins: focus on kinetics and hypoglycemic actions. *Enzyme research*, 57(24), 902-914.
- Khacheba, I., Djeridane, A. & Yousfi, M. 2014. Twenty traditional Algerian plants used in diabetes therapy as strong inhibitors of α -amylase activity. *International Journal of Carbohydrate Chemistry*, 28(72), 81-93.
- Kim, M.-J., Lee, S.-B., Lee, H.-S., Lee, S.-Y., Baek, J.-S., Kim, D., Moon, T.-W., Robyt, J. F. & Park, K.-H. 1999. Comparative study of the inhibition of α -glucosidase, α -amylase, and cyclomaltodextrin glucanotransferase by acarbose, isoacarbose, and acarviosine-glucose. *Archives of Biochemistry and Biophysics*, 371, 277-283.
- Kim, M. S., Hur, H. J., Kwon, D. Y. & Hwang, J.-T. 2012. Tangeretin stimulates glucose uptake via regulation of AMPK signaling pathways in C2C12 myotubes and improves glucose tolerance in high-fat diet-induced obese mice. *Molecular and Cellular Endocrinology*, 358, 127-134.
- Ko, B.-S., Jang, J. S., Hong, S. M., Sung, S. R., Lee, J. E., Lee, M. Y., Jeon, W. K. & Park, S. 2007. Changes in components, glycyrrhizin and glycyrrhetic acid, in raw *Glycyrrhiza uralensis* Fisch, modify insulin sensitizing and insulinotropic actions. *Bioscience, Biotechnology, and Biochemistry*, 71, 60533_1-60533_10.
- Kola, I. & Landis, J. 2004. Can the pharmaceutical industry reduce attrition rates? *Nature Reviews Drug Discovery*, 3, 711-716.
- Korfmacher, W. A. 2005. Foundation review: Principles and applications of LC-MS in new drug discovery. *Drug Discovery Today*, 10, 1357-1367.
- Kota, S. K., Meher, L. K., Jammula, S., Kota, S. K. & Modi, K. D. 2012. Genetics of type 2 diabetes mellitus and other specific types of diabetes; its role in treatment modalities. *Diabetes and Metabolic Syndrome: Clinical Research and Reviews*, 6, 54-58.
- Lai, Z., Tsugawa, H., Wohlgemuth, G., Mehta, S., Mueller, M., Zheng, Y., Ogiwara, A., Meissen, J., Showalter, M. & Takeuchi, K. 2018. Identifying metabolites by integrating metabolome databases with mass spectrometry cheminformatics. *Nature Methods*, 15, 53-56.
- Le Gall, G., Colquhoun, I. J. & Defernez, M. 2004. Metabolite profiling using ^1H NMR spectroscopy for quality assessment of green tea, *Camellia sinensis* (L.). *Journal of Agricultural and Food Chemistry*, 52, 692-700.

- Lee, L.-S., Kim, S.-H., Kim, Y.-B. & Kim, Y.-C. 2014. Quantitative analysis of major constituents in green tea with different plucking periods and their antioxidant activity. *Molecules*, 19, 9173-9186.
- Lee, S. Y., Mediani, A., Ismail, I. S. & Abas, F. 2019. Antioxidants and α -glucosidase inhibitors from *Neptunia oleracea* fractions using ^1H NMR-based metabolomics approach and UHPLC-MS/MS analysis. *BMC Complementary and Alternative Medicine*, 19, 1-15.
- Lesjak, M., Beara, I., Simin, N., Pintać, D., Majkić, T., Bekvalac, K., Orčić, D. & Mimica-Dukić, N. 2018. Antioxidant and anti-inflammatory activities of quercetin and its derivatives. *Journal of Functional Foods*, 40, 68-75.
- Lewis-Beck, M. S. & Skalaban, A. 1990. The R-squared: Some straight talk. *Political Analysis*, 2, 153-171.
- Li, D.-Q., Qian, Z.-M. & Li, S.-P. 2010. Inhibition of three selected beverage extracts on α -glucosidase and rapid identification of their active compounds using HPLC-DAD-MS/MS and biochemical detection. *Journal of Agricultural and Food Chemistry*, 58, 6608-6613.
- Li, J.-y., Cao, H.-y., Liu, P., Cheng, G.-h. & Sun, M.-y. 2014. Glycyrrhizic acid in the treatment of liver diseases: literature review. *BioMed Research International*, 87(21), 39-54.
- Li, X., Wang, R., Zhou, N., Wang, X., Liu, Q., Bai, Y., Bai, Y., Liu, Z., Yang, H. & Zou, J. 2013. Quercetin improves insulin resistance and hepatic lipid accumulation in vitro in a NAFLD cell model. *Biomedical Reports*, 1, 71-76.
- Limanto, A., Simamora, A., Santoso, A. W. & Timotius, K. H. 2019. Antioxidant, α -glucosidase inhibitory activity and molecular docking study of gallic acid, quercetin and rutin: a comparative study. *Molecular and Cellular Biomedical Sciences*, 3, 67-74.
- Lin, J.-K., Lin, C.-L., Liang, Y.-C., Lin-Shiau, S.-Y. & Juan, I.-M. 1998. Survey of catechins, gallic acid, and methylxanthines in green, oolong, pu-erh, and black teas. *Journal of Agricultural and Food Chemistry*, 46, 3635-3642.
- Lin, L.-Z., Chen, P. & Harnly, J. M. 2008. New phenolic components and chromatographic profiles of green and fermented teas. *Journal of Agricultural and food chemistry*, 56, 8130-8140.
- Lipinski, C. A. 2004. Lead-and drug-like compounds: the rule-of-five revolution. *Drug Discovery Today: Technologies*, 1, 337-341.

- Lipinski, C. A., Lombardo, F., Dominy, B. W. & Feeney, P. J. 1997. Experimental and computational approaches to estimate solubility and permeability in drug discovery and development settings. *Advanced Drug Delivery Reviews*, 23, 3-25.
- Martin, A. E. & Montgomery, P. A. 1996. Acarbose: An α -glucosidase inhibitor. *American Journal of Health-System Pharmacy*, 53, 2277-2290.
- Meerza, D., Naseem, I. & Ahmed, J. 2013. Pharmacology of signaling pathways: In type 2 diabetes. *Diabetes & Metabolic Syndrome: Clinical Research & Reviews*, 7, 180-185.
- Mohan, V., Sandeep, S., Deepa, R., Shah, B. & Varghese, C. 2007. Epidemiology of type 2 diabetes: Indian scenario. *The Indian Journal of Medical Research*, 125, 217-30.
- Moore, D. S. & Kirkland, S. 2007. *The basic practice of statistics*, WH Freeman New York.
- Moore, M. C., Coate, K. C., Winnick, J. J., An, Z. & Cherrington, A. D. 2012. Regulation of hepatic glucose uptake and storage in vivo. *Advances in Nutrition*, 3, 286-294.
- Moore, R. J., Jackson, K. G. & Minihane, A. M. 2009. Green tea (*Camellia sinensis*) catechins and vascular function. *British Journal of Nutrition*, 102, 1790-1802.
- Murevanhema, Y. Y., Jideani, V. A. & Oguntibeju, O. O. 2018. Review on potential of seeds and value-added products of bambara groundnut (*Vigna subterranea*): Antioxidant, anti-inflammatory, and anti-oxidative Stress. *Bioactive Compounds of Medicinal Plants*. 141-188.
- Musial, C., Kuban-Jankowska, A. & Gorska-Ponikowska, M. 2020. Beneficial properties of green tea catechins. *International Journal of Molecular Sciences*, 21, 1744.
- Naimi, M., Vlacheski, F., Shamsoum, H. & Tsiani, E. 2017. Rosemary extract as a potential anti-hyperglycemic agent: current evidence and future perspectives. *Nutrients*, 9, 968-987.
- Nathan, D. M. & Group, D. E. R. 2014. The diabetes control and complications trial/epidemiology of diabetes interventions and complications study at 30 years: overview. *Diabetes Care*, 37, 9-16.
- Neveu, V., Perez-Jiménez, J., Vos, F., Crespy, V., du Chaffaut, L., Mennen, L., Knox, C., Eisner, R., Cruz, J. & Wishart, D. 2010. Phenol-Explorer: an online comprehensive database on polyphenol contents in foods. *Database*, 40(1), 1207-1215.
- Ngo, Y. L., Lau, C. H. & Chua, L. S. 2018. Review on rosmarinic acid extraction, fractionation and its anti-diabetic potential. *Food and Chemical Toxicology*, 121, 687-700.

- Nguyen, N. D. T. & Le, L. T. 2012. Targeted proteins for diabetes drug design. *Advances in Natural Sciences: Nanoscience and Nanotechnology*, 3, 013001-013010.
- Ntie-Kang, F. 2013. An in silico evaluation of the ADMET profile of the StreptomeDB database. *SpringerPlus*, 2, 1-11.
- O'Boyle, N. M. 2012. Towards a Universal SMILES representation-A standard method to generate canonical SMILES based on the InChI. *Journal of Cheminformatics*, 4, 22-36.
- O'Neil, R. G., Wu, L. & Mullani, N. 2005. Uptake of a fluorescent deoxyglucose analog (2-NBDG) in tumor cells. *Molecular Imaging and Biology*, 7, 388-392.
- Orellana, E. A. & Kasinski, A. L. 2016. Sulforhodamine B (SRB) assay in cell culture to investigate cell proliferation. *Bio-Protocol*, 6, 1984-1993.
- Ozougwu, V. & Akuba, B. 2018. In vitro Inhibition of Carbohydrate Metabolizing Enzymes and in vivo Anti-hyperglycaemic Potential of Methanol Extract of *Desmodium velutinum* Leaves. *Research Journal of Medicinal Plants*, 48, 56-66.
- Park, S. Y., Kim, M. H., Ahn, J. H., Lee, S. J., Lee, J. H., Eum, W. S., Choi, S. Y. & Kwon, H. Y. 2014. The stimulatory effect of essential fatty acids on glucose uptake involves both Akt and AMPK activation in C2C12 skeletal muscle cells. *The Korean Journal of Physiology & Pharmacology*, 18, 255-261.
- Pei, K., Gui, T., Kan, D., Feng, H., Jin, Y., Yang, Y., Zhang, Q., Du, Z., Gai, Z. & Wu, J. 2020. An overview of lipid metabolism and nonalcoholic fatty liver disease. *BioMed Research International*, 40, 249-261.
- Pereira, A. S., Banegas-Luna, A. J., Peña-García, J., Pérez-Sánchez, H. & Apostolides, Z. 2019. Evaluation of the Anti-Diabetic Activity of Some Common Herbs and Spices: Providing New Insights with Inverse Virtual Screening. *Molecules*, 24, 4030-4072.
- Pessin, J. E. & Saltiel, A. R. 2000. Signaling pathways in insulin action: molecular targets of insulin resistance. *The Journal of Clinical Investigation*, 106, 165-169.
- Petersen, M. 2013. Rosmarinic acid: new aspects. *Phytochemistry Reviews*, 12, 207-227.
- Petersen, M. & Simmonds, M. S. 2003. Rosmarinic acid. *Phytochemistry*, 62, 121-125.
- Petrovska, B. B. 2012. Historical review of medicinal plants' usage. *Pharmacognosy Reviews*, 6, 1-5.
- Pires, D. E., Blundell, T. L. & Ascher, D. B. 2015. pkCSM: predicting small-molecule pharmacokinetic and toxicity properties using graph-based signatures. *Journal of Medicinal Chemistry*, 58, 4066-4072.

- Polonsky, K. S. 2012. The past 200 years in diabetes. *New England Journal of Medicine*, 367, 1332-1340.
- Polychronopoulos, E., Zeimbekis, A., Kastorini, C.-M., Papairakleous, N., Vlachou, I., Bountziouka, V. & Panagiotakos, D. B. 2008. Effects of black and green tea consumption on blood glucose levels in non-obese elderly men and women from Mediterranean Islands (MEDIS epidemiological study). *European Journal of Nutrition*, 47, 10-16.
- Proença, C., Freitas, M., Ribeiro, D., Oliveira, E. F., Sousa, J. L., Tomé, S. M., Ramos, M. J., Silva, A. M., Fernandes, P. A. & Fernandes, E. 2017. α -Glucosidase inhibition by flavonoids: an in vitro and in silico structure–activity relationship study. *Journal of Enzyme Inhibition and Medicinal Chemistry*, 32, 1216-1228.
- Proença, C., Freitas, M., Ribeiro, D., Tomé, S. M., Oliveira, E. F., Viegas, M. F., Araújo, A. N., Ramos, M. J., Silva, A. M. & Fernandes, P. A. 2019. Evaluation of a flavonoids library for inhibition of pancreatic α -amylase towards a structure–activity relationship. *Journal of Enzyme Inhibition and Medicinal Chemistry*, 34, 577-588.
- Reaven, G. M., Hollenbeck, C., Jeng, C.-Y., Wu, M. S. & Chen, Y.-D. I. 1988. Measurement of plasma glucose, free fatty acid, lactate, and insulin for 24 h in patients with NIDDM. *Diabetes*, 37, 1020-1024.
- Rheeder, P. 2019. World Diabetes Day: Innovative Diabetes Care for South Africa done THE UP WAY.
- Saini, V. 2010. Molecular mechanisms of insulin resistance in type 2 diabetes mellitus. *World journal of diabetes*, 1, 68-75.
- Schrodinger 2012. *QikProp 3.5 user manual*, Schrodinger press.
- Schrodinger 2015. *Glide 6.7 User Manual*, Schrodinger Press.
- Septisetyani, E., Santoso, A., Wisnuwardhani, P. & Prasetyaningrum, P. Cytotoxic effects of chemopreventive agents curcumin, naringin and epigallocatechin-3-gallate in C2C12 myoblast cells. *IOP Conference Series: Earth and Environmental Science*, 439, 62-69.
- Sharma, R., Gescher, A. & Steward, W. 2005. Curcumin: the story so far. *European Journal of Cancer*, 41, 1955-1968.
- Shulman, G. I. 2000. Cellular mechanisms of insulin resistance. *The Journal of Clinical Investigation*, 106, 171-176.
- Smith, M. E. & Morton, D. G. 2001. *The digestive system*, Elsevier Health Sciences.

- Spessard, G. O. 1998. ACD Labs/LogP dB 3.5 and ChemSketch 3.5. *Journal of Chemical Information and Computer Sciences*, 38, 1250-1253.
- Srinivasan, K. 2005. Plant foods in the management of diabetes mellitus: spices as beneficial antidiabetic food adjuncts. *International Journal of Food Sciences and Nutrition*, 56, 399-414.
- Şueki, F., Ruhi, M. K. & Gülsoy, M. 2019. The effect of curcumin in antitumor photodynamic therapy: in vitro experiments with Caco-2 and PC-3 cancer lines. *Photodiagnosis and Photodynamic Therapy*, 27, 95-99.
- Tang, C. & Prueksaritanont, T. 2010. Use of in vivo animal models to assess pharmacokinetic drug-drug interactions. *Pharmaceutical Research*, 27, 1772-1787.
- Theerakittayakorn, K. & Bunprasert, T. 2011. Differentiation capacity of mouse L929 fibroblastic cell line compare with human dermal fibroblast. *World Academy of Science, Engineering and Technology International Journal of Medical and Health Sciences*, 5(51), 373-376.
- Tian, M., Yan, H. & Row, K. H. 2008. Extraction of glycyrrhizic acid and glabridin from licorice. *International Journal of Molecular Sciences*, 9, 571-577.
- Tiwari, N., Thakur, A. K., Kumar, V., Dey, A. & Kumar, V. 2014. Therapeutic targets for diabetes mellitus: an update. *Clinical Pharmacology Biopharmaceutics*, 3(1), 1000117-1000127.
- Tolmie, M., Bester, M. J. & Apostolides, Z. 2021. Inhibition of α -glucosidase and α -amylase by herbal compounds for the treatment of type 2 diabetes: A validation of *in silico* reverse docking with in vitro enzyme assays. *Journal of Diabetes*, 13(10), 779-791.
- Tsugawa, H., Cajka, T., Kind, T., Ma, Y., Higgins, B., Ikeda, K., Kanazawa, M., VanderGheynst, J., Fiehn, O. & Arita, M. 2015. MS-DIAL: data-independent MS/MS deconvolution for comprehensive metabolome analysis. *Nature Methods*, 12, 523-526.
- Turner, N., Zeng, X.-Y., Osborne, B., Rogers, S. & Ye, J.-M. 2016. Repurposing drugs to target the diabetes epidemic. *Trends in Pharmacological Sciences*, 37, 379-389.
- Vichai, V. & Kirtikara, K. 2006. Sulforhodamine B colorimetric assay for cytotoxicity screening. *Nature Protocols*, 1, 1112-1116.
- Vidyashankar, S., Varma, R. S. & Patki, P. S. 2013. Quercetin ameliorate insulin resistance and up-regulates cellular antioxidants during oleic acid induced hepatic steatosis in HepG2 cells. *Toxicology In-vitro*, 27, 945-953.

- Vijayakumar, S., Manogar, P., Prabhu, S. & Sanjeevkumar Singh, R. A. 2018. Novel ligand-based docking; molecular dynamic simulations; and absorption, distribution, metabolism, and excretion approach to analyzing potential acetylcholinesterase inhibitors for Alzheimer's disease. *Journal of Pharmaceutical Analysis*, 8, 413-420.
- Voet, D. & Voet, J. G. 2011. *Biochemistry*, New Jersey, John Wiley & sons ,Inc.
- Wang, P.-C., Zhao, S., Yang, B.-Y., Wang, Q.-H. & Kuang, H.-X. 2016. Anti-diabetic polysaccharides from natural sources: A review. *Carbohydrate Polymers*, 148, 86-97.
- Wilson, K. & Walker, J. M. 2010. *Principles and techniques of biochemistry and molecular biology*, Cambridge, UK ;, Cambridge University Press.
- Witkamp, R. F. & van Norren, K. 2018. Let thy food be thy medicine.... when possible. *European Journal of Pharmacology*, 836, 102-114.
- Xia, M.-F., Bian, H. & Gao, X. 2019. NAFLD and Diabetes: Two sides of the same coin? Rationale for gene-based personalized NAFLD treatment. *Frontiers in Pharmacology*, 877(10), 3889-3400.
- Xu, H. 2010. Inhibition kinetics of flavonoids on yeast α -glucosidase merged with docking simulations. *Protein and Peptide Letters*, 17, 1270-1279.
- Yamada, K., Nakata, M., Horimoto, N., Saito, M., Matsuoka, H. & Inagaki, N. 2000. Measurement of glucose uptake and intracellular calcium concentration in single, living pancreatic β -cells. *Journal of Biological Chemistry*, 275, 22278-22283.
- Yamamoto, N., Ueda-Wakagi, M., Sato, T., Kawasaki, K., Sawada, K., Kawabata, K., Akagawa, M. & Ashida, H. 2015. Measurement of glucose uptake in cultured cells. *Current Protocols in Pharmacology*, 71, 12.14. 1-12.14. 26.
- Yang, C.-Y., Yen, Y.-Y., Hung, K.-C., Hsu, S.-W., Lan, S.-J. & Lin, H.-C. 2019. Inhibitory effects of pu-erh tea on alpha glucosidase and alpha amylase: a systemic review. *Nutrition and Diabetes*, 9, 1-6.
- Yilmazer-Musa, M., Griffith, A. M., Michels, A. J., Schneider, E. & Frei, B. 2012. Inhibition of α -amylase and α -glucosidase activity by tea and grape seed extracts and their constituent catechins. *Journal of Agricultural and Food Chemistry*, 60, 8924-8929.
- Zhang, J., Liu, Y., Lv, J. & Li, G. 2015. A colorimetric method for α -glucosidase activity assay and its inhibitor screening based on aggregation of gold nanoparticles induced by specific recognition between phenylenediboronic acid and 4-aminophenyl- α -d-glucopyranoside. *Nano Research*, 8, 920-930.

- Zhang, W. Y., Lee, J.-J., Kim, I.-S., Kim, Y., Park, J.-S. & Myung, C.-S. 2010. 7-O-methylaromadendrin stimulates glucose uptake and improves insulin resistance in vitro. *Biological and Pharmaceutical Bulletin*, 33, 1494-1499.
- Zígolo, M. A., Salinas, M., Alché, L., Baldessari, A. & Liñares, G. G. 2018. Chemoenzymatic synthesis of new derivatives of glycyrrhetic acid with antiviral activity. Molecular docking study. *Bioorganic Chemistry*, 78, 210-219.
- Zou, C., Wang, Y. & Shen, Z. 2005. 2-NBDG as a fluorescent indicator for direct glucose uptake measurement. *Journal of Biochemical and Biophysical Methods*, 64, 207-215.

Annexures

1.32. Annexure A: Binding interactions

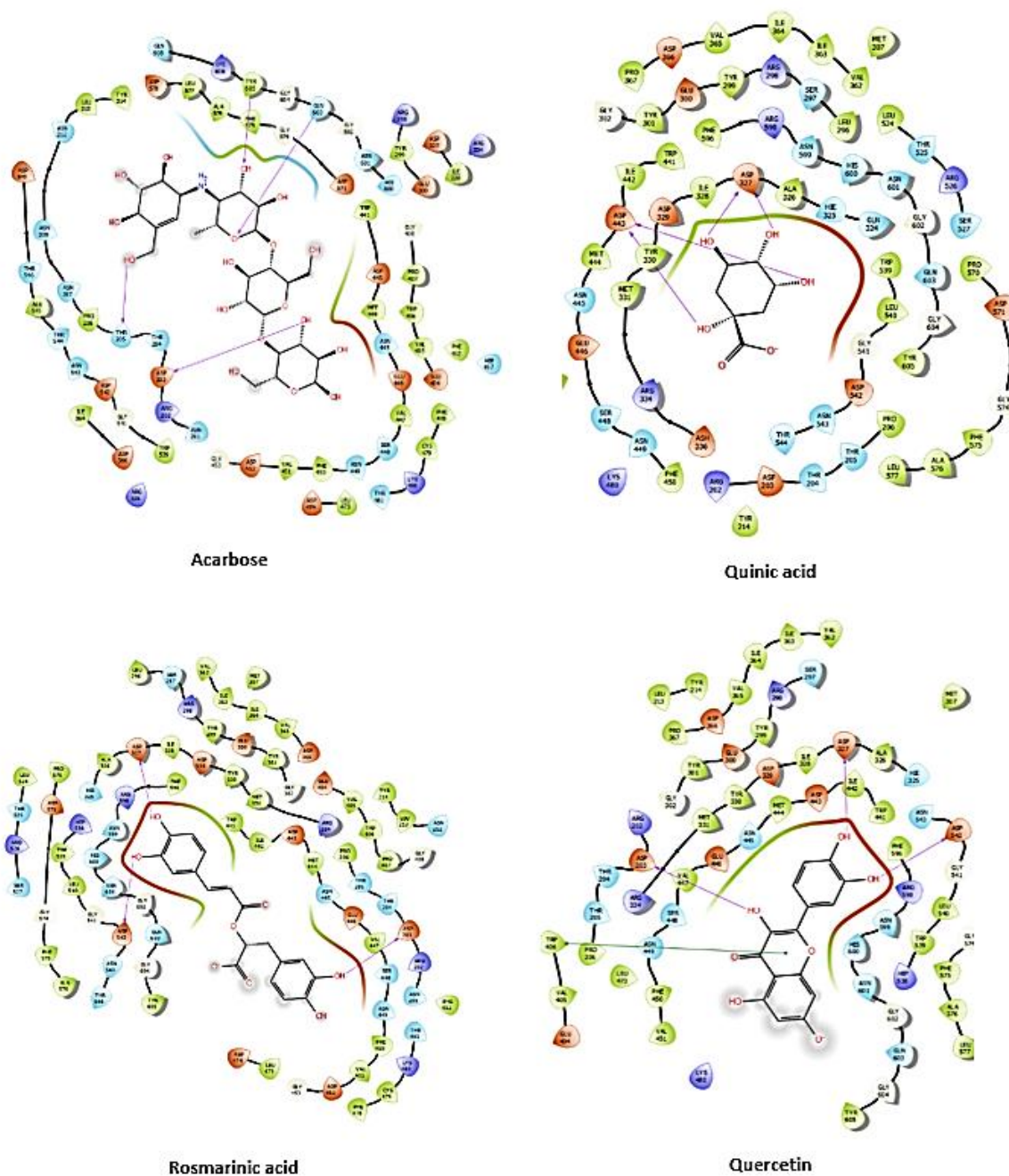


Figure A1. The interactions of acarbose, quinic acid, rosmarinic acid and quercetin in the binding pocket of α -glucosidase. Showing the composition of the binding pocket; hydrogen bonds (purple arrow) and pi-pi stacking (green arrow) interactions between the enzyme and the compounds.

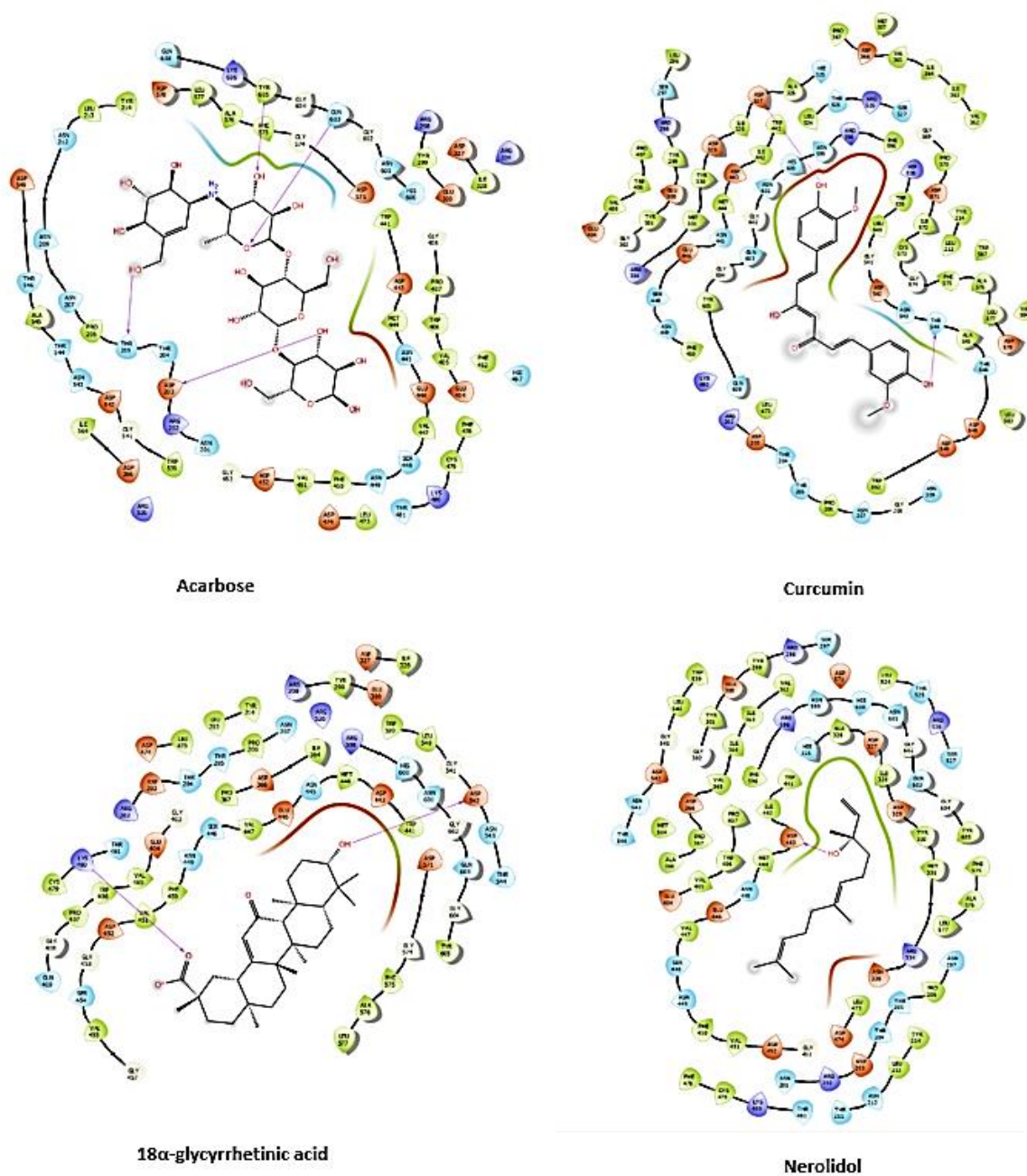


Figure A2. The interactions of acarbose, curcumin, 18α-GA and nerolidol in the binding pocket of α-glucosidase. Showing the composition of the binding pocket; hydrogen bonds (purple arrow) between the enzyme and the compounds.

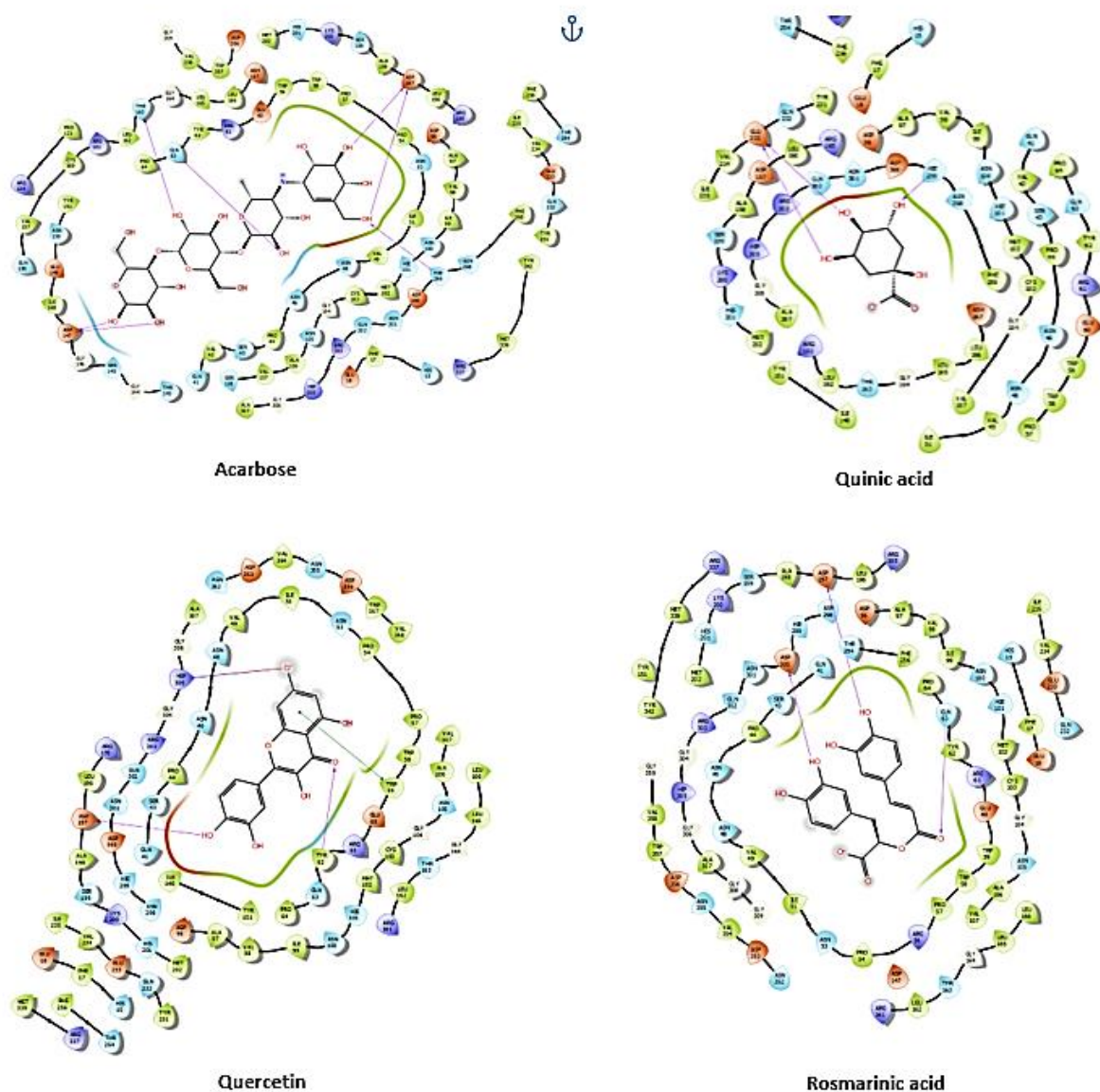


Figure A3. The interactions of acarbose, quinic acid, quercetin and rosmarinic acid in the binding pocket of α -amylase. Showing the composition of the binding pocket; hydrogen bonds (purple arrow) and pi-pi stacking (green arrow) interactions between the enzyme and the compounds.

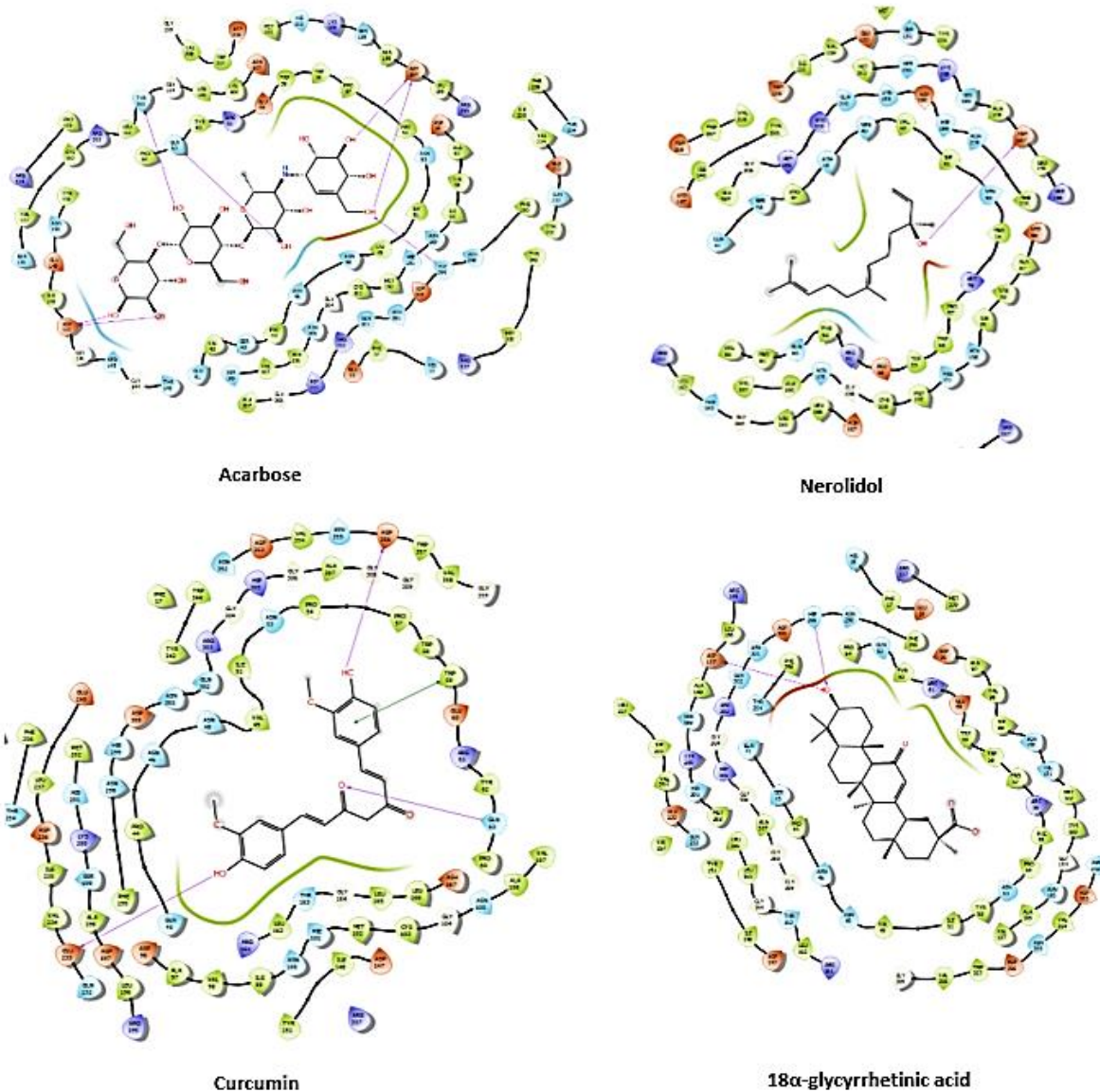


Figure A4. The interactions of acarbose, nerolidol, curcumin and 18 α -GA in the binding pocket of α -amylase. Showing the composition of the binding pocket; hydrogen bonds (purple arrow) and pi-pi stacking (green arrow) between the enzyme and the compounds.

1.33. Annexure B: Lineweaver burk plots

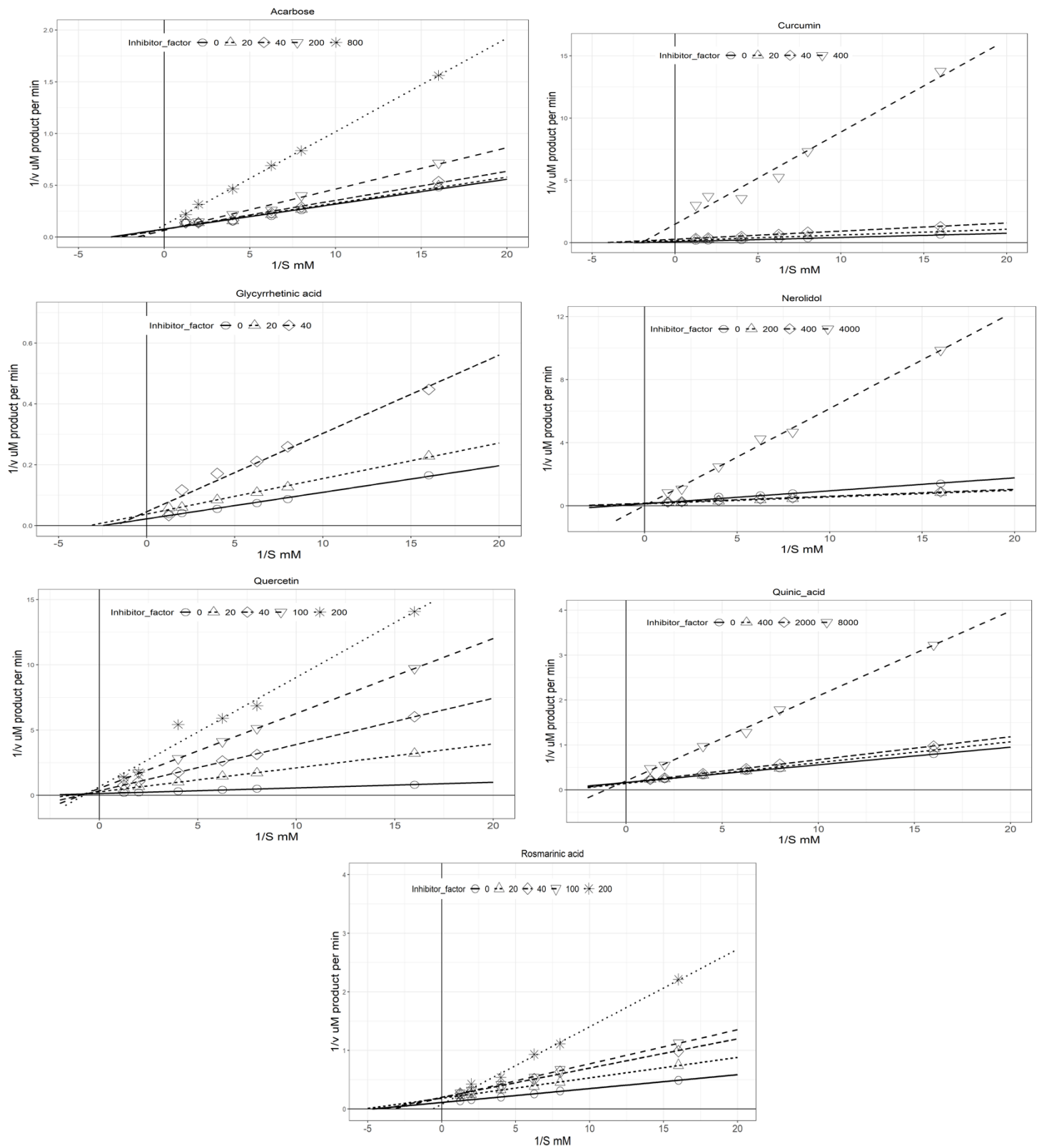


Figure B1. Lineweaver-Burk graphs of the inhibition of α -glucoside by compounds with [I] in μM .

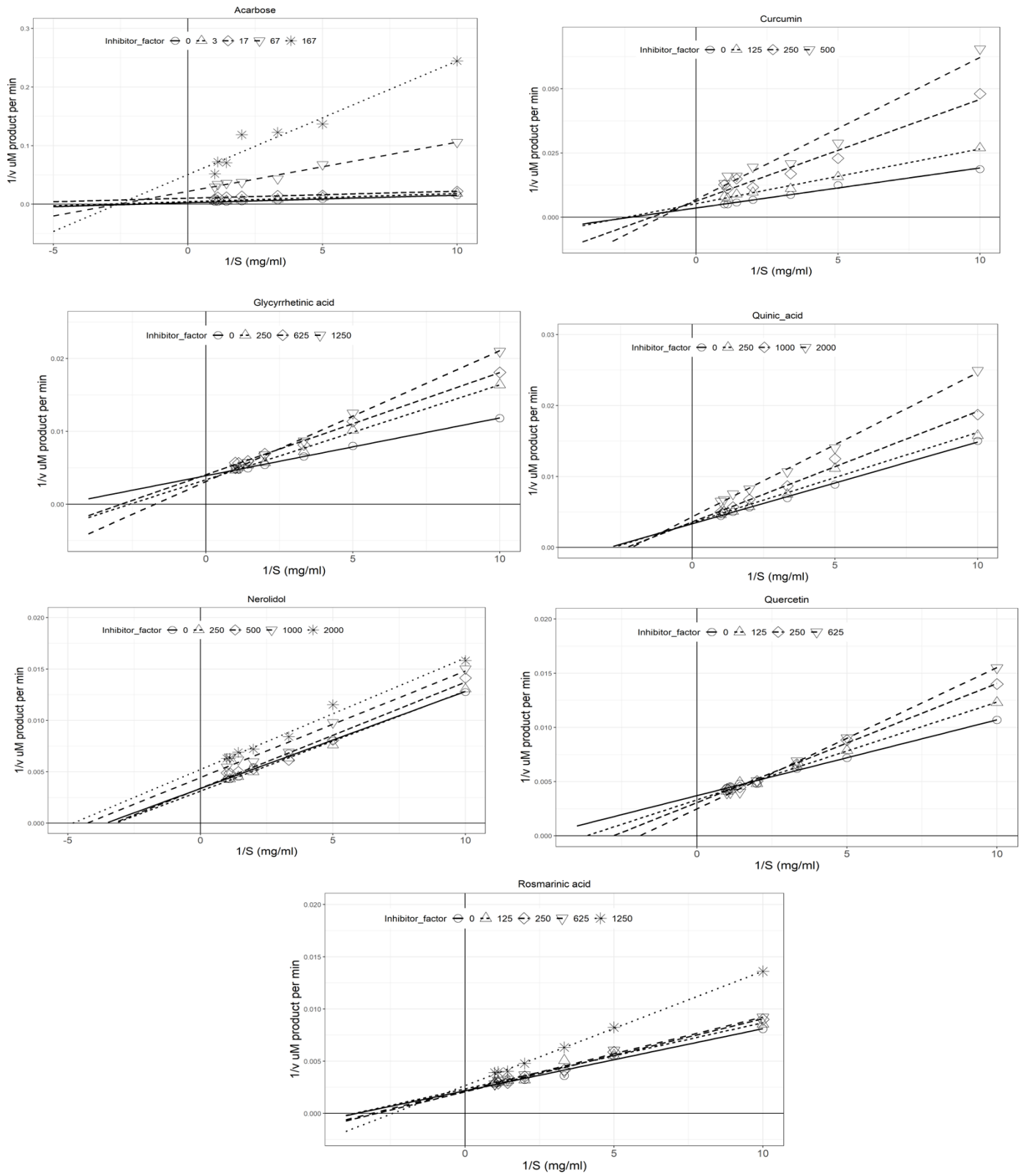


Figure B2. Lineweaver-Burk graphs of the inhibition of α -amylase by compounds with [I] in μM

1.34. Annexure C: Cell viability graphs

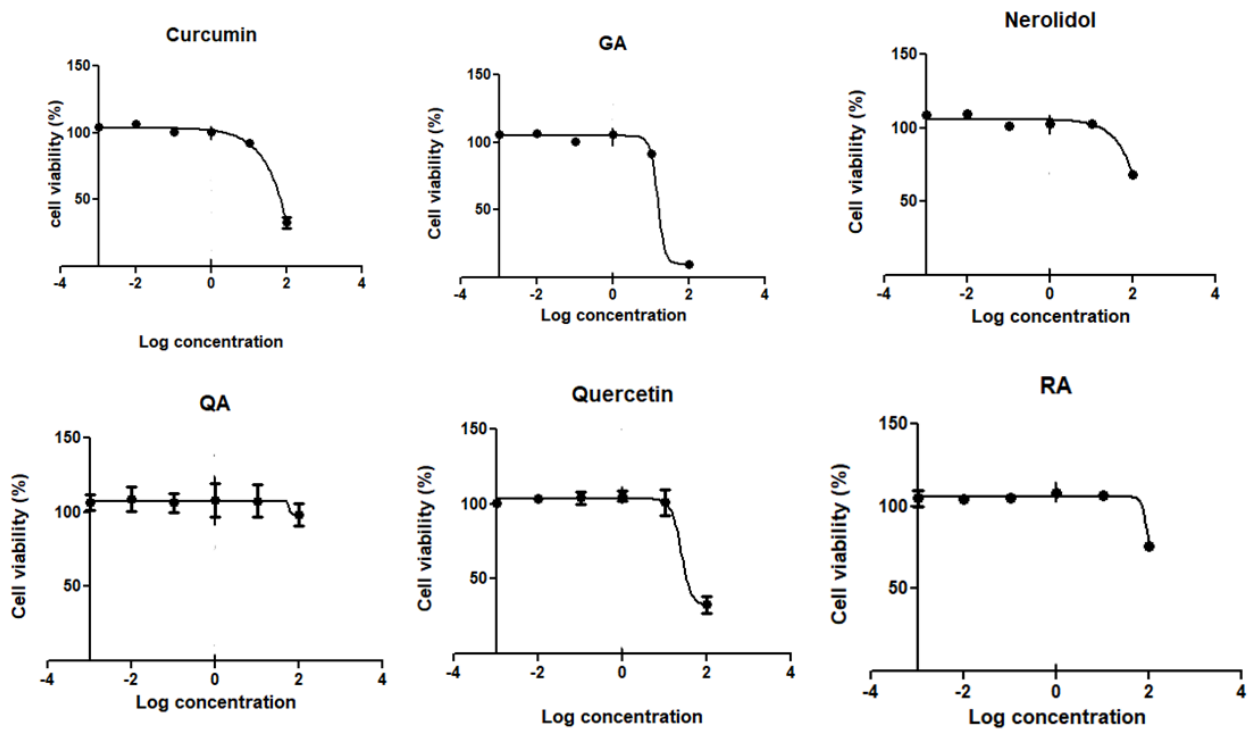


Figure C1. C2C12 cells viability after 72 h exposure to selected compounds (n=3, SEM error bars).

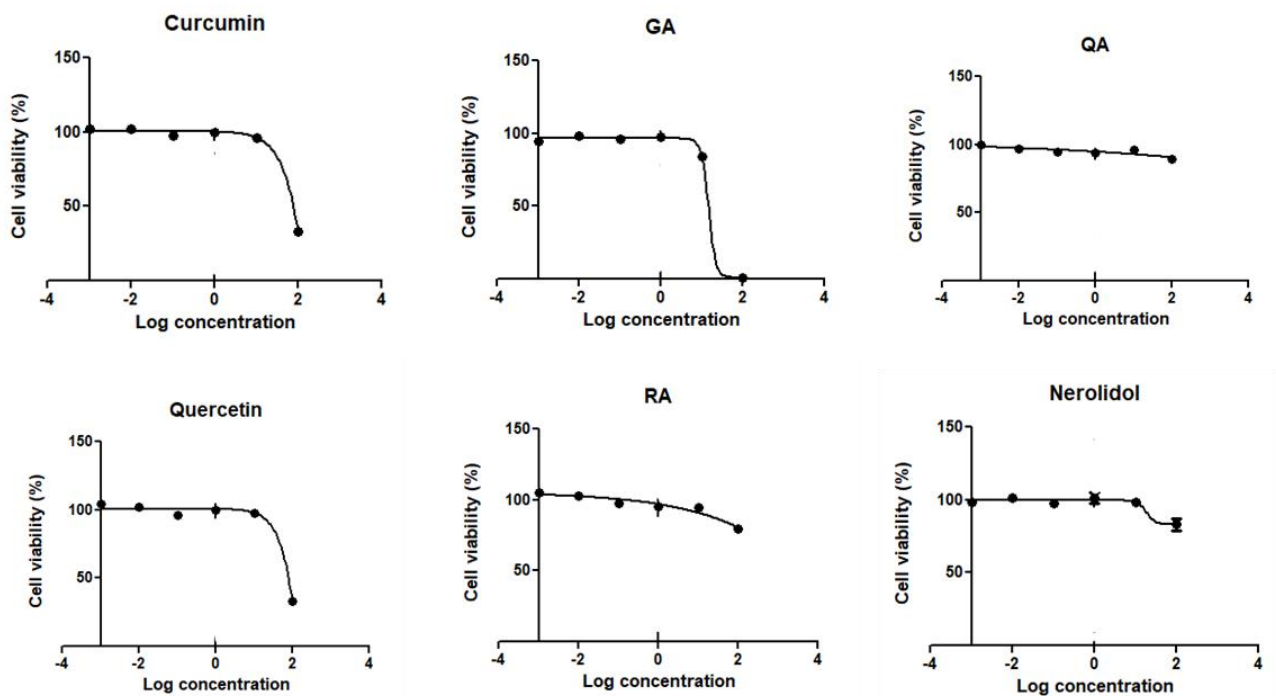


Figure C2. Hepg2 cells viability after 72 h exposure to selected compounds (n=3, SEM error bars).

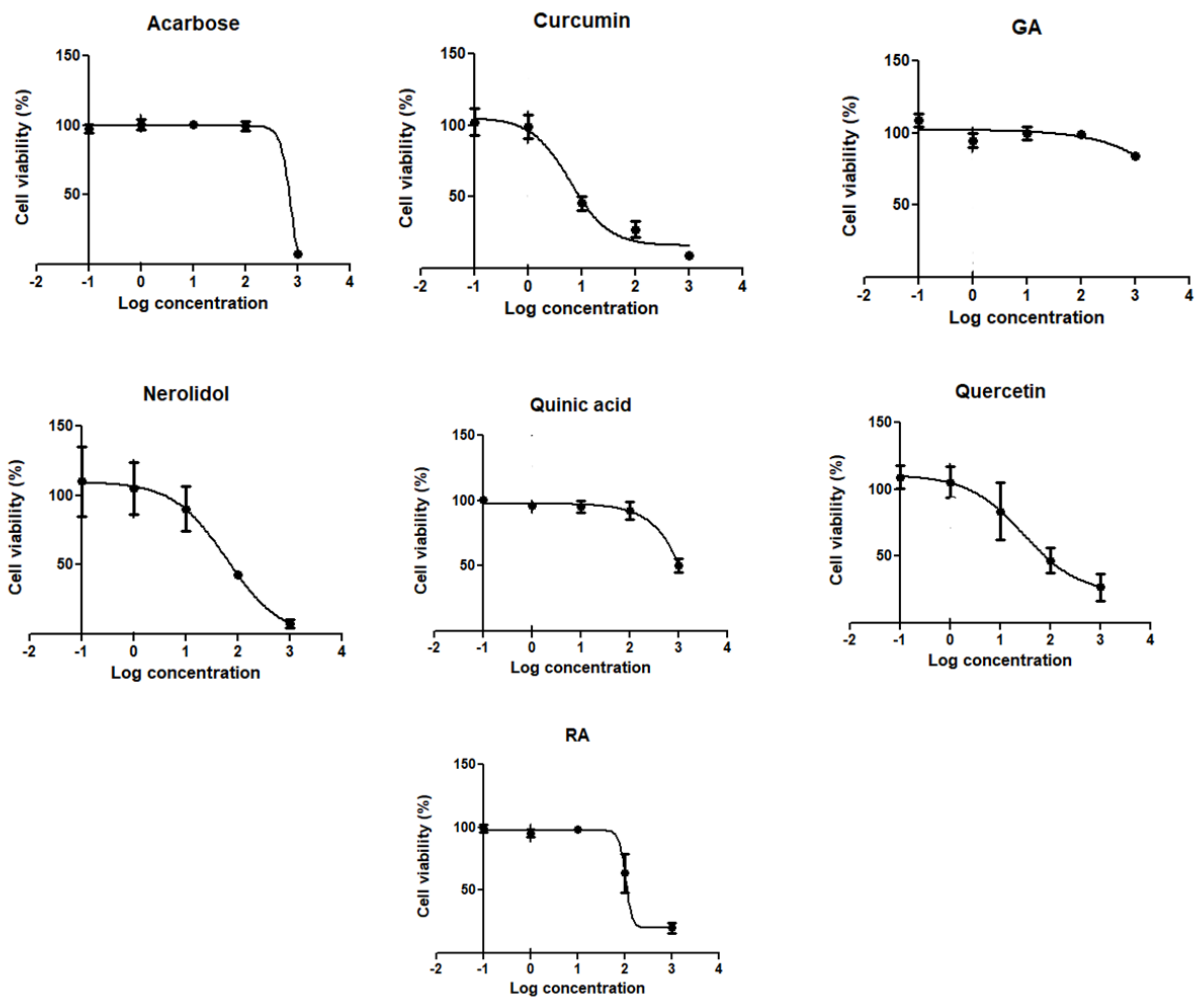


Figure C3. Caco2 cells viability after 72 h exposure to acarbose and selected compounds (n=3, SEM error bars).

1.35. Annexure D: Metabolites detected

Table 1D. Metabolites detected in volcano map and their significance changes between strong and weak inhibitors among the five green tea brands.

	Metabolites	Significance
1	Theogallin	Not significant
2	(-)-Gallicocatechin	Not significant
3	(6-[2-(3,4-Dihydroxyphenyl)-5,7-dihydroxy-4-oxo-4H-chromen-3-yl]oxy}-3,4,5-trihydroxyoxan-2-yl)methyl (2E)-3-(4-hydroxyphenyl)prop-2-enoate	Significant down
4	Cryptochlorogenic acid	Significant down
5	(-)-Epigallocatechin	Not significant
6	3-O-p-Coumaroylquinic acid	Not significant
7	3'-Galloylprodelphinidin B2	Significant down
8	Catechin	Not significant
9	MINEs-444181	Not significant
10	Corilagin	Not significant
11	Chlorogenic acid	Significant down
12	Crypto Chlorogenic acid	Significant down
13	Procyanidin B5	Not significant
14	Vitexin 2'-O-rhamnoside	Not significant
15	Procyanidin isomer	Not significant
16	Epigallocatechin-(4beta->8)-epicatechin 3-O-gallate	Not significant
17	Epicatechin	Not significant
18	Epigallocatechin gallate	Not significant
19	Epigallocatechin gallate isomer	Not significant
20	Isonoeaflavin	Not significant
21	Myricetin 3-galactoside	Not significant
22	Myricetin 3-glucoside	Not significant
23	Kaempferol 3-sophorotrioside	Not significant
24	(-)-Epigallocatechin 3-(3-methyl-gallate)	Significant down
25	Kaempferol 3-sophorotrioside	Not significant
26	(-)-Catechin 3-O-gallate	Not significant
27	Quercetin 3-galactoside	Significant down
28	Kaempferol 3-gentiobioside 7-rhamnoside	significant up
29	Unknown	Significant down
30	Epicatechin 3-O-(4-methylgallate)	Significant down
31	Quercitrin	Significant down

1.36. Annexure E: Tentative identification of peaks

Table 1E. Details on the unidentified peaks according to mass spectra obtained

	Retention time (min)	m/z ratio	[M-H] fragments	Proposed compounds	Reference/s
UP1	2.10	341.11	133, 191	1-O-Caffeoylglucose	KEGG
UP2	2.81	173.09	151	Theanine	(Jin <i>et al.</i> , 2019) PubChem
UP3	6.09	169.01	125	Gallic acid	(Lin <i>et al.</i> , 2008) (Jin <i>et al.</i> , 2019) PubChem
UP4	6.90	343.07	191	Galloylquinic acid 1-O-Caffeoylglucose theogallin	(Jin <i>et al.</i> , 2019) (Lin <i>et al.</i> , 2008)
UP5	8.60	305.07	---	Gallocatechin	(Jin <i>et al.</i> , 2019)
UP6	16.92	771.19	169, 183, 287, 457, 471, 593	Quercetin 3-O-galactosylrutinoside Quercetin 3-O-glucosylrutinoside	(Lin <i>et al.</i> , 2008)
UP7	18.37	755.2	169, 441, 463	Quercetin 3-O-dirhamnosylglucoside Kaempferol 3-O-galactosylrutinoside Kaempferol 3-O-glucosylrutinoside	(Lin <i>et al.</i> , 2008) (Jin <i>et al.</i> , 2019)

1.37. Annexure F: Ethical approval



UNIVERSITEIT VAN PRETORIA
UNIVERSITY OF PRETORIA
YUNIBESITHI YA PRETORIA

Faculty of Natural and Agricultural Sciences
Ethics Committee

E-mail: ethics.nas@up.ac.za

21 October 2020

ETHICS SUBMISSION: LETTER OF APPROVAL

Mr KS Tshiyoyo
Department of Biochemistry, Genetics and Microbiology
Faculty of Natural and Agricultural Science
University of Pretoria

Reference number: NAS183/2020

Project title: In silico and In vitro evaluation of the glucose-lowering effect of some compounds from herbs and spices in the treatment of type 2 diabetes

Dear Mr KS Tshiyoyo,

We are pleased to inform you that your submission conforms to the requirements of the Faculty of Natural and Agricultural Sciences Research Ethics Committee.

Please note the following about your ethics approval:

- Please use your reference number (NAS183/2020) on any documents or correspondence with the Research Ethics Committee regarding your research.
- Please note that the Research Ethics Committee may ask further questions, seek additional information, require further modification, monitor the conduct of your research, or suspend or withdraw ethics approval.
- Please note that ethical approval is granted for the duration of the research (e.g. Honours studies: 1 year, Masters studies: two years, and PhD studies: three years) and should be extended when the approval period lapses.
- The digital archiving of data is a requirement of the University of Pretoria. The data should be accessible in the event of an enquiry or further analysis of the data.

Ethics approval is subject to the following:

- The ethics approval is conditional on the research being conducted as stipulated by the details of all documents submitted to the Committee. In the event that a further need arises to change who the investigators are, the methods or any other aspect, such changes must be submitted as an Amendment for approval by the Committee.
- **Applications using Animals:** NAS ethics recommendation does not imply that Animal Ethics Committee (AEC) approval is granted. The application has been pre-screened and recommended for review by the AEC. Research may not proceed until AEC approval is granted.

Post approval submissions including application for ethics extension and amendments to the approved application should be submitted online via the Ethics work centre.

We wish you the best with your research.

Yours sincerely,

A handwritten signature in black ink, appearing to read 'D. Banda'.